ADDIS ABABA UNIVERSITY

ADDIS ABABA INSTITUTE OF TECHNOLOGY

AFRICAN RAILWAY CENTER OF EXCELLENCE

EVALUATION THE PERFORMANCE OF RAILWAY BALLAST STABILIZED WITH DIFFERENT GEOSYNTHETIC MATERIALS - A CASE OF ADDIS ABABA-DJIBOUTI RAILWAY TRACK LINE

A Thesis in Railway Engineering Civil infrastructure

By

Nigist Abera

Sep, 2019

Addis Ababa, Ethiopia

A Thesis

Submitted in Partial Fulfillment of the Requirements for the Degree of Master of Science

The undersigned have examined the thesis with the title '**Evaluation of the Performance of Railway Ballast Stabilized with Different Geosynthetic Materials, A Case of Addis-Djibouti Railway Track Line'** presented by **Nigist Abera**, a candidate for the degree of **Master of Science** and hereby certify that it is worthy of acceptance.

Tensay G. (Ph.D.)		
Advisor	Signature	Date
Internal Examiner	Signature	Date
External Examiner	Signature	Date
Chairperson	Signature	Date

UNDERTAKING

I certify that research work with the title “Evaluation of the Performance of Railway Ballast Stabilized with Different Geosynthetic Materials, A Case of Addis-Djibouti Railway Track Line” is my own work. The work has not been presented elsewhere for assessment. Where material has been used from other sources it has been properly acknowledged/referred.

…….

Nigist Abera

ABSTRACT

Quality of track depends upon the proper functioning of ballast, which plays a significant role in providing support for the track base and distributing the loads to the subgrade. The freight traffic loads have an inherent effect on the railroad track line such as the deviation of track geometry from required conditions as a result of ballast degradation and substructure layer deformation. In order to overcome this problem and prolong the life of railroad tracks, preserving and enhancing the performance of the ballast layer is necessary. This study aims at evaluating the performance of different types of geosynthetic materials: geotextile, geogrid, and geocomposite for minimizing the deformation level of the ballast layer so as to improve the track capacity.

To evaluate the performance of such geosynthetic materials, numerical simulations have been performed using a two-dimensional plane-strain Finite Element Analysis software PLAXIS-2D. The analysis is comprised of typical unreinforced and geotextile, geocomposite and geogrid reinforced ballasted track. The results show that intrusion of any of the three types of geosynthetics at the ballast sub-ballast interface can improve the ballast performance by minimizing its deformation level. According to the analysis results, the track settlement is reduced by 20%, 30%, and 55% while using geotextile, geogrid, and geocomposite, respectively. Thus, it has been concluded that an intrusion of the geocomposite at the ballast-sub-ballast interface has reduced the track settlement, and the subgrade stress much better than an intrusion of other geosynthetic materials. Furthermore, an attempt is carried out to obtain an optimum location of geosynthetics at which the geosynthetics are of the most effective for minimizing the deformation level of the ballast layer and it has been found out that its location does not have a significant effect on its capacity of reducing the track settlement.

Key Words: **Track Capacity Improvement, Geosynthetic, PLAXIS 2D, Track Settlement , Subgrade stress, Strain Level**

ACKNOWLEDGMENTS

First and for most, Praise and thanks be to the Almighty God for giving me health and strength to overcome obstacles along the way and pass through all confronts during the study periods.

I would like to express my deepest gratitude and respect to my advisor Dr. Tensay Gebremedhn who has given me the basics during the course work and for his valuable advice for the successful completion of this thesis.

I would like to extend my respect and appreciation to the African Railway Center of Excellence for giving me this scholarship program. I also would like to extend my respect to all staff of Addis Ababa Institute of Technology, African Railway Center of Excellence, Librarians and Administrative workers of the institute: without their support, this thesis would not have been possible.

Finally, my special thank goes to my family and intimate friends for their endless love and boundless mental support and for their encouragement.

TABLE OF CONTENTS

LIST OF TABLES

LIST OF FIGURES

NOTATIONS

ERC	Ethiopian Railway Corporation
FEM	Finite Element Modeling
FEA	Finite Element Analysis
2D	Two Dimensional
BSW	Ballast Shoulder Width
BSS	Ballast Side Slope Run
BDD	Depth of Ballast
SBD	Depth of Sub ballast
SBS	Sub ballast side slope run
UIC	International Union of Railways
DUDZ	Dilatant, Unstable Degradation Zone
ODZ	Optimum Degradation Zone
CSDZ	Compressive Stable Degradation Zone
$\emptyset$	Dynamic impact factor
P_s	Static/Nominal Wheel Load
P^D	Design Wheel Load
σ_z	Maximum Vertical Pressure Under the Rail seat
p_a	Average Ballast Pressure
q_r	Rail Seat Load
MC	Mohr-Coulomb model
LE	Linear Elastic model
γ	Unit weight
ν	Poisson's ratio
c	Effective cohesion
$\emptyset$	Effective friction angle
ψ	Dilatancy angle
EA	Elastic normal (axial) stiffness
ε_{max}	Maximum strain / Relative extension
t_{max}	Maximum Tensile Strength
$t_{\varepsilon=X}$	Tensile strength at x% strain
R_{int}	Strength-Reduction Factor
$\emptyset_{int}$	Effective Friction Angle of the Interface

E	Young's Modulus
E_r	Resilient Modulus
σ_C	Confining pressure
S	Shear strength
σ_n	Normal stress on the failure plane
ε_p	Plastic Strain
q_d	Deviatoric Stress
AREMA	American Railway Engineering and Maintenance-of-Way Association

CHAPTER 1 INTRODUCTION

1.1 Background

Ballasted tracks are widely used throughout the world. In this conventional type of track, rails are supported on sleepers, which are embedded in a compacted ballast layer up to 350 mm thickness [1]. Nowadays a ballasted railway track system becomes an integral part of the transportation infrastructure in our country Ethiopia. Such tracks are the most common railroad track structures, owing to have a relatively low cost of construction and ease of maintenance. However, ballast degradation, which is associated with particle breakage, fouling, and ballast migration, as well as deformation of the subgrade may result in a small amount of permanent settlement under each wheel load, occurring due to the periodic forces induced by the trains. Therefore, regular maintenance is required such as by ballast tamping machines. Although the cost of such maintenance is lower than that of replacing the whole system, it is still very high.

The performance of a ballasted railway track is directly dependent on the effective functioning of the ballast layer and the cost of track maintenance can be significantly reduced if the geotechnical behavior of rail substructure is better understood [2]. The problem of track deterioration, lateral instability, and increased maintenance costs becomes more severe under conditions of ballast fouling [3]. During track operations, fine particles migrate within the ballast bed and fill the voids between larger aggregates. Fouling of ballast makes the granular mass effectively less angular, decreases its shear strength, and impairs track drainage. Therefore, Different ballast stabilization techniques have been introduced to improve track conditions and reduce the cost of maintenance. One of these techniques is, using a geosynthetic material, which can improve the track stability and provide optimum filtration, adequate separation, and better drainage for the ballast layer simultaneously [2]. Various types of geosynthetic reinforcements placed in unbound ballast have usually improved the performance of rail transportation systems, but the optimal location of geosynthetic is not yet established.

This thesis focuses on minimizing the track settlement and the deformation level of the ballast layer so as to improve the performance of railway ballasted track by the intrusion of three different types of geosynthetic materials geotextile, geogrid, and geocomposite.

The study numerically investigates the influence of the tensile stiffness of different types of reinforcement on the overall performance of the railroad ballast using a two-dimensional plane-strain Finite Element Analysis PLAXIS 2D, which has already demonstrated its success with limit analysis of geotechnical problems. A number of researchers like [4] used the two-dimensional (2D) plane strain FE modeling to simulate the dynamic response of ballasted railway tracks.

The plane strain railway track modeling requires an assumption that the transversal profile of the track is consistent in the longitudinal direction. However, This is a gross approximation, since the longitudinal rail is discretely supported by the sleepers in the transverse direction of the track [5]. Because of this, a discretely supported rail track structure (3-dimensional problem) is approximated to a 2-dimensional plane strain problem by idealizing the sleeper as a continuous member. From the literature review, the more popular method of idealizing the discretely placed member is by converting the discrete member elements into the continuous plane to simulate a plate with factored properties [6]. This method is applicable to methods of idealization of a discrete member element to plane strain member element for allowing the sleeper to be represented as a continuous member in the 2D plane strain calculations.

In this study, a discreet sleeper support track structure is converted to the continuous support system by equivalencing of strength and stiffness properties of the sleeper. The equivalent Young's modulus $\overline{E}_{sl}$ of the sleeper is determined from the original Young's modulus E_{sl}, the width of the sleeper b_{sl} and the distance between sleepers d_{sl} [7]. Using these equivalent stiffness and strength parameters a typical plane strain track model with three different types of geosynthetics: geotextile, geogrid and geocomposite were numerically simulated by Finite Element discretization and finally, results were compared to show the level/degree of improvement and recommendations are presented.

1.2 Statement of the Problem

Ethiopian Addis-Djibouti railway line needs to fulfill industrial demands for faster, heavier and longer trains. This, in turn, necessitates a better quality of track that depends upon better functioning of ballast. However, the freight traffic loads on this line have an inherent effect such as the deviation of track geometry (alignment, profile, and cross-level) from

required conditions as a result of ballast degradation and substructure layer deformation. In order to overcome this problem of substructure deformation and breakage of ballast under traffic loads new ballast stabilization technique use of geosynthetics has been developed. Therefore, it is significant to investigate the performance of ballast stabilized with different types of geosynthetic material and obtain an optimum location of such geosynthetic materials within the depth of the ballast layer to minimize the level of the ballast layer deformation and track settlement.

1.3 Objective

1.3.1 General Objective

The primary objective of this study is to evaluate the performance of different types of geosynthetic materials in minimizing the track settlement and deformation level of the ballast layer so as to improve the track capacity.

1.3.2 Specific Objective

- To assess the performance of railway ballast reinforced with different types of geosynthetic material for typical national railway track section based on the result of Finite Element Analysis (FEA).
- To stabilize the ballast layer using different types of reinforcement: geogrid, geotextile, and geocomposit.
- To evaluate and compare the performance of different types of reinforcement in minimizing the track settlement and deformation level of the ballast layer.
- To obtain an optimum location of geosynthetics in rail track substructure for improving the track capacity.

1.4 Methodology

In order to achieve the above-mentioned objective, a numerical analysis is performed using a finite element based software PLAXIS-2D. The data sources are from Ethiopian Railways Corporation (ERC), American Railway Engineering and Maintenance of Way

Association (AREMA) manual and other acknowledged publications. The entire procedure is summarized step by step below:

- Data collection and summarizing
- Works of literature regarding the current trend of using geosynthetics in the railway industry will be thoroughly studied and reviewed.
- Geometric modeling of the track section with and without geotextile, geocomposite, and geogrid using a FEM based software package PLAXIS-2D.
- Finite Element Analysis (FEA) of the track section with and without geotextile, geocomposite, and geogrid using a FEM based software package PLAXIS-2D.
- Discussing and interpreting the result of Finite Element Analysis of the track section unreinforced and reinforced with geotextile, geocomposite, and geogrid.

1.5 Significance of the Study

The finding of this study will lead to an efficient track design in order to reduce the required depth of granular layer, minimize the deformation and track settlements, and consequently reduce the track maintenance costs, hence this makes the railway track system economical.

1.6 Scope of the Study

The main focus of this study is to evaluate the performance of different types of geosynthetic materials in minimizing the deformation level of the ballast layer and the track settlement. The study is limited to use only three types of geosynthetic material: geogrid, geocomposite, and geotextile. For the simulations, geogrid is used to obtain an optimum location of geosynthetic material to use its maximum capacity of minimizing the deformation level of the ballast layer and track settlement.

1.7 Thesis Outline

This thesis contains five Chapters. A brief outline of this thesis is given below:

Chapter 1 is an introductory chapter containing the general background, statement of the problem, objectives of the study, methodology, significance, and scope of the study and structure of the thesis.

Chapter 2 is the chapter of literature review which includes: general description of various track components and its function, characteristics of railroad ballast, gradation and mechanical behavior of ballast, ballast degradation and settlement, the resilient and permanent deformation of ballast, factors influencing the permanent deformation and degradation of ballast, forces imposed on track and the significance, material requirement, application location and reinforcement principles are reviewed.

Chapter 3 is about the Finite Element Modeling and Analysis. It is divided into five subtopics; introduction, preliminary input data analysis and the modeling of the geometry and Finite Element Analysis of railway substructure. Before the analysis, an introduction about the general methods and procedures of Finite Element Methods are presented and in which a general description of the project and loading, have been performed. The final subtopic is a Finite Element Analysis of the track section unreinforced and reinforced with three different types of geosynthetic material: geotextile, geocomposite, and geogrid.

Chapter 4 in this chapter the results of the Finite Element Analysis are discussed and presented.

The final chapter, chapter 5 recapitulates the main findings of this study; in which conclusions have been made and finally, recommendations have been made for further research.

CHAPTER 2 LITERATURE REVIEW

In this Chapter, the general description of a typical ballasted railroad track components and its function, properties of ballast, gradation and mechanical behavior of ballast, ballast settlement, ballast fouling, the use and significance of geosynthetics and the current trend of using geosynthetics in the railway industry are reviewed. An introduction into the composition and behavior of different types of geosynthetic materials like geogrid, geotextile and geocomposite and their uses in civil engineering applications, Degradation of ballast in railway engineering has long been an issue because it can lead to misalignment of the rails. The factors, such as a number of load cycles, gradation of aggregates, track confining pressure, and angularity and fracture of individual grains of ballast that can cause ballast degradation and deformation are thoroughly reviewed.

2.1 Railway Track Structure

Railroad track structure is a stable guide-way that serves as safe and comfortable train transportation with appropriate vertical and horizontal alignment. To achieve this role, each component of the system performs its specific functions satisfactorily in response to the traffic loads and environmental factors imposed on the structure [1]. Currently, the two commonly used rail track types are conventional ballasted track and slab track. Most rail tracks are of the traditional ballasted type; however, there are some recent applications of non-ballasted slab tracks depending on the load-deformation characteristics of the subgrade. The type of structure chosen depends upon expected axle loads, speeds, the required service life, the type and amount of maintenance, local conditions, intended purpose and availability of basic materials. This means that the choice of the track system is a technical, economic, social and political question, which has to be answered according to each individual case. The eventual aim is to arrive at minimum costs and maximum benefits throughout the life span of the track.

2.2 Ballasted Track Structure and Its Components

Ballasted tracks are widely used track structures throughout the world. In this conventional type of track, rails are supported on sleepers, which are embedded in a compacted ballast layer up to 350 mm thick [1]. A common problem with this type of track is the progressive

deterioration of ballast with increasing traffic passage. The breakage of sharp corners repeated grinding and wearing of aggregates, and crushing of weak particles under heavy cyclic loading may cause differential track settlement and unevenness of the surface. To maintain the desired safety level, design speed, and passenger comfort, routine maintenance is authoritative in a ballasted track. The main advantages that make ballasted track to be more preferable and widely used throughout the world are; relatively low construction cost and use of homegrown materials, ease of maintenance work (simple replacement of track components), high hydraulic conductivity of track structure (good permeability), simplicity in design and construction, good elasticity and good damping of noise and it requires less soil stabilization. Even though the ballasted track is preferable as of the above advantages, the life history of its usage implementation has shown significant disadvantages. To list some of them, but not limited to; degradation and fouling of ballast particles, leading to large track accumulated plastic deformation and requiring frequent and massive track maintenance work and routine checks; Reduction in hydraulic conductivity due to the clogging of voids by crushed particles and infiltrated fines from the subgrade; Pumping of subgrade clay and silt size particles to the top of ballast layer particularly in areas of saturated and soft subgrade; Emission of dust from ballast resulting from high speed trains; Extremely high maintenance cost; and Traffic interruption at the time of maintenance and so on [1].

A ballasted rail track is categorized into two main divisions of components: the superstructure and the substructure. The superstructure refers to the top part of the track which includes the rails, fastening system and sleepers: and the substructure includes ballast, sub-ballast and the subgrade. Figures 2-1 and 2-2 present the components of a conventional track. The most important element that governs load distribution to the deeper track section is the sleeper-ballast interface [8].

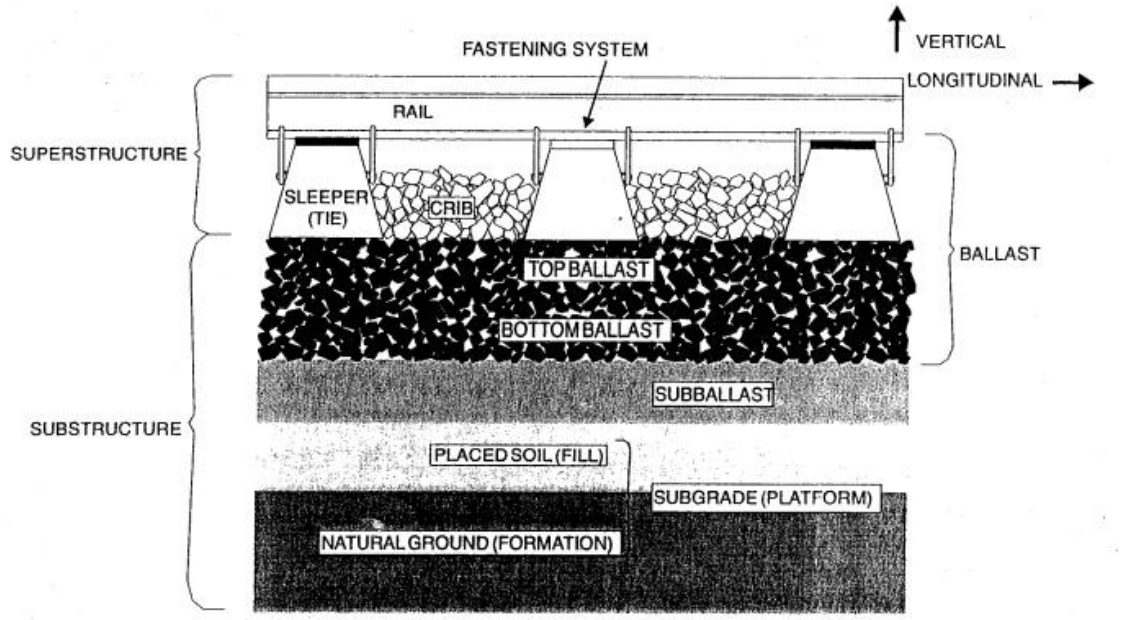

Figure 2-1 Components in a Typical Rail Track [8]

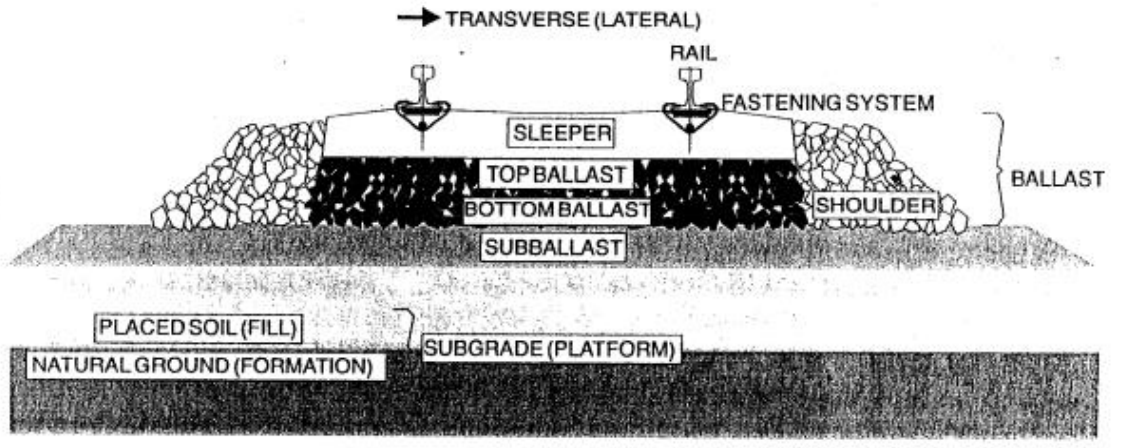

Figure 2-2 Cross-Sectional View of a Typical Rail Track [8]

Rails: are longitudinal steel members that come into direct contact with the train, and guide and support the train wheel loads in the vertical, lateral, and longitudinal directions and successively transfers the concentrated wheel loads to the supporting sleepers, which are equally spaced along the length of the track. Rails must be stiff enough to support train loading without excessive deflection between the sleepers and may also serve as electric signal conductors and ground lines for electric power trains [8] and resist tension failure from longitudinal tensile force caused by rail temperature reduction, resist buckling from

longitudinal compression force caused by rail temperature increase, resist fatigue cracking from repeated wheel loads, in switches and crossings /turnouts/set of points permit tracks to cross over each other and permit trains to switch from one track to another and moreover provides a smooth running surface and distributes accelerating and braking forces by means of adhesion. According to [9] when choosing the size and type of rails, rail properties like wearability, hardness, ductility, manufacture defects in the rail material, and rail straightness should be considered.

Fastening System: includes any system of components used to fasten the rail to the sleeper or other support. According to [8] the purpose of the fastening system is to retain the rail against the sleeper and resist vertical, longitudinal, lateral and overturning movements of the rail. The force system causing this movement is from the wheels and from temperature change in the rails. In addition to this, the fastening system connects sections of rail to permit safe and smooth train operation. [10] States that the choice of fastening greatly depends on the properties and structure of the sleeper. The widely used fastening system, which is elastic fastening, has four primary components; those are clip, anchor, rail-pad, and insulator. According to [11] each of these elements is designed to perform a specific function within the fastening system.

Sleeper: is part of the track superstructure which provides a resilient, even and flat platform for holding the rails, and forms the basis of a rail fastening system. They are laid on top of the compacted ballast layer in a specific distance apart which is called gauge. During the passage of trains, the sleepers receive concentrated vertical, lateral and longitudinal forces from the rails, and distributed to a wider area of ballast to decrease the stress at the sleeper/ballast interface to an acceptable level. The parameters used to select the preferred sleeper material include life-cycle costs, cross sleeper spacing and design methodology, rail fastening systems, cost per sleeper and number of sleepers per mile. Sleeper spacing affects rail flexural stress, compressive stress on ballast and roadbed, lateral resistance of the track structure and the flexural stress in the sleeper themselves [10]. According to AREMA Sec. 4.3.2.1 (2009), the recommended center-to-center spacing of sleepers is between 510 mm and 760 mm, its recommended length is between 236 cm and 274 cm and its width is between 20 cm and 33 cm and sleeper depth between 150 mm and 250 mm is intended for track designs. The use of longer, wider, or stiffer sleepers increases the sleeper-to-ballast bearing.

Sub-ballast: is the layer of aggregates placed between the ballast layer and the subgrade [8]. The sub-ballast layer is compacted to higher stiffness, such that the load distribution to the underlying subgrade is significantly reduced as well as being uniform. Where there is no sub-ballast or where poorly designed sub-ballast is used, saturated subgrade clay and silt-size particles can become slurred or liquefied with infiltrated water. The slurred soil may consequently pump upwards to foul the ballast under high cyclic loading, a phenomenon commonly known as clay pumping [8].

The main functions of the sub-ballast layer are minimizing the subgrade stress by providing additional load distribution, provide a load-bearing foundation beneath the ballast bed, prevent the ballast particles from penetrating the subgrade soils, increase the track resilience, preventing subgrade attrition by ballast and provide drainage to the water from the ballast and transfer it away from the subgrade to ditches at either side of the track thereby preventing the formation of soil slurry, extending the subgrade frost protection, preventing upward migration of fine material springing from the subgrade [8].

An appropriate materials that can be used as a sub-ballast materials are a crushed rock aggregate: with maximum grain size suited for equalizing the stress distribution; fairly broadly graded grain size distribution enabling good compatibility and to fulfill filter requirements; lowest possible fines content; high impact strength; high abrasion strength; lowest possible susceptibility to chemical and frost weathering; cubic, sharp-edged grain shape; high grain surface roughness; and high water permeability and low water retention of fines separating from material [12]. From experience of AREMA and recommendation of researchers the recommended minimum sub-ballast section depth shall be taken as 150 mm to reduce the depth of ballast and consequently intend in reducing the cost of the track.

Subgrade: the railroad subgrade is the load-bearing layer of a track structure, either compacted natural ground or an imported fill embankment, which provides a permanent way to support the trackbed (ballast and sub-ballast layers) [8]. The subgrade is the most significant factor governing track stiffness and hence the deterioration of vertical track geometry. The main functions of subgrade are it provides a stable foundation for the sub-ballast and ballast layers and a stable platform to construct the track, limit progressive settlement from repeated traffic loading, limit consolidation settlement, prevent massive slope failure, and restrict swelling or shrinking from water content change [9]. Subgrade

failure which usually affect the track performance are; overstressed conditions, inadequate compaction or excessive moisture content of the filling material, natural conditions such as weak subgrade soil (silt and clay), high groundwater tables and erosion or sliding of the embankment. For the subgrade to serve as a stable platform these failure types must be avoided and the most economical and commonly used remedial measures, increasing the ballast thickness (ballast + sub-ballast) to reduce subgrade stresses [13].

2.3 Railroad Ballast

Railroad ballast layer, the upper stratum of the substructure upon which the rail-sleeper assembly is laid, is one of the most important components in the railroad track infrastructure [14]. Essentially, the term 'ballast' used in railroad engineering means coarse aggregates placed above sub-ballast (finer-grained) to act as a load-bearing platform to support the track superstructure. Ballast serves two essential roles in rail substructure, to distribute loads from the track into the lower substructure layers and to maintain drainage. It is usually composed of quarried rock aggregates originating from high quality igneous or metamorphic rock quarries. Throughout the life of railroad construction, hard crushed angular stones and rock aggregates having a uniform gradation and free of dust have been considered as acceptable ballast materials [8]. The source of ballast (parent rock) varies from country to country depending on the quality and availability of rock, environmental regulations, and economic considerations. No universal specification of ballast is used throughout the world for its index characteristics such as size, shape, hardness, friction, texture, abrasion resistance and mineral composition that will provide the optimum track performance under all types of loading and subsoil behavior. And a wide variety of materials (e.g. basalt, limestone, granite, dolomite, and quartzite) are used as ballast throughout the world. As a component of the railroad track substructure, the ballast layer can be classified into four zones [9].

- **Crib**: material between the ties
- **Shoulde**r: material beyond the tie ends down to the bottom of the ballast layer
- **Top ballast**: the upper portion of supporting ballast layer that is disturbed by tamping

- **Bottom ballast**: the lower portion of supporting ballast layer, which is not disturbed by tamping and generally is the more fouled

The ballast layer is filled into the cribs to the top of the sleepers for the purpose of providing longitudinal stability to the track and depending on the type of track the ballast shoulders are formed on the sleeper ends to a typical width of 300-600 mm to provide lateral stability to the track. For a track with continuously welded rails track shoulders are heaped 125 mm above the sleeper top level to prevent buckling of the track. Traditionally, the main factors in the choice of ballast materials are its availability and economic reasons. Ideal ballast materials are angular, crushed, hard stones and rocks, uniformly graded, free of dust and dirt, and not prone to cementing action [9].

2.3.1 Characteristics of Railroad Ballasts

A) Constitutive Characteristics of Railroad Ballast Particles: The mechanical characteristics of individual particles significantly influence the behavior of ballast. The ability of the ballast to perform its functions depends on the particle characteristics (e.g. particle size, shape, angularity, hardness, surface texture and durability) together with the in-situ physical state (e.g. grain structure and density) [12]. In the following section, various characteristics of individual grains and their influence on the mechanical behavior of ballast are discussed.

Particle size: Typically, the size of ballast grains are varied in the range of 25 mm – 63 mm in diameter (ASTM D6913). The larger particles within the range of ballast size stabilize the track while the smaller particles above 25 mm reduce contact forces between particles and minimize breakage. Particle breakage in fines less than 25 mm results in poor drainage and larger sizes above 63 mm reduce the angle of internal friction. So the size of particles should be neither too large nor too small. Under a repeated cyclic loading ballast particles breaks to a smaller fine below 25 mm which will clog the ballast and reduce, in the longer term, its drainage properties [15].

Particle shape: influences both the physical state (grain structure and porosity) and the particle interactions (interparticle friction and contact force) of the assembly. In the railway industry, various shape characteristics (i.e. flakiness, elongation, sphericity, angularity, and surface texture) are used [16].

Flat particle: is defined as one in which the ratio of thickness to width of its circumscribing rectangular prism is less than a specified value. From the ballast maintenance point of view, increasing the percentage of the flaky particles could increase the ballast degradation rate and the degree of fouling and thus will increase the ballast maintenance work [16]. The disadvantages of increased flakiness (extent of elongated, thin and flat particles) appear to be increased abrasion and breakage, increased permanent strain accumulation under repeated load and decrease stiffness [16]. Furthermore, better particle interlocking due to the existence of a substantial portion of flaky particles in a ballast sample will make the ballast maintenance work more difficult.

Angularity or roundness: Angularity, or it's inverse, roundness, is a measure of the sharpness of the edges and corners of an individual particle. Roundness defined as the ratio of the average radius of curvature of the corners and edges of a particle to the radius of the maximum inscribed circle. Angularity increases frictional interlock between grains which increases the shear strength of the ballast layer. Angular aggregates give less settlement than rounded aggregates. However, from the ballast maintenance point of view, angular ballast may need more ballast maintenance work because it is easily degraded and deformed under the repeated loading of trains [17].

Surface texture: has a positive effect on ballast performance. A rough particle surface forms a high inter-particle friction force and which makes to increase the shear strength of the ballast and make the track more stable. On the other hand, a smooth surface will create a low inter-particle friction force which will result in an easy rearrangement of particles and cause more ballast-related track deformation [17].

Particle crushing strength: Individual particle crushing strength is an important factor governing particle degradation, including grain splitting and breakage of sharp corners under high and cyclic loadings. Particle crushing strength primarily depends upon the strength of the parent rock, grain geometry, the loading point, and loading direction [12].

Abrasion of particles: Abrasion is a phenomenon where very small particles disintegrate from the grain surface, and this is independent of the stress level. Abrasion takes place in granular materials when particles slip or roll over each other during shear deformation which can occur even at low-stress levels [16].

B) Bulk characteristics of Railroad Ballast Particles: The overall characteristics of the granular mass that govern ballast behavior include particle size distribution (PSD), degree of saturation and the void ratio (or density) [12]. These characteristics are discussed in the following section.

Particle size distribution: The particle size distribution plays a significant role in the strength, deformation, degradation, stability, and drainage of tracks. A specified ballast gradation at first should satisfy the objective of higher shear strength to provide increased stability and minimal track deformation. This can be achieved by specifying a well-graded ballast. However, it should also have a high permeability to provide adequate drainage, readily dissipating excess pore water pressures and increasing the effective stress and this can be insured by specifying uniformly graded ballast [2]. These two objectives are contradictory in terms of the required particle size distribution and the optimum ballast gradation needs a balance between the uniform and well gradation. Uniform gradation provided a higher stiffness compared to well-graded aggregates and well-graded ballast gives lower settlement compared to uniformly graded ballast [17]. It is widely accepted that a narrow gradation would best meet the requirements for railway ballast. Sufficient voids are formed in a narrow gradation and, therefore, provide efficient drainage of water from the ballasted trackbed. The AREMA (2.4.5) manual provides recommended values of ballast gradation size as shown in table 2-1 below:

Table 2-1 Recommended Ballast Gradations [18]

Size No. (see Note-1)	Nominal Size Square Opening	**Percent Passing**									
		3"	**2 ½"**	**2"**	**1 ½"**	**1"**	¾ "	½ "	d"	**No.4**	**No.8**
24	**2 ½" - ¾ "**	100	90-100		25-60		0-10	0-5	-	-	-
25	**2 ½" - d"**	100	80-100	60-85	50-70	25-50	-	5-20	0-10	0-3	-
3	**2" - 1"**	-	100	95-100	35-70	0-15	-	0-5	-	-	-
4A	**2" - ¾ "**	-	100	90-100	60-90	10-35	0-10	-	0-3	-	-
4	**1 ½" - ¾ "**	-		100	90-100	20-55	0-15	-	0-5	-	-
5	**1" - d"**	-		-	100	90-100	40-75	15-35	0-15	0-5	-
57	**1" - No.4**	-		-	100	95-100	-	25-60	-	0-10	0-5
Note 1: Gradation Numbers 24, 25, 3, 4A and 4 are mainline ballast materials. Gradation Number 5 and 57 are yard ballast materials.											

Void ratio and density: It has been well established that aggregates with a lower initial void ratio (i.e. higher initial density) are stronger in shear and generate a smaller settlement than aggregates with a higher initial void ratio (i.e. lower initial density). Track stability can be significantly improved by increasing the bulk density of the ballast bed by further compaction or by using well-graded aggregates. However, care should be given to higher compaction which also increases the risk of particle breakage contributing to a reduction in drainage characteristics [17].

Degree of saturation: The response of ballast to external mechanical forces is adversely affected by an increased degree of saturation. According to [19] water influences track settlement and particle breakage and also leads to traffic problems. [19] conducted one-dimensional compression tests to investigate the effects of saturation on the deformation and degradation of ballast and they observed a sudden ballast settlement increase by about 2.6 mm due to sudden flooding. They also concluded that saturation increased settlement by about 40% of that of dry ballast.

2.3.2 Resilient and Permanent Strain Behavior of Railroad Ballast

Resilient modulus of ballast: The cyclic response of granular materials is usually characterized by resilient modulus. For repeated loads in triaxial testing with constant confining stress, the resilient modulus (E_r) is defined as the ratio of the applied cyclic deviator stress to the recoverable (resilient) axial strain during unloading [19] It is vital to have a good understanding of the resilient behavior of the trackbed material as this is known to have an effect on the degradation and rate of settlement of the rail track. Figure 2-3 illustrates the type strain in a granular material.

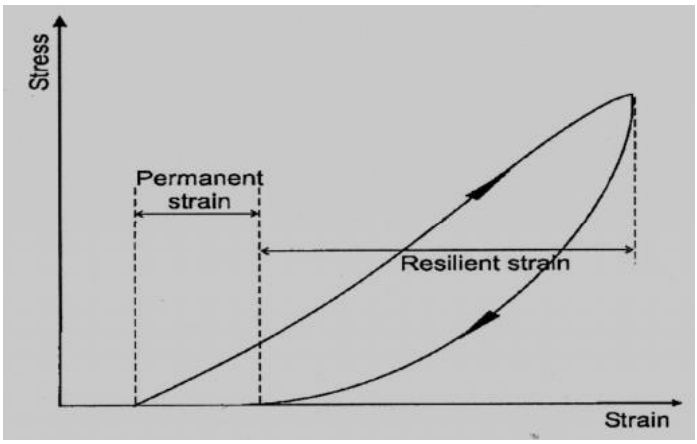

Figure 2-3 Strains in granular materials during one cycle of load application [20].

The resilient behavior of railroad ballast is influenced by different factors. Some of them are stress, confining pressure, the number of loading cycles, aggregate type and particle shape, duration and sequence of load and so on [19]. The resilient modulus (E_r) was found to be increasing with the number of loading cycles, maximum deviator stress magnitude ($q_{max,cyc}$) and confining pressure [19]. Research from the University of Wollongong highlights that resilient modulus is influenced by particle breakage and it is found to be increasing with particle breakage irrespective of the initial effective confining pressure [21].

Permanent Strain Behavior of Granular Material: The irrecoverable strain of granular material as shown in Figure 2-4 is often a trigger for maintenance activities on a rail track. The accumulation of such permanent strain on a rail track is due to the rearrangement of particles as well as particle breakage. The number of loading cycles, Stress level, moisture content, stress history, and density are the most important factors governing the development of permanent deformation in granular materials [12].

The permanent strain accumulated over a certain number of load cycles is directly related to the stress ratio, defined as the ratio of deviator stress q to confining stress σ_3 [22]. According to this report, increasing the stress ratio q/σ_3 will result in increasing the permanent strain as shown in Figure 2-4. The figure also showed that for the same stress ratio, (i.e. 20/5 and 60/15) increasing the stress path length will result in increasing the amount of permanent strain.

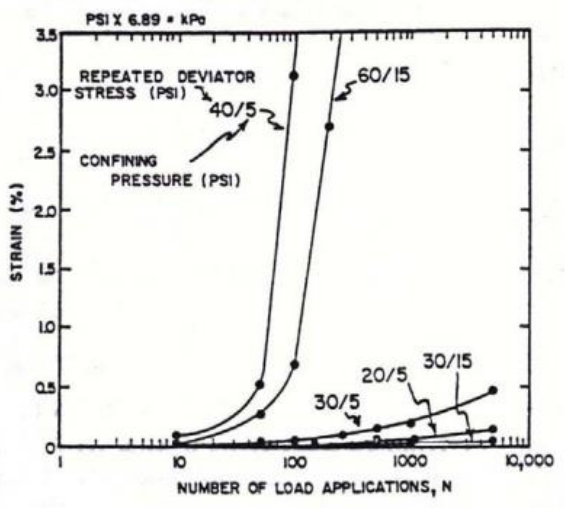

Figure 2-4 Effect of Stress Ratio on Permanent Strain [22]

Factors Influencing the Permanent Deformation and Degradation of Ballast: The deformation and degradation behavior of railroad ballast are influenced by factors such as confining pressure, deviatoric stress, the number of load cycles (N), load history, particle size distribution, degree of compaction, loading frequency (f), and the parent rock strength [19] Each parameter is presented in the subsequent sections.

Effect of confining pressure: in conventional rail track design the confining pressure on the ballast layer has not often been seriously considered as an important factor. This is due to the fact that a confining pressure, applied on tracks by the shoulder ballast and sleepers, is small when compared with a relatively high vertical stress [19].

A number of drained cyclic triaxial tests have been conducted on latite basalt, to examine the role of confining pressure on ballast degradation, and to quantify an optimum confining pressure in the track to reduce particle breakage [19]. In a practical sense, from their test result they have concluded that, by increasing the track confinement by a small amount, a significant reduction in ballast breakage can be achieved. The results of this cyclic triaxial tests on railway ballast have revealed that particle degradation behavior can be divided into three zones. (I) dilatant, unstable degradation zone (DUDZ): (II) optimum degradation zone (ODZ), and (III) the compressive stable degradation zone (CSDZ).

Dilatant unstable degradation zone (DUDZ): At low confining pressures of the region (I) where $\sigma_3' < 30$ kPa, ballast specimens are subjected to rapid and considerable axial and expansive radial strains. This leads to an overall volumetric increase or dilation. In this region, particles do not have adequate time to rearrange, and due to the excessive axial and radial strains, considerable degradation occurs via shearing and attrition of angular projections. Because of the small confining pressures applied here, specimens in this degradation zone are characterized by a limited coordination number, as well as relatively small particle-to-particle contact areas [19].

Optimum degradation zone (ODZ): As the confining pressure is increased to the optimum region ($30 < \sigma_3' < 75$ kPa), the axial strain rate is greatly reduced due to increased apparent stiffness. Small increases in confining pressure result in enhanced particle contact areas adopting a more favorable internal stress distribution, causing less degradation. It is noted that the overall volumetric behavior is slightly compressive. In this region, particles are held together in an optimum array with sufficient lateral confinement so as to provide

an optimum contact stress distribution and increased inter-particle contact areas. This leads to the reduction of the risk of breakage associated with stress concentrations, thereby reducing the wet attrition value [19].

Compressive stable degradation zone (CSDZ): As σ_3' is further increased to the compressive stable region ($\sigma_3' > 75$ kPa), particles are forced to move against each other within a limited space for sliding and rolling. Therefore, breakage is significantly increased. In this region, particles fail not only at the beginning of loading when the axial strain rates are the greatest, but also by the process of fatigue as the number of cycles increases [19].

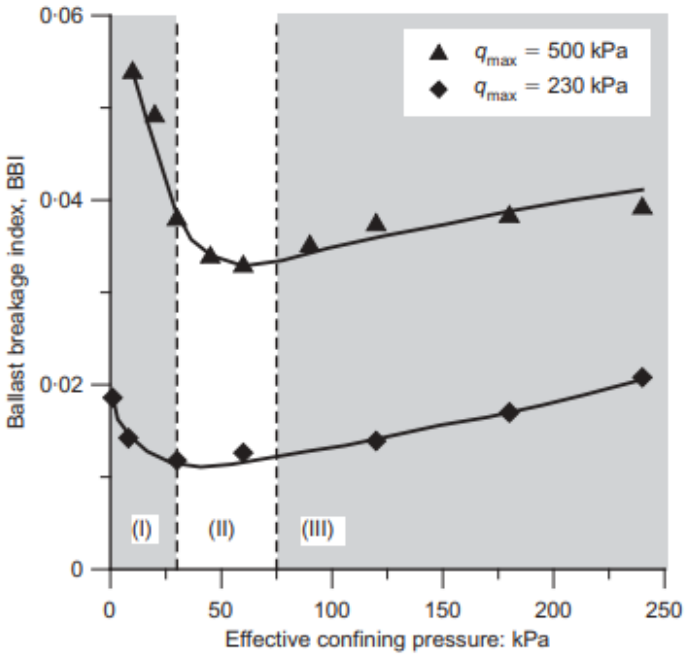

Figure 2-5 Effective Confining Pressure on BBI [19]

Effect of deviatoric stress, q: Indraratna et al (2005) studied the effect of deviatoric stress (q) on the deformation and degradation behavior of ballast and concluded that the deformation and degradation of ballast are increased significantly with increasing applied deviatoric stress for a given confining stress [19].

Effect of a number of load cycles: A material, which is subjected to repeated loading can respond in four different ways [23].

- **Purely elastic**: when the magnitude of the cyclic loading is sufficiently small, the material does not exhibit any permanent strains (stage 1 in Figure 2-6).

- **Elastic shakedown**: when the applied load level is appropriate to induce some permanent strains, yet the material behaves completely elastic after a finite number of cycles i.e. leading to zero permanent strain. At this point, the material is said to have reached "elastic shakedown" and the resilient strain becomes constant resulting in constant resilient modulus.

- **Plastic shakedown**: when the loads are higher than the critical loads which cause elastic shakedown, the material behavior will be either "cyclic plasticity" where a closed cycle of permanent strain is formed (stage 3 in Figure 2-6) or

- **The incremental collapse or ratcheting**: wherein permanent strain increases indefinitely (stage 4 in Figure 2-6) with each successive loading until the material fails [23].

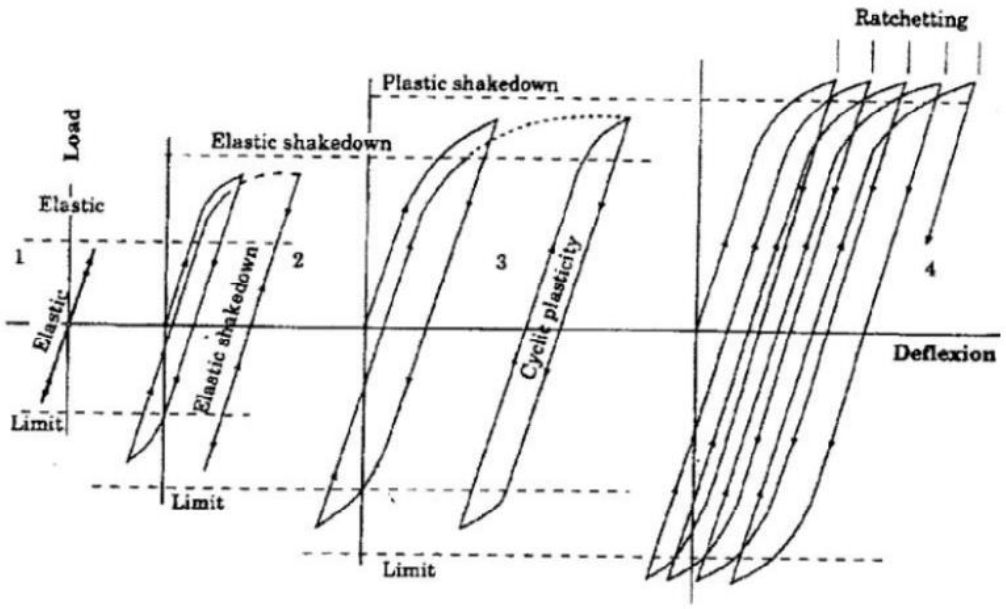

Figure 2-6 Four types of Responses of Structures to Repeated Loading Cycles [23]

Effect of particle size distribution: The grain size distribution of ballast significantly controls track performance, which should provide sufficient shear strength and the porosity to allow free drainage. [24] carried out large-scale cyclic triaxial tests on four different distributions of basalt aggregate and from the test result they have concluded that the

ballast breakage decreases with an increase in the value of C_u [24]. Furthermore, The test results showed that a distribution similar to the moderate grading would give improved track performance with lower permeability.

The ballast gradation with a uniformity coefficient of exceeding 2.2, but not more than 2.6, is most appropriate and recommended [21]. Figure 2-7 illustrates the relationship between the coefficient of uniformity C_U and particle breakage. Ballast breakage decreases when the value of C_U increases, with the exception of the gap-graded.

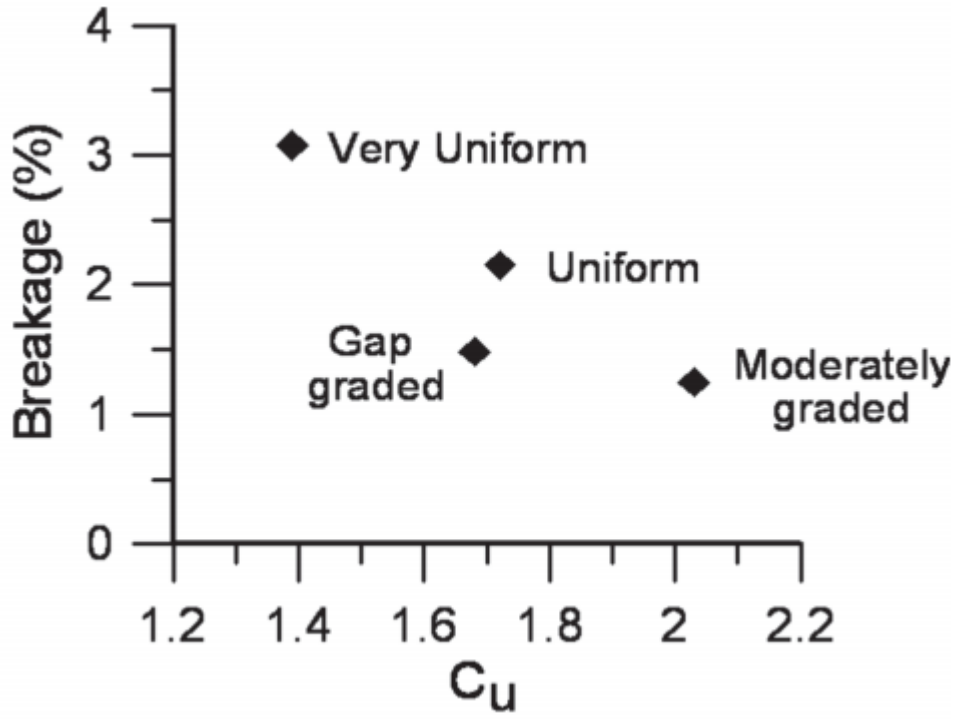

Figure 2-7 Effect of Grading on Particle Breakage [25]

Effect of degree of compaction: the degree of compaction is the most important factor that influences the permanent deformation behavior of ballast. According to [8] the material should be compacted at 95% instead of 100% of maximum compaction density.

Effect of loading frequency, f: as the loading frequency increases from 10 to 20 Hz and from 30 to 40 Hz the particle degradation, evaluated in terms of ballast breakage index (BBI), increases significantly. However, there exists an optimum frequency between 20 and 30 Hz at which the ballast densifies without any significant change in the BBI [26].

Effect of parent rock strength: The parent rock strength is an important parameter that influences the tensile strength of aggregates which often governs the particle breakage. [27] conducted cyclic tests on three different types of rocks and reported that the vertical settlements to be the highest in the case of granite, followed by basalt and quartz.

2.4 Forces Imposed on Track

The forces imposed on the railway track structure could be classified as mechanical forces (both static and dynamic) and Thermal forces. These forces are applied to the track structure in the form of repeated vertical, lateral and longitudinal forces resulting from traffic and changing temperatures. Lateral and longitudinal forces are more complex and harder to predict than vertical forces, which act perpendicular to the plane of the rails [8] In this thesis, only vertical forces resulting from traffic wheel loadings are considered. Vertical loads applied to the track from moving trains are a combination of a static load and a dynamic component. The static wheel load is the dead weight of the train divided by the number of wheels while the dynamic component is caused by interactions between the wheels and the rails and is a function of the track, vehicle, and train characteristics, such as track irregularities and train speed [8].

In order to design and analyze a ballasted railroad track structure, the type and magnitude of loads that are imposed during its lifetime must be quantified. The requirements for the bearing strength and overall quality of the track depend largely on the vertical load per axle which determines the required strength of the track, tonnage born as the sum of the axle loads which determines the deterioration of track quality, such as, increase in geometrical deviations, increase in rail fractures, and rail wear, alerts an indication for maintenance and renewal needed, and the running speed which determines the dynamic load of horizontal and vertical track geometry [10]. In order to design the track substructure effectively, it is essential to know the magnitude of sleeper/ballast contact stress and the distribution of stresses with depth through the ballast, sub-ballast and subgrade layers. The ballast thickness required for a track structure should depend on maximum stress intensity at the sleeper/ballast interface, acceptable bearing pressure of the underlying layer (sub-ballast or subgrade) and stress distribution within the ballast body. Typical distribution of wheel load to the rails, sleepers, ballast, sub-ballast and subgrade, is shown in Figure 2-8.

The vertical force consists of static and dynamic components. The static load is due to the dead weight of the superstructure and train, whereas the dynamic load is a function of the speed of the train and the track conditions. The vertical downward force at the rail-wheel contact point, as shown in Figure 2-8, tends to lift up the rail and sleeper some distance away from the contact point. With the advancing wheel, the uplifted sleeper will be forced down creating a high impact load onto the ballast particles and the track structure as a whole. As previously mentioned, the impact force is very much dependent on train speed and load. Meanwhile, this movement can cause a pumping action in the ballast, which can cause deterioration of track structure components and increase the ballast settlement by exerting a higher force on the ballast and pumping up fouling materials from sub-layers [28]. In addition to a dynamic variance, the vertical wheel force consists of a static component, equal to the weight of the train divided by the number of wheels [18] The total vertical wheel load on the rail could be classified into two groups: quasi-static load and dynamic load, as shown in equation 2.2 the quasi-static load is composed of the static, centrifugal and dynamic load components [29].

$$Q_{total} = Q_{quasi-static} + Q_{dynamic} \quad (2\text{-}1)$$

$$\mathbf{Q_{quasi-static} = Q_{static} + Q_{centrifugal} + Q_{dynamic}} \quad (2\text{-}2)$$

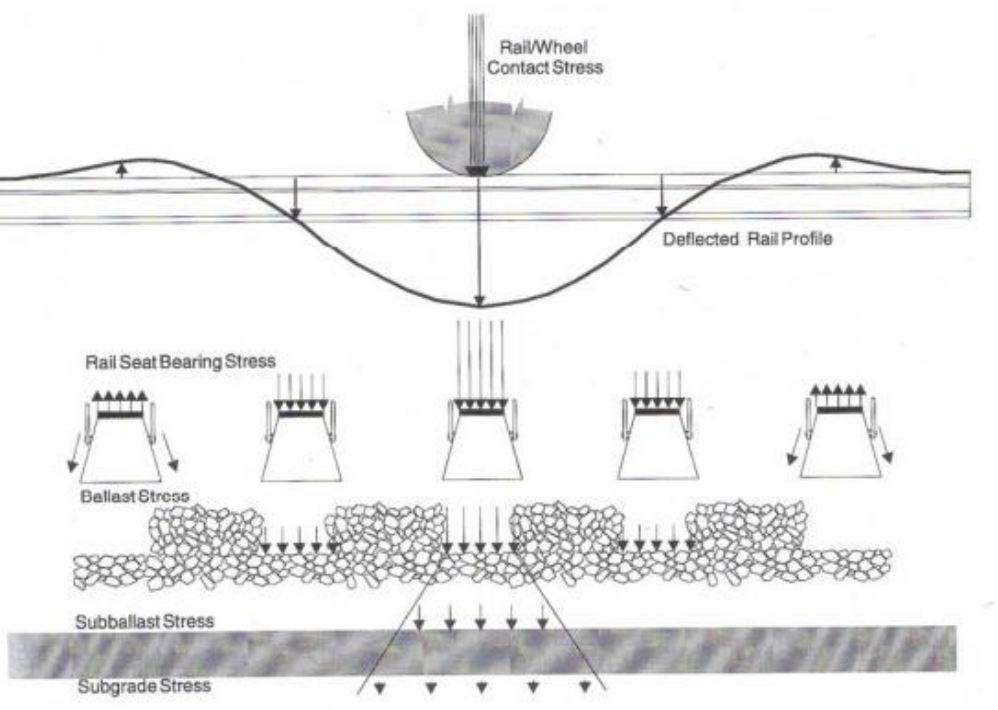

Figure 2-8 Ballasted Railroad Stress Distribution and Track Deflection Profile [8]

2.5 Geosynthetics Applications on Track

Applications of geosynthetics represent a rapidly growing field of geotechnical engineering. Geosynthetics are products manufactured from plastics which are used in conjunction with soils and aggregates in constructed projects for purposes such as earth retention, drainage and seepage control [8]. Geosynthetics reinforcement (geogrids, geotextile, and geocomposite) installed over unstable subgrades may eliminate the necessity of replacing this unstable subgrade soil, increasing the load-bearing capacity of the system due to better stress distribution. When installed within the ballast or sub-ballast layers, geosynthetics may help to reduce settlements associated with the lateral spreading of the ballast and sub-ballast materials. The main geosynthetic characteristics that must be considered for this function are the interaction between geosynthetic-soil/ballast, resistance to mechanical damage. In railroad construction, geosynthetics may be installed within or beneath the ballast or sub-ballast layers. There are different types of geosynthetics some of them along with their specific functions are listed in Table 2-2.

Table 2-2 Types of Geosynthetics with Functions [8]

Types of geosynthetics with functions	
Type	Functions
Geotextiles Woven Non-Woven	Separation Filtration Transmission Reinforcement
Geomembranes	Isolation Separation Reinforcement
Geogrids	Reinforcement
Geonets	Transmission
Geowebs	Reinforcement
Geocomposites	Combinations

A field trial were conducted on an instrumented track at Bulli, New South Wales, Australia, with a specific aim of studying the benefits of a geocomposite installed at the ballast-capping interface, and evaluate the performance of moderately graded recycled ballast in comparison to traditionally very uniform fresh ballast [30]. It was found that recycled ballast can be effectively reused if reinforced with a geocomposite. It was also found that geocomposite can effectively reduce vertical and lateral strains of the ballast with obvious implications for improved track stability and reduced maintenance costs.

A series of tests have been conducted using fresh ballast and recycled ballast with and without geocomposite so as to observe the effectiveness of using geocomposite and Predefined Vertical Drains (PVD) through field measurements and finite element predictions [3]. In which it has been confirmed that a geocomposite layer can improve the track performance by reducing the vertical deformations when ideally placed at the ballast-subballast interface. According to this investigation, PVDs also decrease the buildup of excess pore water pressure during cyclic loading and the dissipation of the pore water pressure during the rest period makes the track more stable for the next loading stage. Even with the relative short PVDs, both FEM predictions and field data proved that the lateral displacement can be abridged. It has also been showed that the equivalent plane strain Finite Element Analysis is adequate to predict the behavior of track improved by both geocomposit as well as short PVDs. Figure 2-9 shows a reduction in average vertical deformations of recycled ballast at a large number of cycles when a geocomposite reinforcement is used.

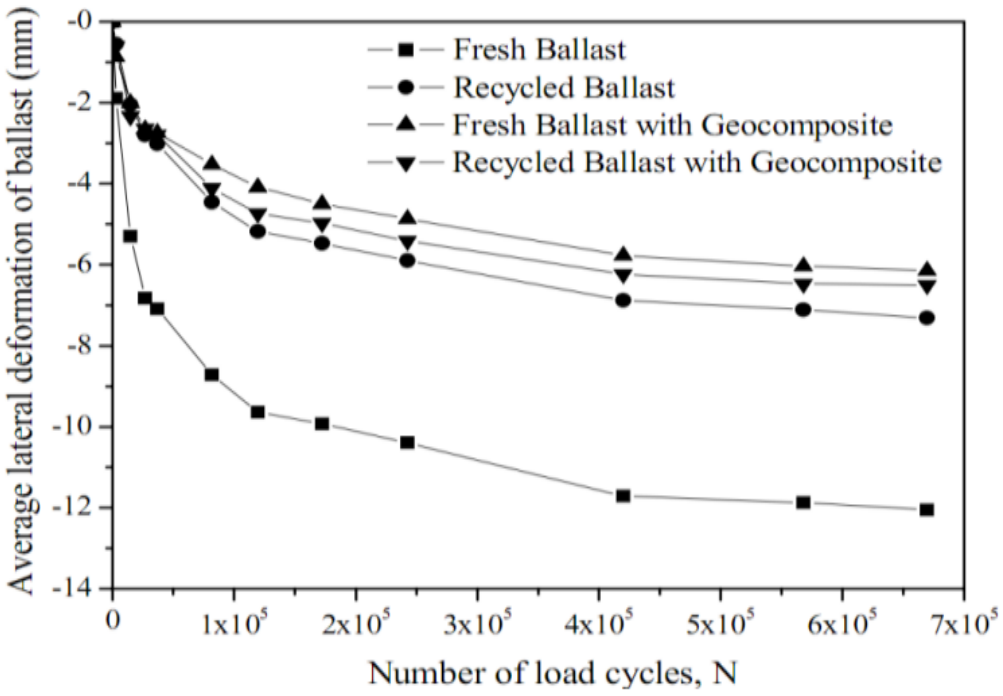

Figure 2-9 Vertical Deformation of the Ballast Layer [30]

2.5.1 Geotextile in Track Application Consideration

Geotextiles, also known as filter fabrics, are permeable textiles in either woven or non-woven form. A porous geotextile with small enough opening sizes can separate two adjacent layers of soils or aggregates. If the fabric has holes that are not too small, and if excess water pressure exists in the soil causing seepage, then the fabric will allow water to pass through while the soil particles will be retained. This is the filtration function. If the fabric is thick enough nonwoven. According to [8] the two functions of geotextiles in the track that are most likely to be of interest are:

- Maintain separation of substructure soil and/or aggregate layers of such different particle sizes and gradations that they would otherwise intermix under repeated loading.

- Permit seepage of water out of the track substructure layers while retaining the soil particles

There are five different substructure interlayer alternatives involving geotextiles need to be evaluated [8]: Between ballast and subgrade as a sub-ballast alternative, between sub-ballast and subgrade, between the ballast and sub-ballast, between replacement ballast and the surface exposed by undercutting, creating a sub-ballast layer by encapsulating a geotextile within the sub-ballast.

2.5.2 Geogrids in Track Application Consideration

Polymer geogrid has been proposed and tried as a reinforcement material, especially in the base course layer of flexible pavements. Geogrids are plastic sheets in the form of a grid with strands stretched to align the long-chain polymer molecules for high strength and stiffness [8]. The grids interlock with the soil to create tensile reinforcement when the soil strains are extensional in the plane of the grid.

Geogrids are also used as a reinforcing material on the rail track. Significant performance has been documented when geogrids are included within the ballast or sub-ballast layers of a roadbed section. The effects of the reinforcement are particularly apparent where the roadbed is placed on soft or medium strength subgrades. The reinforcement mechanism, often termed “mechanical stabilization”, occurs when larger aggregate particles partially penetrate and interlock within the apertures of the geogrid. Subsequent compaction results

in the aggregate and geogrid being “interlocked”; forming a semi-rigid mat that helps to distribute train loads and thereby reducing stresses on the subgrade.

According to [18] the benefits of using geogrid reinforcement within the roadbed section are Increased ballast life (life cycle cost savings), Reduced roadbed thickness (initial cost savings), Reduced track deflection resulting in less wear and tear of the mechanical components of the rail track, Maintenance of good drainage within the roadbed section and Smoother transitions between areas with differing subgrade strengths.

Geogrid uses the interlocking effect of soil particles, which penetrate the apertures and are locked into position between the strands of the geogrid. This immobilization of the particles leads to a strong horizontal shear resistance, which will increase the bearing capacity of the soil. Figure 2-10 shows the interlocking mechanism of a typical tensor polymer geogrid. Polymer geogrids were described as a plastic sheet in the form of a grid with aligned long-chain polymer molecules stretched to achieve high stiffness and strength [8].

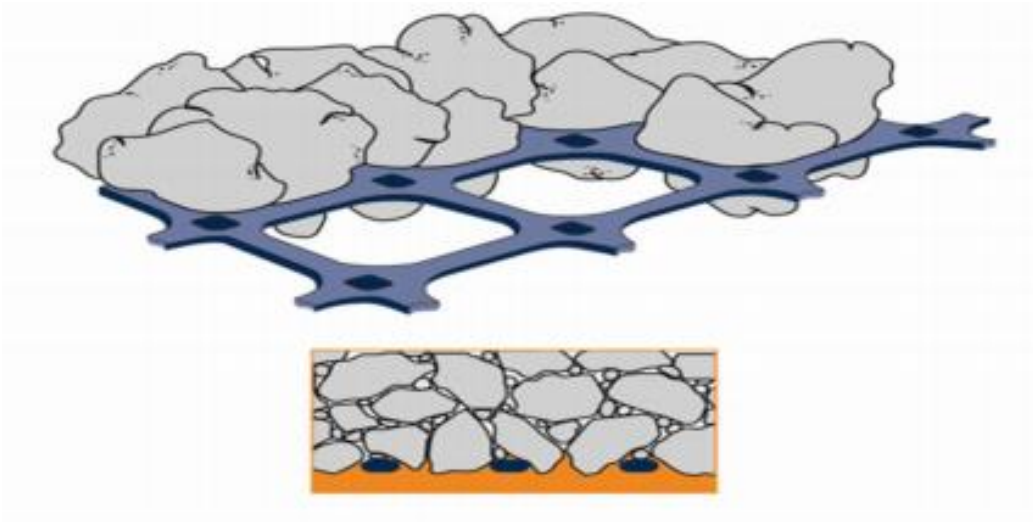

Figure 2-10 Interlock Mechanism of Polymer Geogrid [18]

The geogrids can be used in two main locations within the roadbed section [18]

- At the bottom of the ballast or within the ballast (Figure 2-11) this provides direct ballast reinforcement and thereby reduces the rate of track settlement. It, therefore, increases the length of the maintenance cycle. This approach is generally favored when the roadbed is founded on a relatively firm subgrade. and

- At the bottom of the sub-ballast, directly on the existing or prepared subgrade (Figure 2-12), this is done in order to increase the bearing capacity of the track foundation. This approach is generally favored when the roadbed is founded on a relatively soft subgrade.

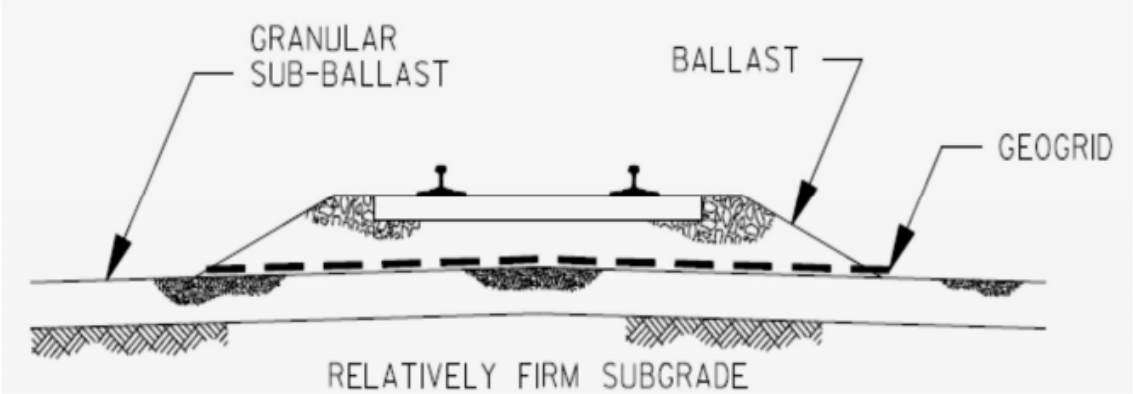

Figure 2-11 Geogrids at the Bottom of the Ballast, or within the Ballast [18]

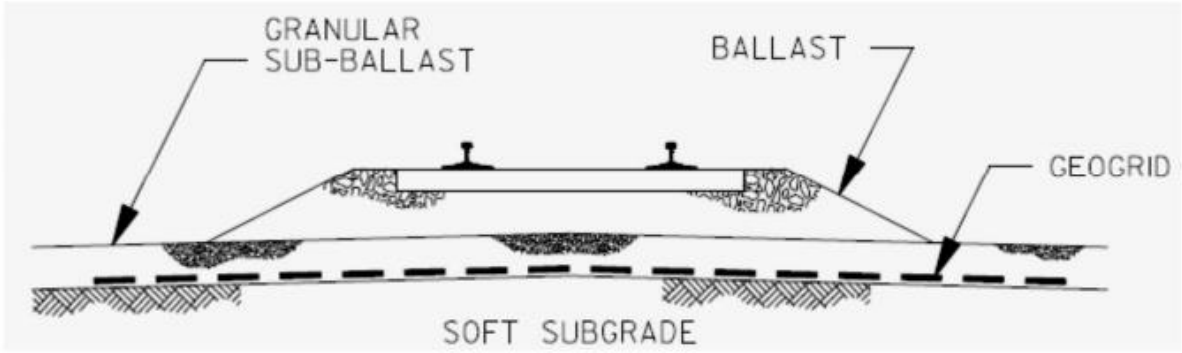

Figure 2-12 Geogrids at the Bottom of the Sub-Ballast, Directly on the Subgrade [18]

Material Requirements: In order to perform as reinforcement effectively, a geogrid should be able to transfer load through interaction with the surrounding aggregate. The material properties shown in Table 2-3 are recommended for geogrids used in ballast and sub-ballast reinforcement applications [18].

Reinforcing principle: A geosynthetic placed strategically in construction at the position of maximum tensile plastic strain is able to reduce such strain by carrying tensile stress in itself. This requires a good transfer of stress from the soil to the geosynthetic. In the case of a geogrid, this requires a good interlock. Applying this to the ballasted railway track, as

shown in Figure 2-13 the geosynthetic resists granular extension strains with confinement provided by the tensile strength of the polymer geogrid.

Table 2-3 Physical Properties for Geogrids Used in Track Stabilization [18]

Property	Test Method	Units	Minimum Value (sub-ballast reinforcement)	Minimum Value (Ballast reinforcement)
Aperture size (min. – max.)	Direct measurement	Inches (mm)	0.70 - 1.6 (17.8- 40.6)	1.70 - 2.50 (43.2 x 63.5)
Open area	Direct measurement	%	70	75
Rib thickness	ASTM D1777	Inches (mm)	0.05 (1.27)	0.05 (1.27)
Junction thickness	ASTM D1777	Inches (mm)	0.16 (4.0)	0.17 (4.4)
Aperture stability modulus @ 20cm-kg	US Army Corps of Engineers 62	lb-ft/deg (kg-cm/deg)	0.470 (6.5)	0.419 (5.8)
Flexural rigidity (Machine diretion)	ASTM D1388	(lb-ft) (mg-cm)	0.0542 (750,000)	0.0325 (450,000)
Tensile modulus @ 2% strain (Machine x cross machine diretion)	ASTMD6637-01	lb/ft (kN/m)	18,500 x 30,000 (270 x 437)	19,000 x 32,500 (277 x 474)
Junction strength	GRI GG2-87	lb/ft (kN/m)	1080 (15.7)	956 (13.9)
Junction efficiency	GRI GG2-87	%	90	90
Carbon black	ASTM 4218	%	0.5	0.5

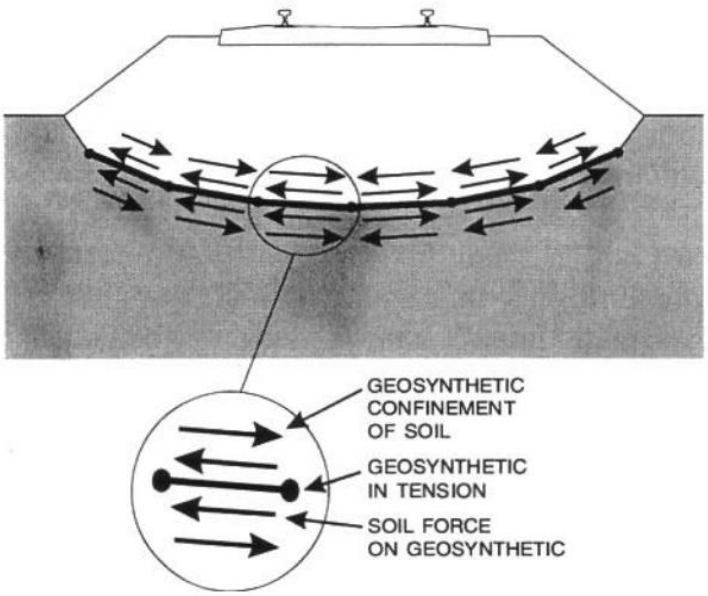

Figure 2-13 Reinforcing Effect of Geogrid [8].

There are four separate reinforcement mechanisms [10]. These reinforcement mechanisms are: Confinement of aggregates by the geogrid results in a reduction of lateral spreading, Confinement results in an increase in the lateral stress within the aggregate, thereby increasing its stiffness [10]. This reduces the dynamic (recoverable) deformation for each load cycle. An increase in the modulus of aggregate results in a reduction of vertical stress underlying subgrade. The effect is that the surface deformation will be less and becomes more uniform, a reduction in the shear stress within the subgrade leading to lower vertical strain. It is widely agreed that an appropriate stiffness and an ability to interlock effectively with the material is vital to achieving the reinforcing effect of a polymer geogrid. The geogrid works on the premise that the ballast penetrates the apertures and interlocks with the grid. This interlock leads to a strong horizontal shear resistance and restrains the ballast from lateral movement even when dynamic loading is applied. In practice, this means that the settlement rate is reduced.

2.5.3 Geocomposite in Track Application Consideration

Geocomposite is a composite material made from different geosynthetics products to serve their both functions simultaneously. In the railroad ballast, the geocomposite is usually comprised of a layer of geotextile bonded with the geogrid [30].

Figure 2-14 Use of Geocomposite at Subballast-Ballast Interface in Track [30].

Figure 2-14 above shows the layer of geocomposite being placed at subballast - ballast interface in a rail track at Bulli, New South Wales, Australia.

Under this chapter literature regarding an understanding of how a conventional rail track functions with an added focus on the behavior of ballast material and application of geosynthetic materials in railway track substructure were reviewed. The remainder of this thesis will examine and discuss the modeling and analysis of unreinforced and geogrid, geotextile, and geocomposite reinforced railway ballast with the aid of FEA package PLAXIS-2D.

CHAPTER 3 RAILROAD FINITE ELEMENT MODELLING

3.1 Introduction

The Finite Element Method (FEM) is the dominant discretization technique in structural mechanics. The basic concept in the physical interpretation of FEM is the subdivision of the mathematical model into disjoint (non-overlapping) components of simple geometry called finite elements. The response of each element is expressed in terms of a finite number of degree of freedom characterized as the value of unknown's functions at a set of nodal points. Three-dimensional modeling can incorporate complex longitudinal stress-strain distribution and cross-anisotropic behavior but often requires numerous input parameters and significant computational power [31]. In engineering practices, where possible, it is advantageous to simplify the complex 3D problems into equivalent two-dimensional (2D) plane strain such as railroad tracks where the longitudinal strain (ε_2) is negligible [31].

For the purpose of this thesis, a Finite Element based software PLAXIS is used. In order to predict the track behavior with and without geosynthetics, a numerical simulation was performed using a two-dimensional plane-strain Finite Element Analysis, i.e. (PLAXIS 2D), which has already demonstrated its success with limit analysis of geotechnical problems. A number of researchers like [4] used the two-dimensional (2D) plane strain FE modeling to simulate the dynamic response of ballasted railway tracks. Figure 3.1 shows a typical example of a 2D plane strain modeling of a ballasted railway track. The plane strain railway track modeling requires an assumption that the transversal profile of the track is consistent in the longitudinal direction. However, this is a gross approximation, since the longitudinal rail is discretely supported by the sleepers in the transverse direction of the track [5].

In this thesis, an equivalent method is used to approximate a discretely supported rail track structure (3-dimensional problem) to a 2-dimensional plane strain problem by idealizing the sleeper as a continuous member. This is because the plane strain railway track modeling requires an assumption that the transversal profile of the track is consistent in the longitudinal direction [32].

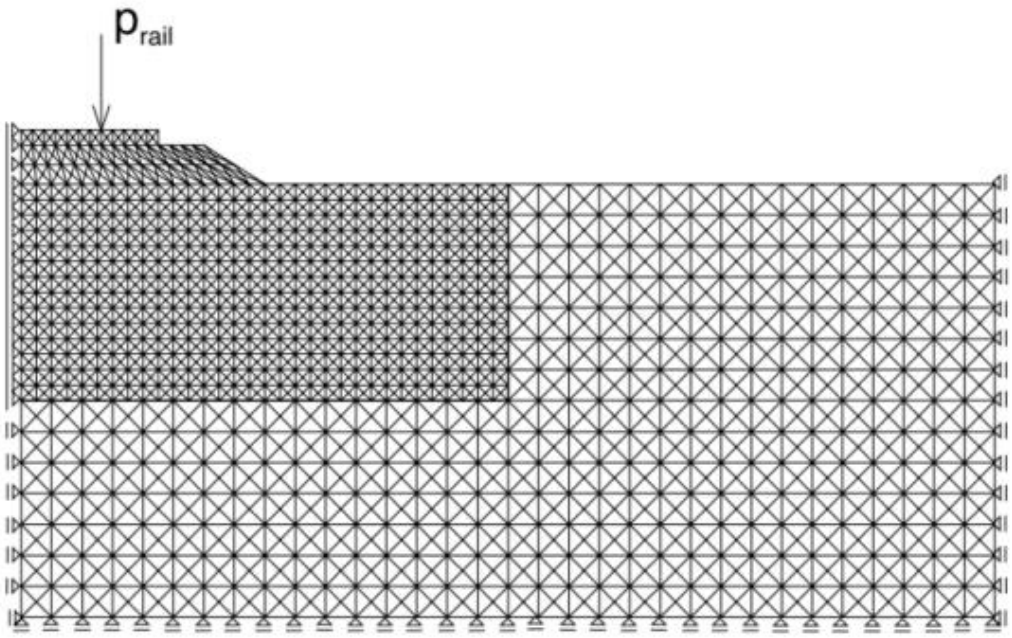

Figure 3-1 Example of a 2D plane strain FE modeling of the track and soil [5]

The use of FEM in geotechnical analysis, have emerged many methods of idealization. From the literature review, however, it is observed that the more popular method of idealizing the discretely placed member element is by converting the discrete member elements into the plane to simulate a plate with factored properties [6]. This method is applicable to methods of idealization of a discrete member element to plane strain member element for allowing the sleeper to be represented as a continuous member in the 2D plane strain calculations.

In this study, a discreet sleeper support track structure is converted to the continuous support system by equivalencing of strength and stiffness properties of the sleeper. The equivalent Young's modulus $\overline{E}_{sl}$ of the sleeper is determined from the original Young's modulus E_{sl}, the width of the sleeper b_{sl} and the distance between sleepers d_{sl} [7]. Using this strength and stiffness parameters a typical plane strain track model with three different types of geosynthetics: geotextile, geogrid and geocomposite were numerically simulated by Finite Element discretization and compared with the behavior of unreinforced track embankment. The selection of the material properties, loading of the track and Finite Element Analysis (FEA) are presented. The parameters observed during numerical simulation include vertical displacement (track settlement), subgrade stress and subgrade

stress strain curve. Furthermore, a comparison between unreinforced track and track reinforced with geotextile, geocomposite, and geogrid has been made.

3.2 Project Description

The Addis Ababa/Sebeta – Port of Djibouti railway line starts at the highlands of Ethiopia and traverses along the rift valley and terminates in the low lands of Djibouti. The landform and terrain condition varies from highland and plateau in Ethiopian to return plain land in Djibouti [33]. Except in a few undulating sections, most of the railway line can be considered flat terrain with acceptable altitude differences [33].

The strata along the railway line are largely covered with tertiary-quaternary basalt, trachyte, tuff, volcanic lava and Mesozoic sedimentary rocks and Paleozoic substratum are sparsely exposed [33]. Covering soils are mainly hard plastic-like black cotton soil, silty clay and soft soil with large thickness differences [33].

The railway line has been built in areas of the highland terrace, shallow hill, and plain, with wide terrain and small undulating in some sections. There is basically no natural disaster and major unfavorable geological features such as landslide, collapse, debris flow, coal bed and gob along the whole line [34] Main engineering geological problems are seismic faults, expansive soils, loose rock, and bedrock soft interlayer, unstable slope and soft soil [35].

key parameters and dimensions are [35].

- Loading capacity 70 t
- Dead weight 25 t
- Design Speed 120 km/h

The technical parameters of the bogie used in this thesis are [35].

- Fixed Wheel Base 1830 mm
- Wheel Diameter 840 mm
- Railway Gauge 1435 mm
- Axle Load 25 t

- Design speed 120 km/h

According to [18] the current practice for designing the railway track is based upon satisfying several criteria for the strength of individual components. Some of these criteria are: allowable rail bending stress, allowable sleeper bending stress, allowable ballast pressure and allowable subgrade pressure

3.2.1 Loading

The nominal vehicle axle load is usually measured for the static condition; however, the vertical load can be much greater or much smaller than the nominal value due to the inertial effects of the moving train traveling over varying geometry on a track with defects [9]. The passage of trains over the track causes the initial track geometry to deform. The inertia of the moving train causes the vertical wheel force to vary above and below the nominal wheel load. The major factors that influence the magnitude of the dynamic vertical forces are nominal wheel load, train speed, wheel diameter, vehicle unsprung mass, smoothness of the rail and wheel surfaces, track geometry and track modulus or vertical track stiffness [9]. Therefore, in the design of the railway track, the actual stress in the various components of the track structure and in the rolling stock must be determined from the dynamic vertical and lateral forces imposed by the design vehicle moving at speed. According to [29] the dynamic wheel load increases the rail stress values above those of the static condition because of lateral bending of the rail, eccentric vertical loading, transfer of the wheel loads due to the rolling action of the vehicles, vertical impact of wheel on the rail due to speed, Irregularities and non-uniformities in the track and the wheel and rail profiles.

The traditional approach for representing the geometry-driven dynamic wheel load is to multiply the nominal wheel load by an impact factor, ϕ which is a percentage increase over static vertical loads intended to estimate the dynamic effect of wheel and rail irregularities . The impact factor recommended by AREMA (2003, chap. 16) is a function of the train travel speed and the wheel diameter, as given in equation 3-2.

$$P^D = \phi P_s \quad (3\text{-}1)$$

Where: P^D is design wheel load (kN), P_s is static/nominal wheel load (kN) and ϕ is dimensional impact factor (always >1).

$$\phi = 1 + 5.21 * \frac{V}{D} \quad (3\text{-}2)$$

Where: V is Design Speed $\left(\frac{km}{h}\right)$ and D is Wheel Diameter (mm)

Hence: $P_s = \frac{\text{axle load}}{2} = \frac{25\ t * 1000\ \frac{kg}{t} * 9.81\ \frac{m}{sec^2}}{2} = 122600\ N = 122.6\ kN$

$$\phi = 1 + 5.21 * \frac{120\ \frac{km}{hr}}{840\ mm} = 1.75$$

Design wheel load, $P^D = \phi P_s = 1.75 * 122.6\ kN = 214.6\ kN$

Percentage of axle load (distribution factor, DF) carried by a single tie = 50%

$$q_r = 0.5 * P^D = 0.5 * 214.6\ kN = 107.3\ kN$$

3.2.2 Geometry and Cross-Section

In this section, the components of a typical section of track substructure: Ballast Shoulder Width (BSW), Side Slope (BSS), Ballast & Sub-ballast depth with recommended values in AREMA are presented. Each component of the track section is shown in Figure 3-2.

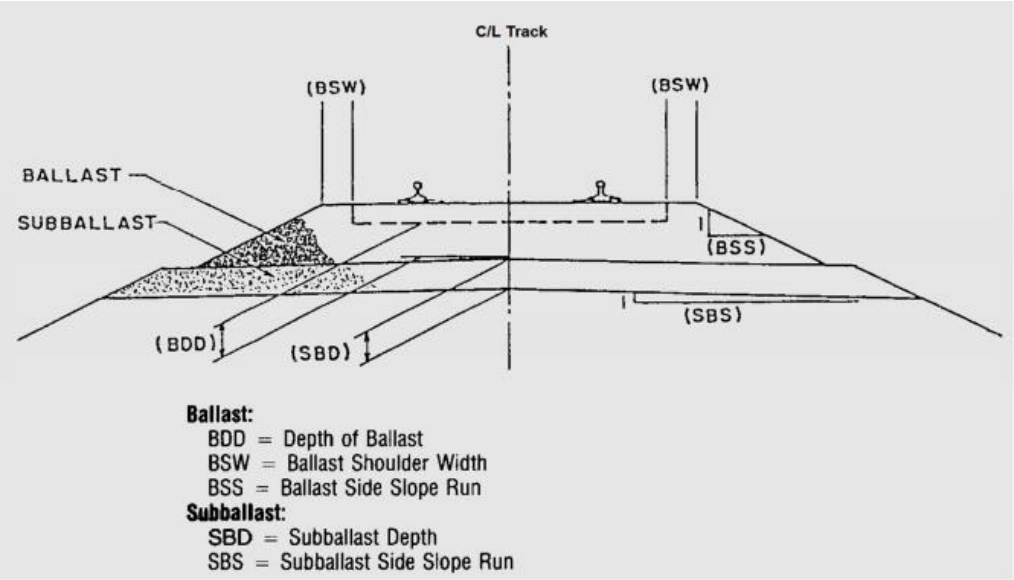

Figure 3-2 Typical Section of Track Substructure [18]

Ballast Shoulder Width (BSW): For Standard Gage construction of continuous welded rail in main track service, AREMA (2.1.1.5.2.2) recommends a value for BSW of not less than 12 inches (300mm).

Side Slope (BSS): AREMA (2.1.1.5.2.3) The Side Slope run component of the Ballast Section is designed to provide a confining pressure for the Ballast Section that is expected to transmit the vertical load from the bottom of the cross-tie to the top of the sub-ballast layer. The BSS run component is measured in the plane of the top of the cross-tie, and the rise component is measured perpendicular to the run component. A BSS value of 2:1 is commonly used.

Ballast and Subballast Depth

- Ballast pressure

According to AREMA 4.1.2.5.1.1, a tie-to-ballast pressure is not uniformly distributed along the bottom of a cross tie; The average pressure at the bottom of the tie is equal to axle load, modified by distribution and impact factors, and divided by the bearing area of the tie:

$$p_a = \frac{q_r}{A} \tag{3-3}$$

Where: p_a is an average ballast pressure, q_r is a rail seat load (N), and A is a bearing area of the cross tie which is equal to (1/3 of the total base area) (mm^2)

Average ballast pressure, $p_a = \frac{107.3*10^3}{314560} = 0.34 \text{ MPa} < 0.586 \text{ MPa}$

As AREMA 4.1.2.5.1.1 states, the recommended ballast pressure should not exceed 85 psi (0.586 MPa) for high-quality, abrasion-resistant ballast. If lower quality ballast materials are used, the ballast pressure should be reduced accordingly.

In accordance with the UIC classification, the behavior of the subgrade may macroscopically be characterized by and classified as follows [36].

- Low settlements and very good support of train loads. This subgrade is designated as S_3

- Medium behavior in settlement and non-satisfactory support of loads. This subgrade is designated as S_2.
- Large settlements and non-satisfactory support of loads. This subgrade is designated as S_1.
- Extensive settlements and a very bad performance in withstanding loads. The quality of such a subgrade is designated as S_0.

For ease of comparison two cases are considered:

- Excellent subgrade: based on maximum allowable subgrade pressure recommended by AREMA with a pressure of 25 psi (0.172 MPa) or CBR between 20 % and 30 %.
- Poor subgrade: assume loose to medium dense sand; firm to stiff clays and silts; alluvial fills. Assume allowable pressure of 6.94 psi (0.10 MPa) is adopted.

The AREMA design manual (2010) indicates that the load distribution through a roadbed structure is approximately the same regardless of the relative thickness of the subballast and ballast layers. Therefore, the combined depth of sub-ballast and ballast is calculated as a single unit to ensure that the pressure imposed on the subgrade does not exceed the allowable bearing pressure for a particular set of subsoil conditions. The most notable and most widely used empirical relationship is the equation recommended and developed by Talbot (1919). According to him the maximum vertical pressure σ_z(kPa) under the rail seat for any particular ballast depth is defined as:

$$\sigma_z = P_a \left[\frac{1}{5.9\, z^{1.25}}\right] \tag{3-4}$$

$$Z_{min} = \left[\frac{P_a}{5.9\, \sigma_z}\right]^{\frac{4}{5}} \tag{3-5}$$

Where: P_a is an average uniform pressure between the sleeper and the ballast in (kPa) and z is ballast depth in (m)

Thus for the first case of excellent subgrade

$$Z = \left[\frac{340}{5.9 * 172}\right]^{\frac{4}{5}} = 0.41 \text{ m}$$

For the second case of poor subgrade

$$z = \left[\frac{340}{5.9 * 100}\right]^{\frac{4}{5}} = 0.62 \text{ m}$$

AREMA (2.1.1.5.3) recommends a minimum value of 6 inches (152 mm) compacted sub-ballast layer to perform the separation of layers and shielding of the roadbed from weather functions.

3.3 Finite Element Analysis

The numerical analysis can be used to determine the impact of different types of geosynthetic materials: geogrid, geotextile, and geocomposite, on-track performance. In this study, the construction of a Finite Element Model was conducted in PLAXIS 2D using several sources for the geometry of the track segment. This 2D model will provide insight into whether the use of these geosynthetic materials influence the performance of the railroad structure.

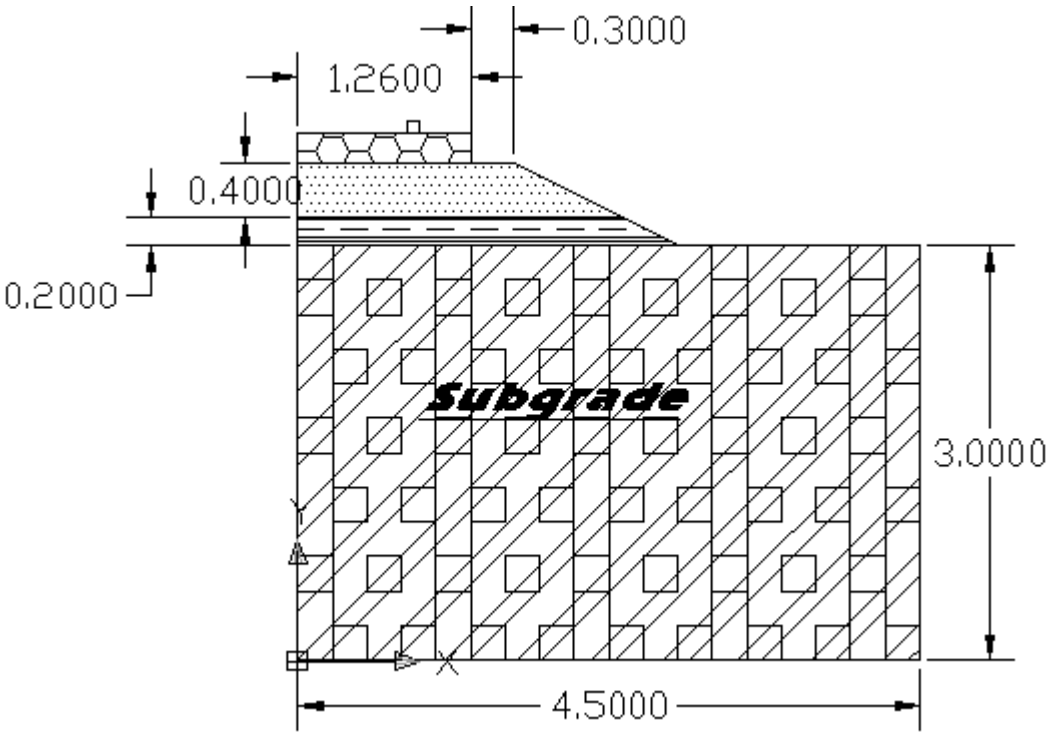

Figure 3-3 Geometry of the Half-Track Section

For the purpose of this thesis, a 3 m high and 4.5 m wide plane strain geometric of half-track section i.e. half of the geometry of the track section as shown in (Figure 3-3) is modeled with and without geosynthetics using PLAXIS 2D.

A series of Finite Element Analysis of ballasted railroad embankment were conducted: unreinforced ballast embankment used as control, and ballast embankment reinforced with geogrid, geotextile, and geocomposite. For the purpose of obtaining, an optimum location of geosynthetic, embankment reinforced with geogrid is modeled more than two times. One is when the geogrid is placed at the ballast-subballast interface and the others are when geogrid is placed within the ballast layer.

3.3.1 Assumptions

Throughout the analysis, the following assumptions have been made.

- For ease of simplification symmetry of the system is considered;
- The analysis is completely quasi-static and considers vertical track force only;
- The effect of wind, curving, and hunting of the bogies is excluded or lateral and longitudinal forces are not incorporated.

3.3.2 Symmetry

The appropriate use of symmetry will often expedite the modeling of a problem. The use of symmetry allows us to consider a reduced problem instead of the actual problem; hence a reduced number of finite elements needed to represent it. In this thesis due to symmetry in geometry, construction sequence, materials, ground and loading conditions, only one half of the track section is considered in the numerical model (Figure 3-3).

3.3.3 Material Properties

The material properties used for FEA are from manuals, manufacturer's specifications and actual design specification of the Addis Ababa/Sebeta-Djibouti railway project.

Rail: In this analysis, the rail is simplified as a square element with a cross-section dimension of 83.5 mm x 83.5 mm. The rail is simulated using a linear elastic model with a nonporous material type. A linear elastic model is too limited for the simulation of the soil behavior and it is primarily used for stiff structures like reinforced concrete and steel structures that are found within the soil [37].

Table 3-1 Rail dimensions for FEM Analysis, a Rail Profile of UIC54 [34]

Section weight Kg/m	54.77
Rail height mm	159.00
Head width mm	70.00
Web thickness mm	16.00
Foot width mm	140.00
Moment of inertia, I_{XX} (cm^4)	2337.90

Concrete sleeper: In the ballasted railway track, the longitudinal rail is discretely supported by the sleepers in the transverse direction of the track. However, the plane strain railway track modeling requires an assumption that the transversal profile of the track is consistent in the longitudinal direction[32] In this study, the sleeper is idealizing as a continuous member of the plane with a simplified dimension of a rectangular element with a length of 2.52 m and a width of 0.211 m. These are driven from the given dimensions in Table 3-2 (sleeper type B58). The material model used to simulate a concrete sleeper is also a linear elastic model with a nonporous material type.

Table 3-2 Sleeper Dimensions for FEM analysis [34]

Parameters	Value
Concrete volume	Approximately 0.127 m^3
Length	2520 mm
Width	300 mm
Sleeper height	233 mm
Height of center of the rail base	225 mm
Height sleeper center	175 mm
Support surface (total)	639.2 cm^3

The use of FEM in geotechnical analysis, have emerged many methods of idealization. From the literature review, however, it is observed that the more popular method of idealizing the discretely placed member element is by “converting” the discrete elements into the plane to simulate a plate with factored properties [6]. This method is applicable to methods of idealization of a discrete member element to the plane strain member element. This allows the sleeper to be represented as a continuous member in the plane and hence enable 2D plane strain calculations.

Converting a discrete support system to the continuous support system requires a comparison and subsequent equivalencing of strength and stiffness properties of the sleeper [6]. The equivalent Young’s modulus $\overline{E}_{sl}$ of the sleeper is determined from the

original Young's modulus E_{sl}, the width of the sleeper b_{sl} and the distance between sleepers d_{sl} [7].

$$\overline{E}_{sl} = \frac{E_{sl}\, b_{sl}}{d_{sl}} \tag{3-6}$$

$$\overline{E}_{sl} = \frac{36000\ \text{MPa} * 0.211\ \text{m}}{0.6\ \text{m}} = 12660\ \text{MPa}$$

The sleeper mass m_{sl} is used to calculate a uniformly distributed mass

$$\overline{m}_{sl} = \frac{m_{sl}}{d_{sl}} \tag{3-7}$$

$$\overline{m}_{sl} = \frac{2300\ \frac{\text{kg}}{\text{m}^3} * 0.211\ \text{m}}{0.6\ \text{m}} = 808.834\ \frac{\text{kg}}{\text{m}^3}$$

Ballast: The material model used to simulate the behavior of ballast material is a Mohr-Coulomb model. The Mohr-Coulomb model which is a linear elastic perfectly plastic soil model is the first approximation of the soil behavior [37]. The PLAXIS manual [37] states that the linear elastic part of the Mohr-Coulomb model is based on Hooke's law of isotropic elasticity and the perfect plastic part is based on the Mohr-Coulomb failure criterion, formulated in a non-associated plasticity framework.

Sub-ballast: In this study, the material model used to simulate the sub-ballast behavior is the Mohr-Coulomb model. This model is a simple and well-known linear elastic-perfectly plastic model and it can be used as a first approximation of soil behavior [37]. This model requires a total of five parameters: Young's Modulus, E; Poisson's ratio, v; Cohesion, c; Friction angle,∅ and Dilatancy angle, ψ [37].

The values of Young's Modulus for ballast and subballast materials as recommended by AREMA are to be within the range of 150 to 200 MPa. Therefore, in this study, the values of young's Modulus for ballast and subballast materials are taken to be 150 MPa and 170 MPa respectively.

The shear strength parameter , friction angle of both the ballast and sub-ballast layer are not available in the actual site condition. So the friction angles can be obtained from the chart given in Figure 3-4 using the dry density and the relative density of the ballast and subballast that are calculated from the given equations. The relative density of subballast

and ballast are calculated using equation 3.8 and the dry density of both ballast and subballast are also calculated using equation 3-9 [38].

$$D_r = \frac{(e_{max} - e)}{e_{max} - e_{min}} \quad (3\text{-}8)$$

Where e_{max} and e_{min} are the void ratio at loosest and densest condition respectively and e is the current void ratio. The current void ratio is assumed to be between the void ratio of the loosest and densest condition and it is taken to be 0.56 for subballast and 0.54 for ballast. The void ratio at loosest and densest conditions is 0.68 and 0.53 respectively as presented in Table 3.3.

$$\gamma_{dry} = \frac{\gamma_{bulk}}{1+w} \quad (3\text{-}9)$$

Where γ_{bulk} and γ_{dry} are the bulk and the dry unit weight of the ballast or subballast respectively and w is the water absorption, which is the weight of water absorbed by the particle divided by the dry particle weight in percentage. As recommended by AREMA specifications for the ballast aggregate characterization tests the maximum Absorption is provided as 1% and this is used to calculate the dry unit weight.

- Subballast

$$D_r = \frac{0.68 - 0.56}{0.68 - 0.53} = 0.8 \ = 80\%$$

- Ballast

$$D_r = \frac{0.68 - 0.54}{0.68 - 0.53} = 0.8 \ = 93.33\%$$

Since the unit weight of ballast and subballast are equal the dry unit weight for both layers is calculated as

$$\gamma_{dry} = \frac{22\ kN/m^3}{1 + 0.01} = \ 21.78\ kN/m^3 \ = 135\ lb/ft^3$$

So from the chart given in Figure 3.4 for the dry density of $135\ \mathrm{lb/ft^3}$ and relative density of 80%, the friction angle, ∅ of the subballast, is found to be 42^0.

For the dry density of $135\ \mathrm{lb/ft^3}$ and a relative density of 93.33% the friction angle of ballast, ∅ is found to be about 45^0.

Table 3-3 Unit weight/volume relationships of ballast [38]

Ballast condition	Unit weight (lb/ft^3)	Void ratio	Void volume (%)
Loose	95	0.68	41
Compact	110	0.53	35
Moderately fouled	125	0.35	26
Heavily fouled	135	0.25	20

Source: Sussmann, T.R. et al., J. Transport. Res. Board, 2289, 87–94, 2012

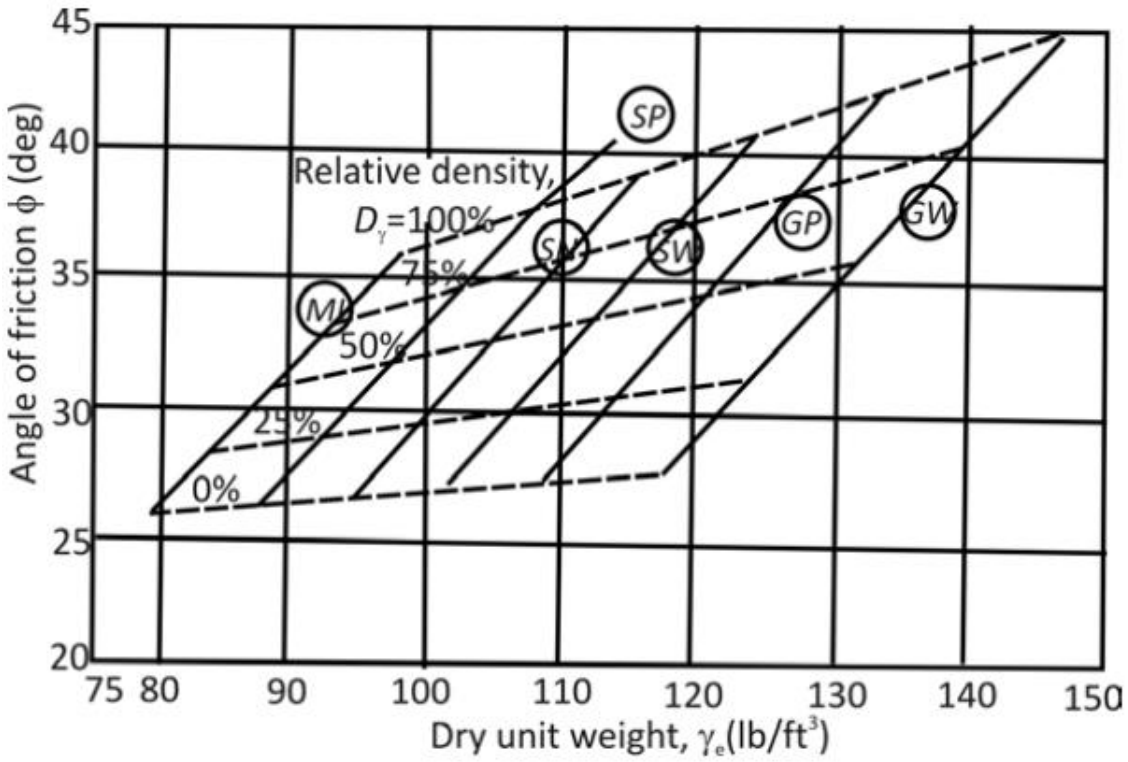

Figure 3-4 Range of relative density and the corresponding range of angle of friction for coarse-grained material [38]

Sub-grade: The sub-grade behavior of the track is also simulated using a Linear Elastic-Perfectly Plastic soil model (Mohr-Coulomb model). The type of subgrade used in this study is silty clay and this is the type of subgrade that exists at the chainages DK29+268.01 - DK29+955 along the route of Addis/Sebeta-Djibouti railway project. The material and constitutive models used for each component of the track layer are given in Table 3-4.

Table 3-4 Parameters of Railway Track Layers Used in Finite Element Analysis [18]

Parameters	Rail	Concrete sleeper	Ballast	Sub-ballast	Subgrade
Model	LE	LE	MC	MC	MC
Material type	Non- porous	Non- porous	Drained	Drained	Drained
$\gamma(kN/m^{3)}$	76	23	22	22	18
$\gamma_{equivalent}(kN/m^{3)}$	76	8.088	22	22	18
V	0.3	0.3	0.3	0.3	0.25
E(MPa)	206,000	36,000	170	150	30
$E_{equvalent}$ (MPa)	206,000	12660	170	150	30
c $(kN/m^{2)}$	-	-	0	0	24
∅ (degrees)	-	-	45	42	12
ψ (degrees)	-	-	15	12	0

Where, MC = Mohr Coulomb model, LE = Linear Elastic model, γ = unit weight, ν = Poisson's ratio for loading conditions, c = effective cohesion, ∅ = effective friction angle, ψ = dilatancy angle.

Geosynthetics: In this study, the three geosynthetics materials: geogrid, geotextile, and geocomposite are modeled in PLAXIS under the geogrid dataset with their specific normal (axial) stiffness. The dimensions and properties of the geosynthetics are selected based on the recommendations stated in AREMA and based on tested dimensions from literatures.

Geotextile: A woven geotextile offers adequate permeability to rapidly dissipate the excess pore pressures (if generated) in the track [17].

Geogrid: The geogrid used in this study is a bi-oriented geogrid that is made of polypropylene and manufactured by extrusion and biaxial orientation to enhance its tensile properties. This geogrid has high tensile strength, high elastic modulus, and strong resistance to construction damage and environmental exposure [1]. AREMA section 10.6 recommended that for subballast layers the aperture size of the geogrid does not exceed the average (D_{50}) particle size of the fill materials. For ballast layers, however, researchers have shown that a larger aperture geogrid (greater than 1.7 inches (43.18 mm) provides strong mechanical interlock with coarse ballast grains and this always leads to optimum performance.

Geocomposite: A geogrid-geotextile composite is manufactured by bonding the geogrid with a nonwoven geotextile. This composition enables the geocomposite to provide both the reinforcement function and filtration and separation functions [1]. In a geocomposite, the geogrid gives a strong mechanical interlock within the ballast grains and produces reinforcement, whereas the non-woven geotextile provides filtration and separation, and allows partial in-plane drainage.

3.3.4 Axial Stiffness of Geosynthetics

Geosynthetics are tensile reinforcing elements (geotextiles, geogrids, and geocomposite) defined by their starting and endpoints and by the axial (normal) stiffness J_z (kN/m) [39]. The axial normal stiffness of geosynthetics always differs by the factors of the aperture dimensions, the tensile strength of the manufacturing material and the rib thickness.

The minimal (initial) axial stiffness of geotextiles from a short-term experiment (load rate according to EN ISO 10 319) for x-%-strain is given by

$$J_{\varepsilon=X} = E.A = \frac{T_{\varepsilon=X}}{\varepsilon} \tag{3-10}$$

where: $\varepsilon - x\% - \text{strain(relative extension)according to EN ISO 10319}$

According to [39] the maximum (theoretically attainable) axial stiffness of geotextiles for a short-term axial strength is determined as follows

$$J_{\varepsilon\,max} = E.A = \frac{T_{max}}{\varepsilon_{max}} \tag{3-11}$$

where: $\boldsymbol{\varepsilon_{max}}$ is a maximum strain (relative Extention) according to EN ISO 10319

In order to evaluate the performance of the three types of geosynthetics materials: geogrid, geotextile, and geocomposite the axial (normal) stiffness of each geosynthetic material is calculated using Eq. 3.10 by assuming a 2% strain and using the corresponding tensile strength. The tensile strength of each geosynthetic material: geotextile, geogrid and geocomposites are given in Table 3-4.

Table 3-5 Tensile Strength of the Three Geosynthetic Materials [17]

Geosynthetic materials	Tensile strength at 2 % strain (kN/m)
Geogrid	10.5
Geotextile	7.2
Geocomposite	12

Geogrid: $J_{\varepsilon=X} = E.A = \frac{T_{\varepsilon=X}}{\varepsilon} = = \frac{10.5\ kN/m}{0.02} = \quad 525\ kN/m$

Geotextile: $J_{\varepsilon=X} = E.A = \frac{T_{\varepsilon=X}}{\varepsilon} = = \frac{7.2\ kN/m}{0.02} = 360\ kN/m$

Geocomposite: $J_{\varepsilon=X} = E.A = \frac{T_{\varepsilon=X}}{\varepsilon} = = \frac{12\ kN/m}{0.02} = 600\ kN/m$

3.3.5 The Idealization of Two-Dimensional Railway Substructure

To fulfill the computational requirements of more refined mesh the 3 m high and 4.5 m wide track embankment is modeled with 1.435 m gauge length, 0.3 m shoulder width of ballast and a 1:2. side slope of the rail track embankment. The boundary effects are generally considered small due to symmetry. The axial wheel load is simulated as a line load representing an axle trainload of 25 tones with a dynamic impact factor of 1.75, (calculated from Equation 3.1).

3.3.6 Elements

The subgrade soil and track layers were modeled using 15-node linear strain triangular elements, which provides a fourth-order interpolation for displacements and the numerical integration by Gaussian integration scheme involves twelve Gauss points (stress points).

3.3.7 Boundary Conditions

The nodes along the bottom boundary of the section were restrained in both vertical and horizontal directions (standard fixities). The left and right boundaries were restrained in the horizontal direction to represent smooth vertical contacts and to prevent lateral displacement in the x-direction. The bottom boundaries were also restrained in both vertical and horizontal directions from any displacement.

3.3.8 Geogrid and Interface in PLAXIS Software Package

Geogrids: Slender structures with a normal stiffness but with no bending stiffness**,** are used to model soil reinforcements. Its material property is an elastic normal (axial) stiffness EA. which can be specified in the material database. When 15-node soil elements are employed then each geogrid element is defined by five nodes whereas 3-node geogrid elements are used in combination with 6-node soil elements. Axial forces are evaluated at the Newton-Cots stress points, which coincide with the nodes the location of the nodes and stress points in geogrid elements are indicated in Figure 3-4.

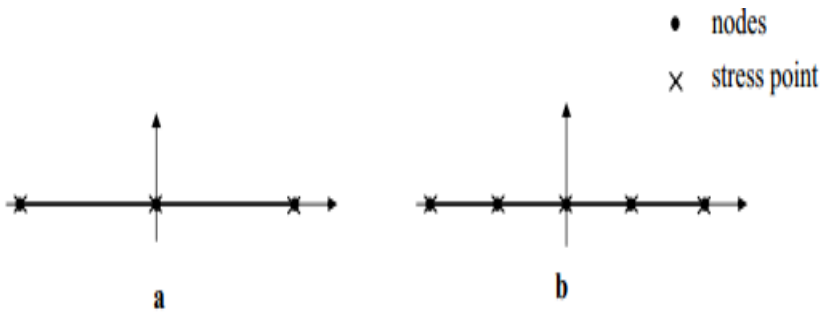

Figure 3-5 Positions of Nodes & Stress Points in 3 and 5 Node Geogrid Elements [36]

Interfaces: are composed of interface elements when using 15-node soil elements, the corresponding interface elements are defined by five pairs of nodes, whereas for 6-node soil elements the corresponding interface elements are defined by three pairs of nodes. Figure 3-5 shows how to connect the interface elements with soil elements.

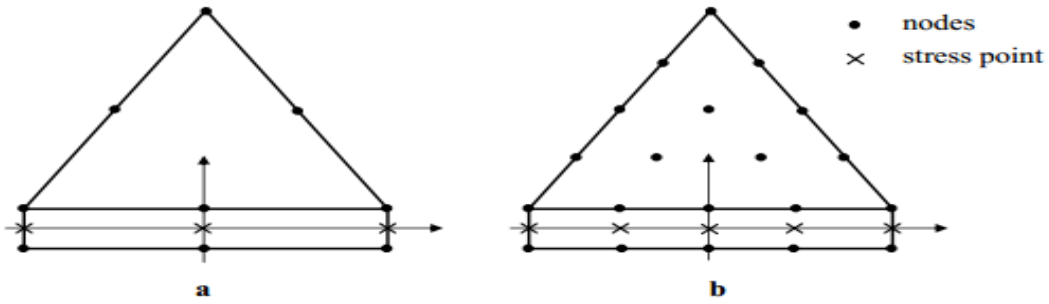

Figure 3-6 Interface Elements & Their Connection to Soil Elements [36]

In this thesis, zero-thickness fully bounded interface elements, which are available in PLAXIS 2D 8.2 were used to model the frictional behavior between the reinforcement and the ballast and subballast layer. This interface is simulated by five-node line elements and it can still capture the interface strength through the effective friction angle at the interface, which will be lower than the maximum interparticle friction or dilation angle at low confining pressure. The role of this aggregate-geogrid interaction is captured through the strength-reduction factor R_{int} obtained as [37].

$$\tan \emptyset'_{\text{int}} = \text{R}_{\text{int}} * \tan \emptyset'_{\text{m}} \quad (3\text{-}12)$$

Where: $\emptyset_{int}$ is an effective friction angle of the interface. However In this study, R_{int} is assumed to be 2/3 for the ballast-geogrid and sub-ballast-geogrid interface.

3.3.9 Meshing

The unreinforced track model in Figure 3-7 consisted of 2079 elements and 16915 nodes and the reinforced track model in Figure 3-8 consists of 2735 elements and 24049 nodes.

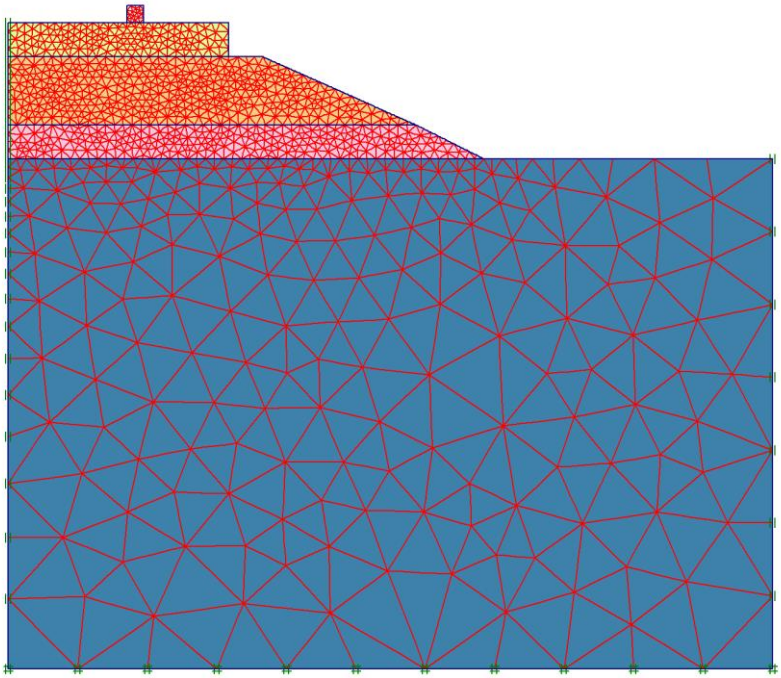

Figure 3-7 Mesh of Unreinforced Ballasted Railway Track Embankment, PLAXIS 2D

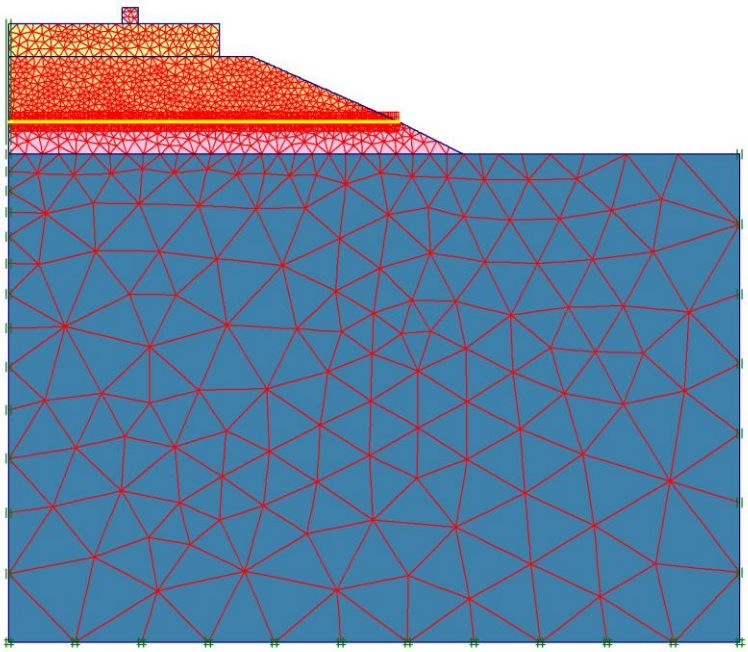

Figure 3-8 Mesh of Reinforced Ballasted Railway Track Embankment , PLAXIS-2D

CHAPTER 4 ANALYSIS RESULTS AND DISCUSSIONS

4.1 Discussion of Results

In this section, the results obtained from the Finite Element Modeling in PLAXIS are presented.

A series of static analyses have been carried out: -

- Unreinforced ballast embankment,
- Ballast embankment reinforced with geogrid
- Ballast embankment reinforced with geotextile
- Ballast embankment reinforced with geocomposite
- Ballast embankment reinforced with geogrid at the ballast-subballast interface and within the ballast layer at a depth of 150 mm, 200 mm, 250 mm, 300 mm and 350 mm below the sleeper are modeled for the purpose of obtaining an optimum location of a geogrid for its threshold depth.

The parameters like track settlement and subgrade stress and strain level are analyzed. The analysis results for track settlement (vertical settlement) and subgrade stress are presented hereunder.

I. Unreinforced Ballast Embankment

Figure 4-1 illustrates the analysis output from PLAXIS for unreinforced ballast embankment settlement versus depth of the track. As can be seen from this figure; the deformation is 8 mm at the point of load application and gradually decreases to zero.

The analysis output from PLAXIS for the variation of vertical track settlement within the depth of the unreinforced ballast layer is shown in Figure 4.2 and the full analysis results are presented in Appendix-b. As can be seen from this figure; the track settlement is gradually decreased from 6.9 mm at the top surface of the ballast layer to 6 mm at the bottom surface of the subballast layer or top surface of the subgrade layer.

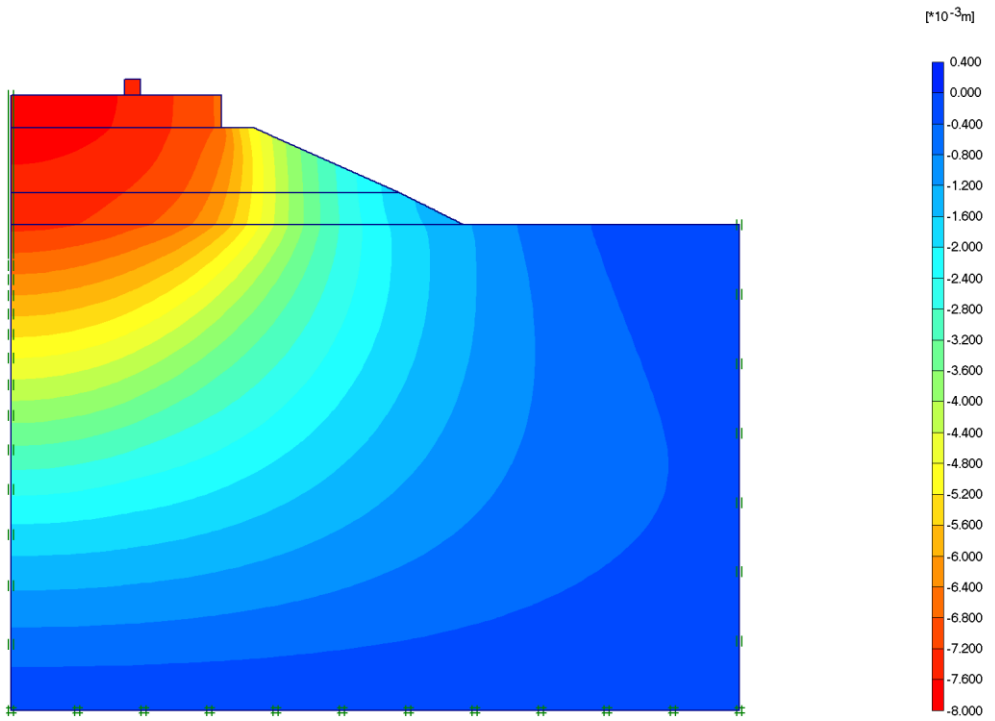

Figure 4-1 Vertical Displacement within the Depth of Unreinforced Ballasted Track

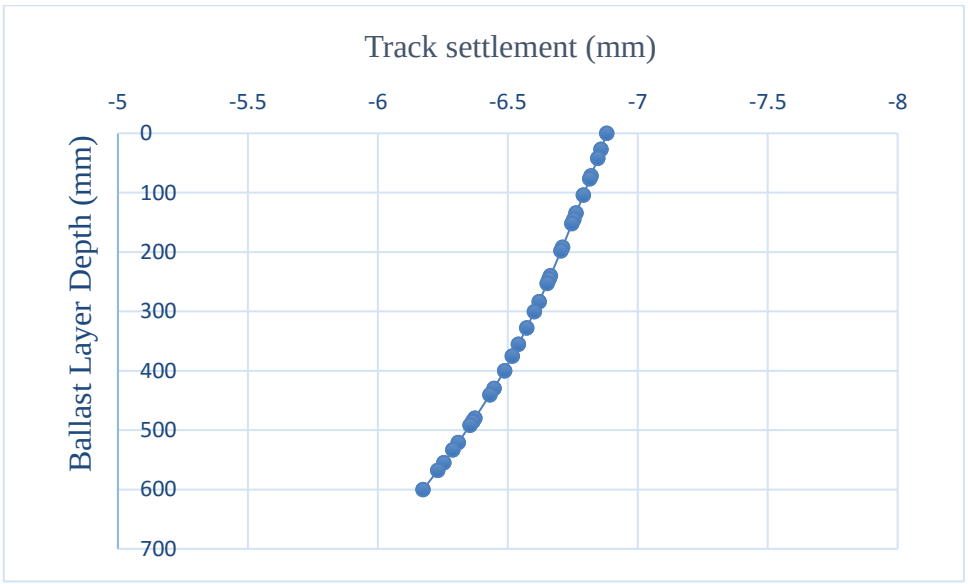

Figure 4-2 Variation of vertical displacement within the depth of unreinforced ballast layer

Figure 4.3 shows the analysis output from PLAXIS for unreinforced ballast embankment subgrade stress (load transmitted underneath the ties) as a function of the depth of the track. As can be seen from this figure; the subgrade stress is 49.3 kPa at the sub-ballast-

subgrade interface and gradually decreases to 24 kPa at a depth of 3 m below the bottom of the ballast.

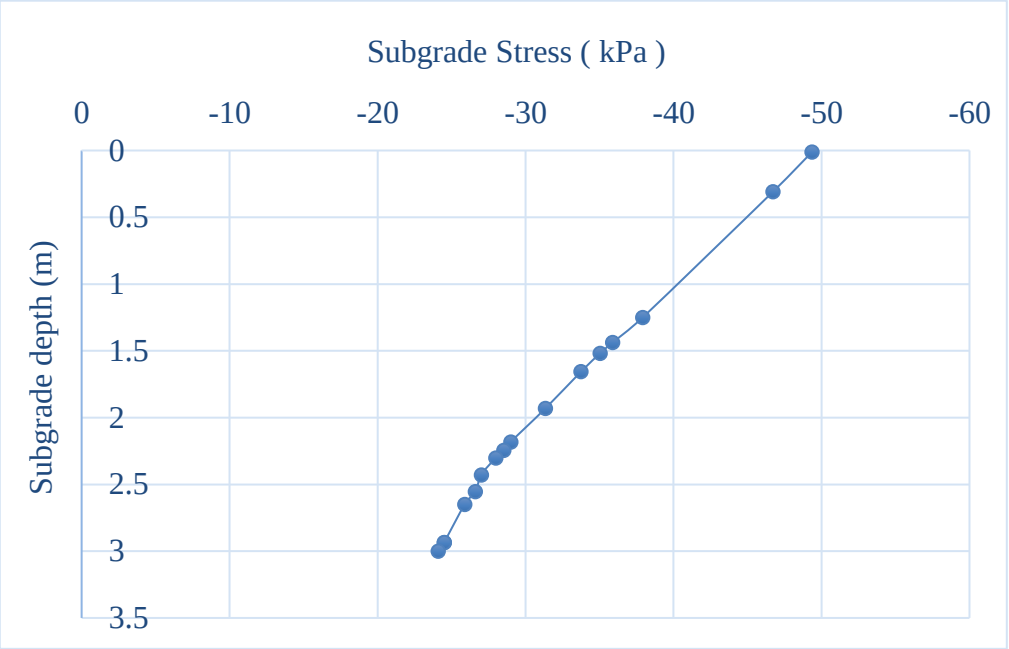

Figure 4-3: Subgrade Stress Versus Track Depth of Unreinforced Ballast, PLAXIS

II. Ballast Embankment Reinforced with Geotextile

For ballast embankment reinforced with geotextile, the output of the Finite Element Analysis from PLAXIS for the variation of vertical settlement throughout the track depth is illustrated in appendix c. As can be seen from the figure; the deformation is 6.4 mm at the point of load application and gradually decreases to zero

The vertical displacement within the depth of the geotextile reinforced ballast layer is also shown in Figure 4-4 and the full analysis result is presented in appendix c. The vertical track settlement is varied with the depth of the ballast layer. As can be seen from this figure; the track settlement is gradually decreased from 6.1 mm at the top surface of the ballast layer to 5.4 mm at the bottom surface of the subballast layer or top surface of the subgrade layer.

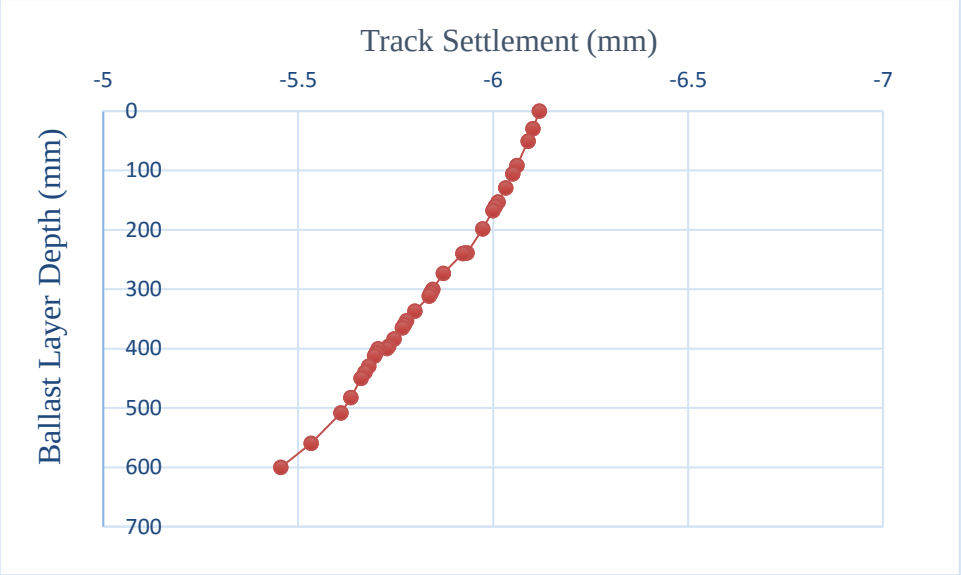

Figure 4-4 Vertical Displacements within the Depth of Geotextile Reinforced Ballast Layer

Figure 4.5 shows the analysis output from PLAXIS for geotextile reinforced ballast embankment subgrade stress (load transmitted underneath the ties) as a function of the depth of the track. As can be seen from this figure; the subgrade stress is 39.5 kPa at the sub-ballast-subgrade interface and gradually decreases to 18 kPa at a depth of 3 m below the bottom of the ballast.

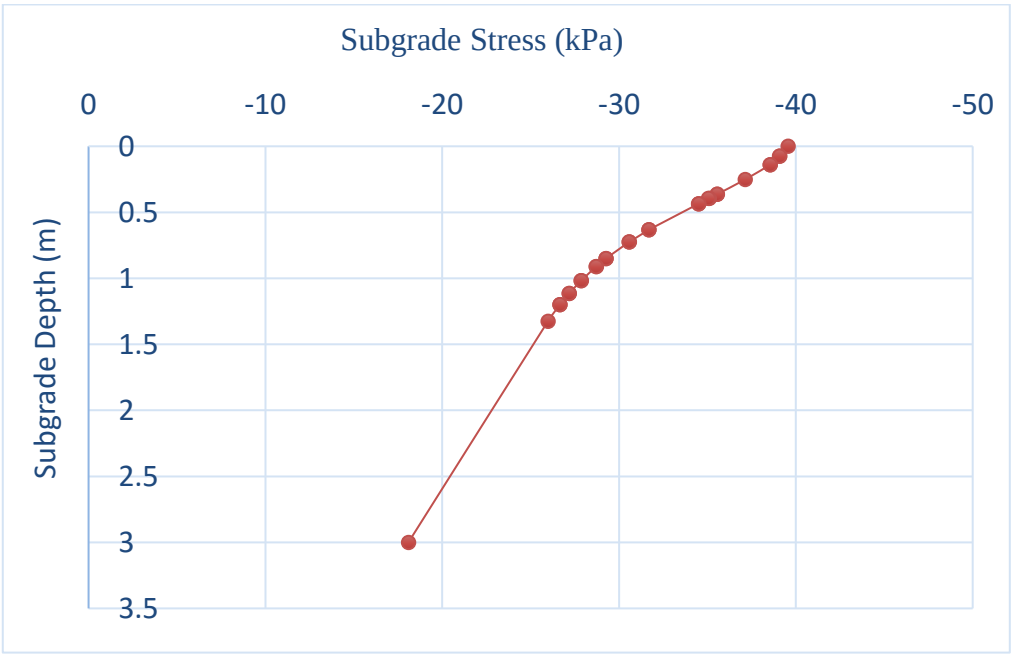

Figure 4-5: subgrade stress versus track depth of geotextile reinforced ballast, PLAXIS

III. BALLAST Embankment Reinforced with Geogrid

The analysis output from PLAXIS for geogrid reinforced ballast embankment settlement versus depth of the track is illustrated in Appendix-d. The location of maximum deformation is assumed to be at the track center which is in line with the point of wheel load application. As can be seen from the figure; the deformation is 5.2 mm at the point of load application and gradually decreases to zero.

Figure 4-6 illustrates the analysis output from PLAXIS for geogrid reinforced ballast embankment settlement versus depth of the track and the full analysis result is presented in Appendix-d. As can be seen from this figure the track settlement is gradually decreased from 4.95 mm at the top surface of the ballast layer to 4.3 mm at the bottom surface of the subballast layer, or top surface of the subgrade layer (which are less than the magnitude of the track settlement in unreinforced and geotextile reinforced track embankment).

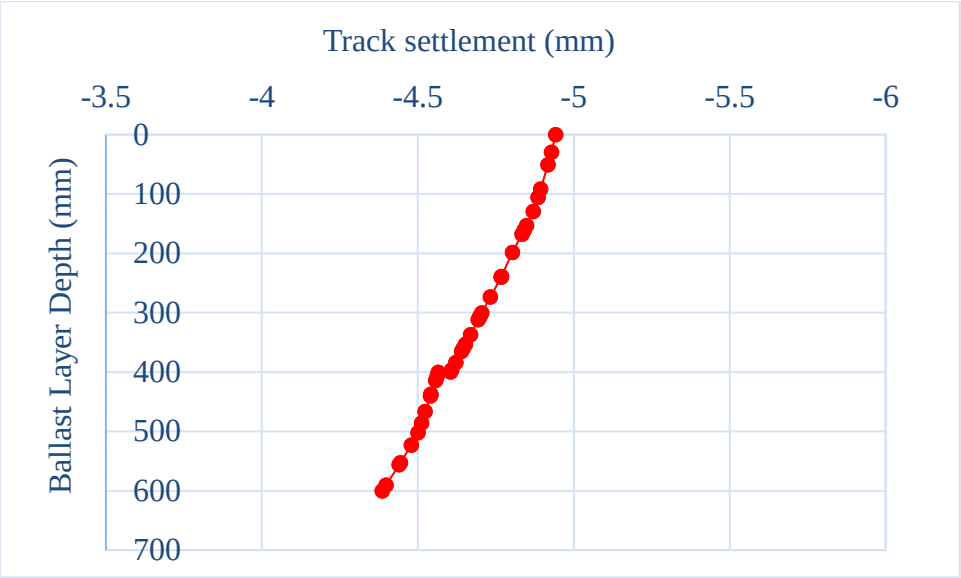

Figure 4-6: Vertical Displacement within the Depth of the Geogrid-Reinforced Ballast layer

Figure 4-7 also illustrates the analysis output from PLAXIS for geogrid reinforced ballasted track embankment subgrade stress (load transmitted underneath the ties) as a function of the depth of the track. As can be seen from this figure; the subgrade stress is 25.7 kPa at the sub-ballast-subgrade interface and gradually decreases to 13.5 kPa at a depth of 3 m below the bottom of the ballast.

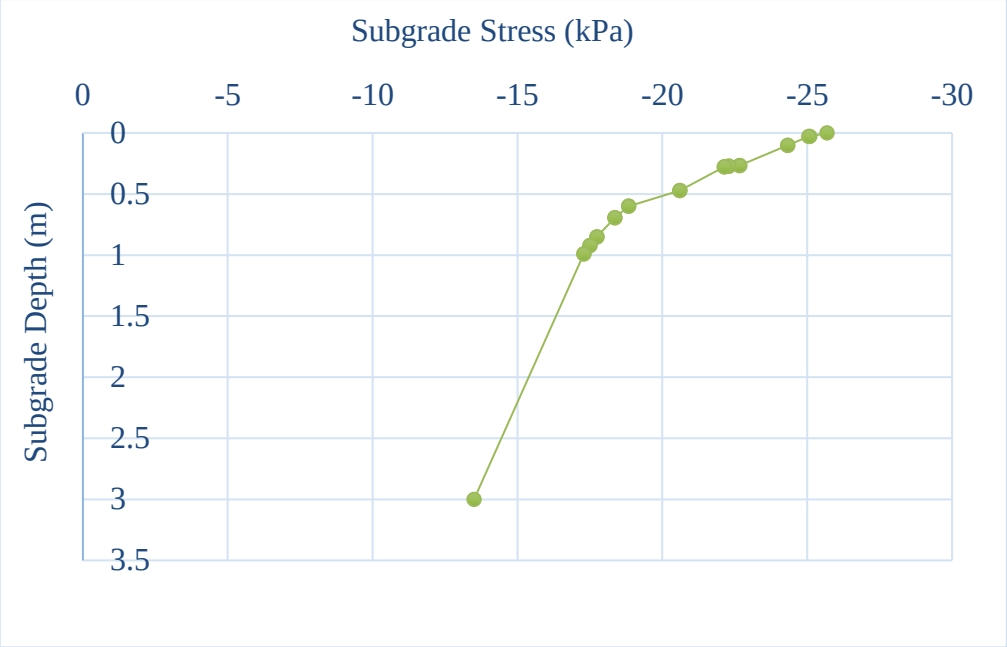

Figure 4-7 Subgrade stress versus track depth of geogrid reinforced ballast, PLAXIS

IV. Ballast embankment reinforced with geocomposite

The analysis output from PLAXIS for the variation of vertical track settlement throughout the depth of the track for geocomposite reinforced ballast embankment is illustrated in Appendix-e. The location of maximum deformation is assumed to be at the track center which is in line with the point of wheel load application. As can be seen from the figure; the deformation is 3.6 mm at the point of load application and gradually decreases to zero.

The variation of track settlement in geocomposite reinforced ballast embankment throughout its depth is shown in Figure 4-8 (full analysis results presented in Appendix-e. As can be seen from the figure; the track settlement is 3.4 mm at the top surface of the ballast layer and gradually decreases to 2.9 mm at the bottom surface of the subballast layer.

Figure 4.9 also shows the analysis output from PLAXIS for geocomposit reinforced ballast embankment subgrade stress (load transmitted underneath the ties) as a function of the depth of the track. As can be seen from this figure; the subgrade stress is 18.71 kPa at the subballast-subgrade interface and gradually decreases to 12.5 kPa at a depth of 3 m below the bottom of the ballast.

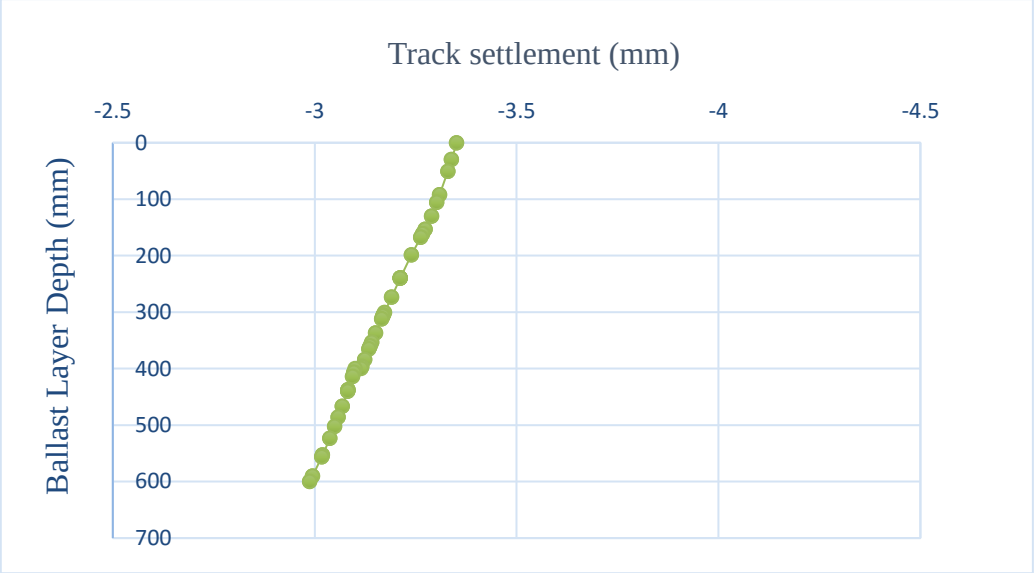

Figure 4-8 Vertical Displacement in the Depth of Geocomposit Reinforced Ballast

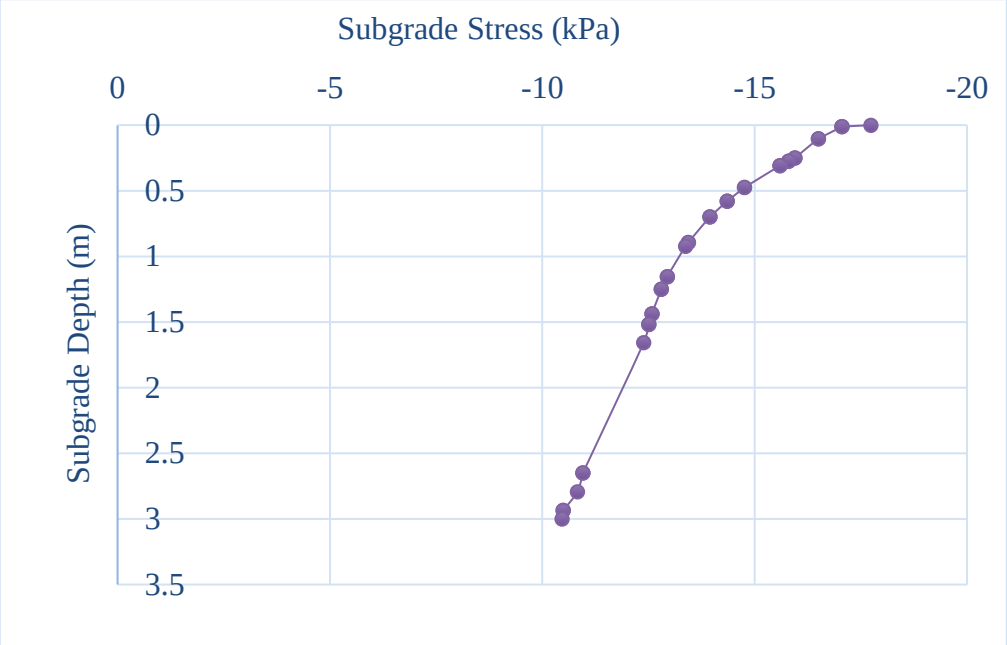

Figure 4-9 Subgrade Stress Versus Track Depth of Geogrid Reinforced Ballast, PLAXIS

4.2 Comparison of the Different Cases

In order to determine important parameters such as vertical settlement, subgrade stress, and stress-strain curve a series of simulations were conducted on the railway track embankment. After conducting the simulations, a comparison was made between unreinforced ballasted track and those of tracks reinforced with Geotextile, Geocomposit, and Geogrid regarding the level of track settlement and subgrade stress.

4.2.1 Unreinforced Versus Reinforced with Geotextile

- **Track settlement**

According to the analysis results from PLAXIS, the use of geotextile at the ballast-subbalast interface can reduce the track settlement by about 11.5%. As can be seen from Figure 4-10, when geotextile is used at the ballast-subballast interface the track settlement is reduced from 6.2 mm to 5.4 mm at the bottom surface of the sub-ballast layer and from 6.9 mm to 6.1 mm at the top surface of the ballast layer when a geotextile reinforcement is used.

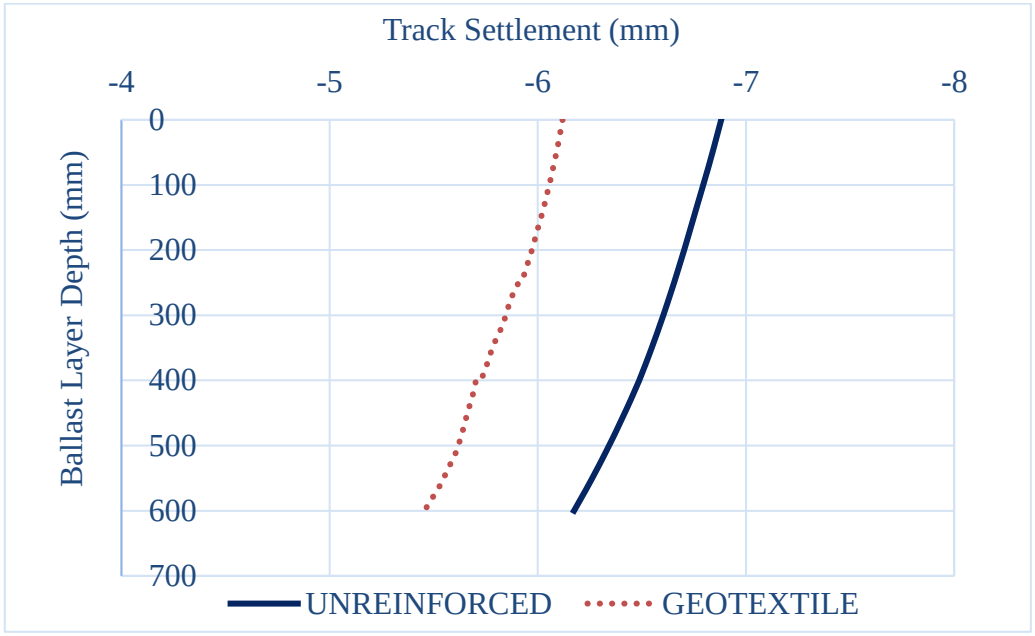

Figure 4-10 Vertical Displacement in Unreinforced & Geotextile Reinforced Ballast

- **Subgrade Stress**

The distribution of the rail loads over a wider area is also advantageous as it mobilizes more of the subgrade's strength and resistance, unlike the singular peak loads that induce shear when no reinforcement is present. Therefore one great advantage of geosynthetic material is its redistribution of stress over a wider area. The peak stress was reduced by approximately 20 % when using geotextile as shown in figure 4.11.

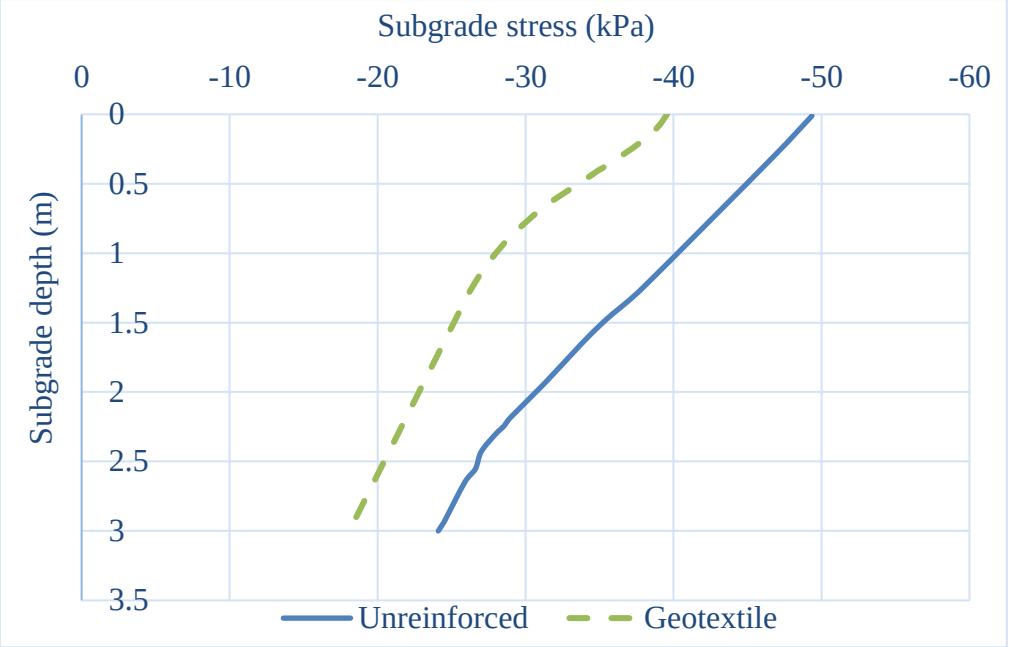

Figure 4-11 Subgrade stress in unreinforced & geotextile reinforced ballast

4.2.2 Unreinforced Versus Reinforced with Geogrid

- **Track settlement**

According to the analysis results, the use of geogrid reinforcement reduced the vertical track settlement by about 29%. Figure 4-12 shows that the track settlement is reduced from 6.17 mm to 4.38 mm at the bottom surface of the sub-ballast layer and from 6.9 mm to 4.94 mm at the top surface of the ballast layer when geogrid is used at the ballast subballast interface. The reinforcement mechanism (aggregate particles partially penetrate and interlock within the aperture of the geogrid) is effective in preventing excessive settlement by providing a relatively rigid mat and reducing the track settlement.

- **Subgrade Stress**

Confinement of ballast with geogrids results in an increase in the lateral stress within the aggregate, thereby increasing its stiffness this reduces the stress transferred to the subgrade. The peak stress was reduced by approximately 47% when geogrid is used at the ballast subballast interface. Geogrids also distribute the stress more evenly; it reduced the magnitude of the subgrade stresses when placed over a very compressible foundation or in an embankment consisting of weak ballast. The subgrade stress (underneath the ties) as a function of the track depth for unreinforced and geogrid reinforced track embankment is

shown in (Figure 4-13) and as it can be seen from the figure the intrusion of geogrid reduced the peak stress from 49.35 kPa to 25.68 kPa.

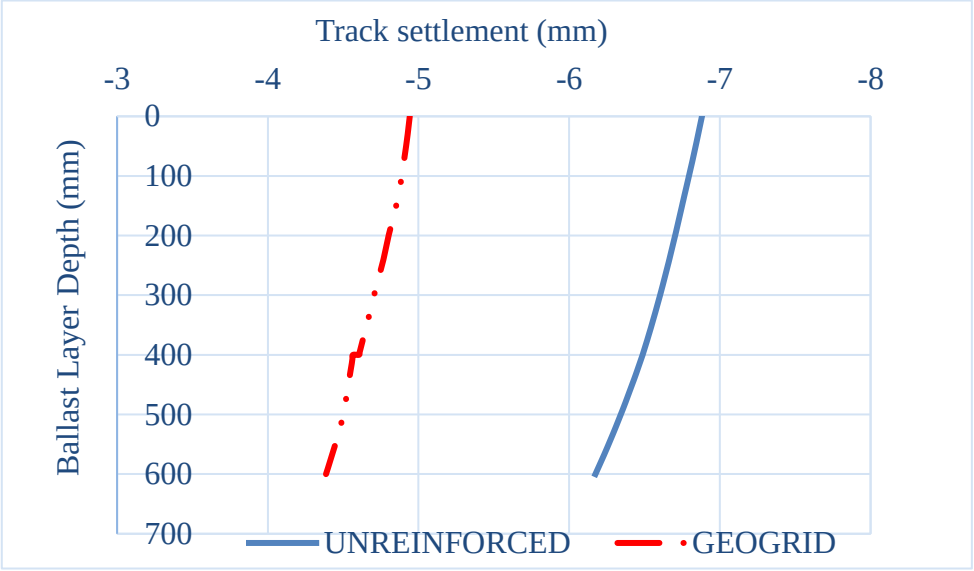

Figure 4-12: Vertical Displacement in Unreinforced and Geogrid Reinforced Ballast Layer

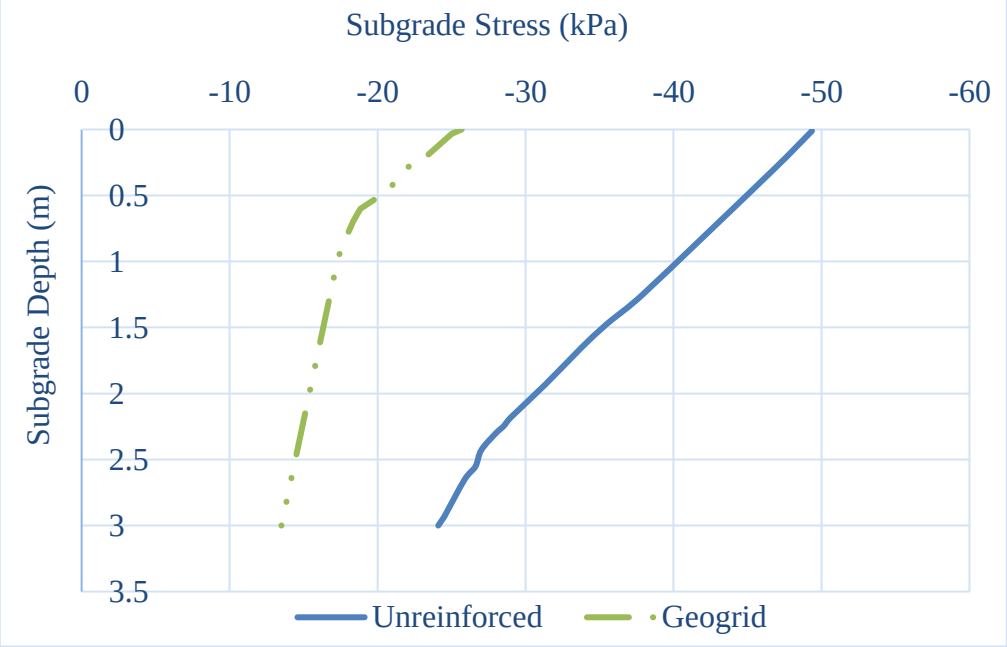

Figure 4-13 Subgrade Stress Vs Track Depth of Unreinforced & Geogrid Reinforced Track, PLAXIS-2D

4.2.3 Unreinforced Versus Reinforced with Geocomposite

- **Track settlement**

Ballast embankment reinforced with geocomposite at the ballast-subballast interface is also analyzed and, the PLAXIS analysis output is presented in Figure 4-14. According to the analysis results, the use of geocomposite at the ballast-subballast interface reduces the track settlement significantly by about 51.7%, which is much larger than how other types of geosynthetic materials did. As can be seen from Figure 4-14 the track settlement is reduced from 6.17 mm to 2.98 mm at the bottom surface of the subballast layer and from 6.88mm to 3.35 mm at the top surface of the ballast layer when geocomposite is used at the ballast subballast interface.

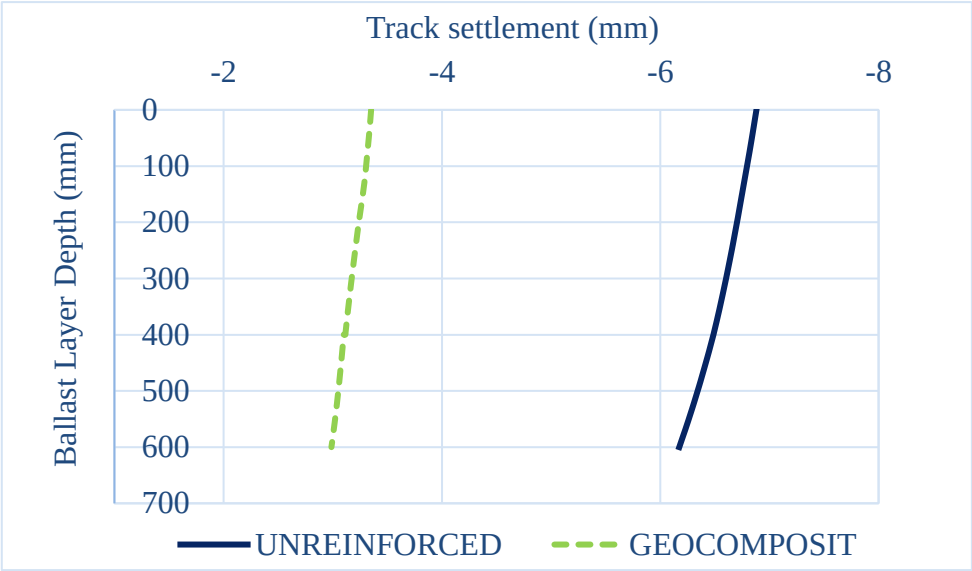

Figure 4-14 Track Settlement in Unreinforced & Geocomposit Reinforced Ballast Layer

- **Subgrade stress**

The subgrade stress (underneath the ties) as a function of the track depth for unreinforced and geocomposite reinforced track embankment is shown in (Figure 4-15) and as it can be seen from the figure the intrusion of geocomposit reduced the peak stress approximately by about 60% from 49.35 kPa to 17.7 kPa.

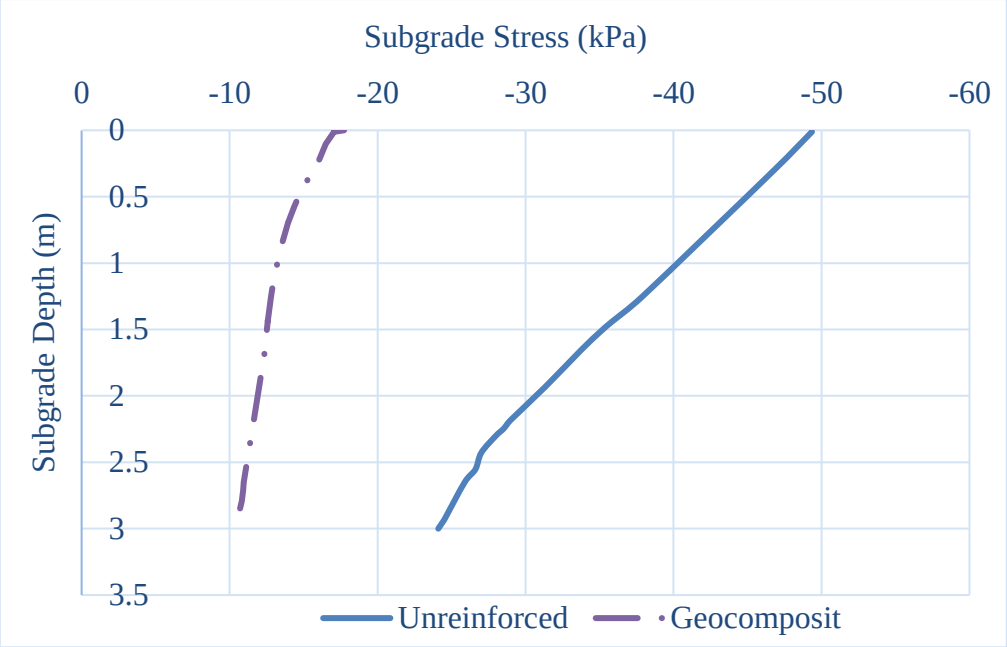

Figure 4-15 Subgrade Stress in Unreinforced & Geocomposit Reinforced Ballasted track Embankment

4.2.4 Unreinforced Versus Reinforced with Geocomposite, Geogrid & Geotextile

- **Track settlement**

As can be understood from the previous discussions the intrusion of any of the three types of geosynthetics used in this study can improve the track performance. In this section, the performance of each geosynthetic materials in improving the track capacity will be compared. From the analysis results, it can be understood that the vertical settlement is varied within the depth of the ballast layer. The variation of vertical settlement within the depth of the ballast layer for unreinforced and geotextile, geogrid and geocomposit reinforced ballasted track embankment is shown in Figure 4-16. As can be seen from this figure minimum track settlement is observed when geocomposit is used at the ballast-subballast interface.

As can be seen from Figure 4-16 the geogrid reinforced ballast has a minimum vertical settlement than the geotextile reinforced ballast. Therefore, a geogrid has a better performance in reducing track settlement. It can also be observed that when geogrid and geotextile is used the track settlement at the top surface of the ballast layer is 6.1 mm and 4.94 mm respectively which is less than the track settlement of unreinforced track embankment but larger than that of the geocomposit reinforced track embankment.

Therefore, it can be concluded that the capacity of geocomposit in reducing track settlement is better than both geogrid and geotextile.

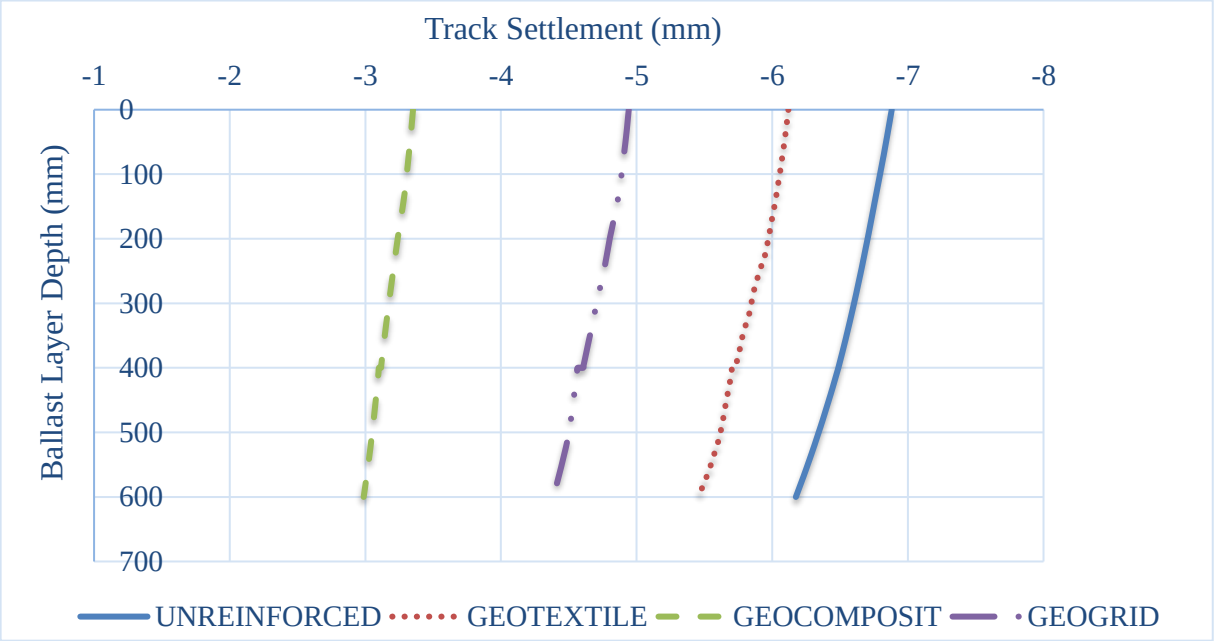

Figure 4-16 Track Settlement in Unreinforced & Geotextile, Geogrid, and Geocomposit Reinforced Ballast Layer

- **Subgrade stress**

The subgrade stress (underneath the ties) as a function of the track depth for unreinforced and geogrid, geocomposit and geotextile reinforced track embankment is shown in Figure 4-17. As can be seen from the figure the intrusion of each geosynthetic material increases the performance of the track by distributing the stress uniformly. The relative performance of each geosynthetic materials in redusing the stress transferred to the subgrade is presented in Figure 4-17. As can be seen from the figure the performance of geocomposit in reducing the subgrade stress is better than the others.

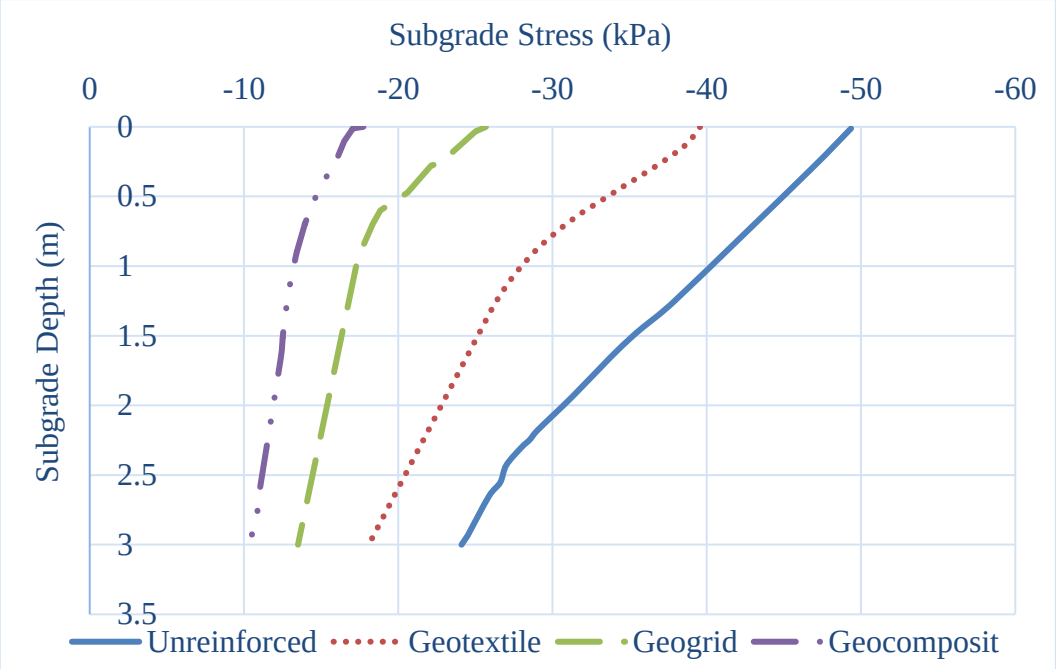

Figure 4-17 The Subgrade Stress as a Function of Track Depth for Unreinforced & Reinforced Track Embankment

Table 4-1 Summary of Finite Element Analysis for Geotextile, Geogrid, and Geocomposit Reinforced Ballasted Track Embankment

Parameter	Unreinforced (mm)	Reinforced with		
		Geotextile	Geogrid	Geocomposit
Settlement (mm)	8	6.4	5.6	3.6
% Reduction	-	20	30	55
Subgrade stress (KPa)	49.35	39.56	25.7	17.7
% Reduction	-	19	47.9	64

4.3 Investigation of an Optimum Location for Geosynthetics

Inclusion of geosynthetics for minimizing the deformation and degradation characteristics of the ballast layer and improving the track capacity could be anywhere beneath the sleeper and within the ballast layer. However, to allow for tamping, geosynthetics must not be placed at a depth of less than 150 mm below the sleeper [13]. In this study, an attempt is carried out using the Finite Element Analysis to obtain an optimum location of geosynthetics for minimizing the track settlement and the deformation level of the ballast layer. The placement depth of geogrid is first modeled at 400 mm beneath the sleeper (i.e.

at the ballast subballast interface) and then decreased by intervals of 50 mm so that the placement depth of geosynthetics can be tried at 350, 300, 250, 200, and 150 mm. The results are given in Figure 4-18.

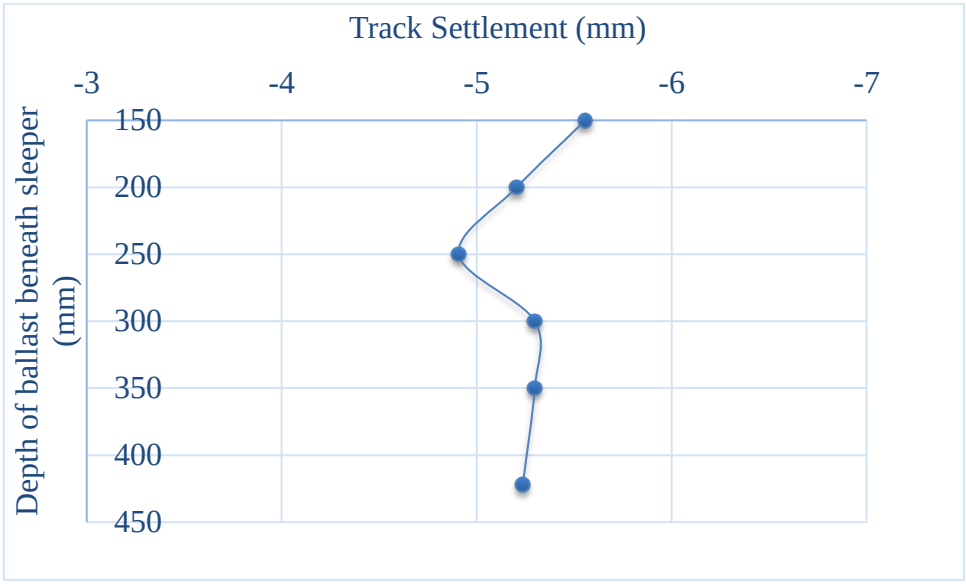

Figure 4-18 Optimum Location of Geosynthetics by the Finite Elements

As can be seen from Figure 4-18. the difference in the level of the track settlement when the geogrid is placed at various depth of location within the ballast layer is not significant. However, from the figure relatively minimum deformation is observed when geogrid is placed at 250 mm below the sleeper. From this, it can be concluded that using geogrid reinforcement where ever it is placed within the ballast layer can reduce the track settlement and its location does not significantly affect the performance of the reinforcement.

CHAPTER 5 CONCLUSIONS AND RECOMMENDATIONS

Numerical simulations of ballasted track unreinforced and reinforced with geogrid, geotextile, and geocomposit have been carried out and based on the analysis results the following conclusions and recommendations are made.

5.1 Conclusions

Reinforcing ballast using geotextile is effective in reducing both vertical deformation and subgrade stress. Placing geotextile at the ballast-subbalast interface reduces the track settlement by about 20%. In addition to this, an intrusion of geotextile increases the performance of reducing the stress as well as the strain.

The reinforcement of ballast using geogrid was quite effective in reducing vertical deformations. The magnitudes of deformation were reduced significantly by about 30%. In addition to reducing vertical deformation, an intrusion of geogrid also gave an added performance to the track in reducing the stress as well as the strain

Ballast embankment reinforced with geocomposite at the ballast-subballast interface was also quite effective in reducing track settlement. According to this thesis results, for ballast embankment reinforced with geocomposit, the track settlement is reduced very significantly by about 55%. In addition to this, the intrusion of geocomposite at the ballast subballast interface can also increase the performance of the track in reducing the stress as well as the strain.

Generally, numerical analysis reveals that an intrusion of any of the three types of geosynthetics can improve the ballast performance and has a direct benefit of extending the maintenance cycles (the period between ballast cleaning and replacement operation) and increases the effective bearing capacity of underlying subgrade. The magnitude of track settlement and subgrade stress reduced when geocomposite is used at the ballast-subballast interface are much larger than the magnitude of track settlement and subgrade stress reduced when geogrid and geotextile are used.

5.2 Recommendations

Even though the Finite Element Analysis has given a promising result further justification by constructing an instrumented track section in the field is needed. This will help in demonstrating the various benefits provided by the composition of geogrid-ballast, geotextile-ballast and geocomposit-ballast to improve the ballast performance and to characterize the materials of the track components effectively. These tests could also include full-scale railway geometry and loading patterns representative of the exact train wheel passes.

Discrete Element Method (DEM) is a numerical method used to compute the stress and displacements in a volume containing a large number of particles as grains of sand, the granular material is modeled as an assembly of rigid particles and the interaction between each particle is explicitly considered. However, a FEM considers the soil as a continuum and describes the soil by pointwise mathematical expressions. Therefore, it is better to use DEM for more confined results.

Optimization of the aperture size of the geogrid and the grain size needs a thorough investigation since the principles of reinforcement of the geogrid lies on the interlock of the geogrid and the ballast. For this reason, a more detailed study is required.

REFERENCES

[1] B. Indraratna, W. Salim, and C. Rujikiatkamjorn, *Advanced Rail Geotechnology – Ballasted Track*. London, UK: CRC Press/Balkema, 2011.

[2] B. Indraratna, S. Nimbalkar, and C. Rujikiatkamjorn, "Stabilising railway embankments with geosynthetic grids and drains and a class A prediction of track behaviour," in *International Symposium on Sustainable Geosynthetics and Green Technology for Climate Change (SGCC)*, 2012, pp. 21–40.

[3] B. Indraratna, C. Rujikiatkamjorn, and S. Nimbalkar, "Use of geosynthetics in railways including geocomposites and vertical drains," in *Geotechnical Special Publication*, 2011, pp. 4733–4742.

[4] A. Gomes Correia *et al.*, "Dynamic analysis of rail track for high speed trains. 2D approach," in *Applications of Computational Mechanics in Geotechnical Engineering - Proceedings of the 5th International Workshop on Applications of Computational Mechanics in Geotechnical Engineering*, 2007, pp. 461–472.

[5] A. S. J. SUIKER, "The Mechanical Behaviour of Ballasted Railway Tracks," Delft University, 2002.

[6] L. C. Hsien, "Finite Element Study of 2d Equivalence to 3d Analysis of a Discrete Soil Nail Problem with Applications to Serviceability Design," National University of Singapore, 2003.

[7] J. P. Freitas da Cunha, "Modelling of Ballasted Railway Tracks for High-Speed Trains," University of Minho, 2013.

[8] J. M. Selig, Ernest T and Water, *Track Geotechnology and Substructure Management*. London: Thomas Telford, 1994.

[9] E. T. Selig, "Railway Track Design," in *Handbook of Transportation Engineering*, M. Kutz, Ed. 2004.

[10] C. Esveld, *[Modern Railway Track]*, Second Edi. 2001.

[11] & J. M. M. J. G Romero, J. R. Edwards, C. P. Barkan, B. Wilson, "Advancements in Fastening System Design for North American Concrete Crossties in Heavy-Haul Service," in *AREMA 2010 Annual Conference & Exposition*, 2010.

[12] Be. (Hons) Wee Loon Lim, "Mechanics of Railway Ballast Behaviour," The universty of Nothingham, 2004.

[13] S. S. Radampola, "Evaluation and modeling performance of capping layer in rail track substructure," Central Queensland University, 2006.

[14] B. Aursudkij, "A Laboratory Study of Railway Ballast Behaviour under Traffic Loading and Tamping Maintenance," University of Nottingham, 2007.

[15] C. F. Bonnett, *Practical Railway Engineering*, 2nd editi. London: Imperial College

Press, 2005.

[16] H. Bereket "Performance Evaluation of ELASTOTRACK Polyurethane Stabilized Railroad ballast," Addis Ababa University, Ethiopia, 2017.

[17] B. Indraratna, M. A. Shahin, and W. Salim, "Use of geosynthetics for stabilizing recycled ballast in railway track substructures," in *Proceedings of NAGS2005/GRI 19 Cooperative Conference, USA: North American Geosynthetics Society.*, 2005, pp. 1–15.

[18] AREMA, "Manual for railway engineering.", 2010

[19] B. Indraratna, J. . Lackenby, and D. Christie, "Effect of confining pressure on the degradation of ballast under cyclic loading," *Geotechnique*, vol. 55, no. 4, pp. 325–328, 2005.

[20] F. Lekarp, U. Isacsson, and A. Dawson, "State of the Art. II: Permanent Strain Response of Unbound Aggregates," *J. Transp. Eng.*, vol. 126, no. 1, pp. 76–83, 2000.

[21] B. Indraratna, J. S. Vinod, and J. Lackenby, "Influence of particle breakage on the resilient modulus of railway ballast," *Geotechnique*, vol. 59, no. 7, pp. 643–646, 2009.

[22] R. M. Knutson, "Factors influencing the Repeated Load Behaviour of Railway Ballast," The University of Illinois at Urban-Champaign, 1976.

[23] I. F. Collins and M. Boulbibane, "Geomechanical Analysis of Unbound Pavements Based on Shakedown Theory," *J. Geotech. Geoenvironmental Eng.*, vol. 126, no. 1, pp. 50–59, 2000.

[24] H. K. & J. L. B. Indraratna, "Behaviour of railway ballast under dynamic loads based on large-scale triaxial testing," in *Proceedings of AusRAIL Plus*, pp. 17–19.

[25] B. Indraratna, W. Salim, and Mohammad Hadi Khabbaz, "Stabilisation of rail tracks employing geosynthetics with recycled ballast," in *5th International Conference on Ground Improvement*, pp. 27-40.

[26] B. Indraratna, P. K. Thakur, and J. S. Vinod, "Experimental and numerical study of railway ballast behavior under cyclic loading," *Int. J. Geomech.*, vol. 10, no. 4, pp. 136–144, 2010.

[27] T. Jeffs, "Towards Ballast Life Cycle Costing Railways in Action," in *4th International Heavy Haul Railway Conference: Railways in Action; Preprints of Papers,*1989, pp. 439–445.

[28] X. Shi, "Prediction of Permanent Deformation in Railway Track," University of Nottingham, 2009.

[29] N. F. Doyle, "Railway track design: a Review of Current Practice (No.UIC Cat 54 0 12)," 1980.

[30] B. Indraratna, S. Nimbalkar, D. Christie, C. Rujikiatkamjorn, and J. Vinod, "Field Assessment of the Performance of a Ballasted Rail Track with and without Geosynthetics," *J. Geotech. Geoenvironmental Eng.*, vol. 136, no. 7, pp. 907–917, 2010.

[31] B. Indraratna and S. Nimbalkar, "Stress-strain degradation response of railway ballast stabilized with geosynthetics," *J. Geotech. Geoenvironmental Eng.*, vol. 139, no. 5, pp. 684–700, 2013.

[32] M. A. Sayeed, "Design of Ballasted Railway Track Foundations using Numerical Modelling with Special Reference to High Speed Trains," Curtin University, 2016.

[33] ERC, "Techno-Economic Feasibility Study: Addis Ababa/Sebeta -Djibouti Railway Project," 2012.

[34] K. Abdu, "Assessment of Degradation and Performance Improvement of Railway Ballast with Geosynthetics - A Case Study of National Railway Network," Addis Ababa University, 2015.

[35] ERC, "Rolling Stocks Specifications: Operation and Service Division, Equipment Supply &Technical Service Department.," 2012.

[36] V. A. Profillidis, *Railway Management, and Engineering*, Fourth edi. 2016.

[37] S. Panagoulias, R. B. J. Brinkgreve, and L. Zampich, "PLAXIS MoDeTo Manual 2018," 2018.

[38] D. Li, J. Hyslip, T. Sussmann, and S. Chrismer, "Substructure," in *Railway Geotechnics*, London, UK: CRC Press, 2015.

[39] O. Holý and L. Mica., "Determination of axial stiffness of geosynthetics for numerical modeling - part 1," in *Paper in conference proceedings Civil engineering structures in view of geomechanics*, 2019.

APPENDIX A

In order to model and analyze a series of track embankments with and without reinforcement. input data are collected from ERC and different literature. The General information about the material properties used in the analysis that are extracted from the FEM software PLAXIS-2D 8.2 are

Material properties used in PLAXIS

Soil and Interfaces Info

Linear Elastic | Mohr-Coulomb

ID	Name	Type	γ_{unsat} [kN/m^3]	γ_{sat} [kN/m^3]	k_x [m/day]	k_y [m/day]	v [-]
3	04 - Concrete sleepert	Non-porous	8.1	8.1	0.0000	0.0000	0.3
4	05- Railt	Non-porous	76.0	76.0	0.0000	0.0000	0.3

OK | Print... | Copy | Help

Soil and Interfaces Info

Linear Elastic | Mohr-Coulomb

ID	Name	Type	γ_{unsat} [kN/m^3]	γ_{sat} [kN/m^3]	k_x [m/day]	k_y [m/day]	v [-]
1	01- Ballatt	Drained	22.0	23.0	3.2411E+3	3.2411E+3	0.30
2	02- Subballastt	Drained	22.0	23.0	3.2411E+3	3.2411E+3	0.30
5	03-Subgradet	Drained	18.0	19.0	0.8643	0.8643	0.25

OK | Print... | Copy | Help

Soil and Interfaces Info

Linear Elastic | Mohr-Coulomb

ID	Name	ν [-]	E_{ref} [kN/m 2]	c_{ref} [kN/m 2]	φ [°]	ψ [°]	E_{incr} [kN/m 3]
1	01- Ballatt	0.30	1.7E5	0.0	45.0	15.0	0.0
2	02- Subballastt	0.30	1.5E5	0.0	42.0	12.0	0.0
5	03-Subgradet	0.25	30000.0	24.0	12.0	0.0	0.0

OK | Print... | Copy | Help

Loading condition extracted from PLAXIS

This study considers only vertical load and in the analysis, a dynamic impact factor, which is a function of wheel diameter and velocity of the train, is used to consider the dynamic effect.

Point loads

Load no.	Load system	Node	X [10 -3 m]	Y [m]	Fx [kN]	Fy [kN]
1	A	1048	750.000	3.900	0.000	-107.300

Material data set for the three geosynthetic materials: geotextile, geogrid and geocomposit

1. **Material data set for Geotextile**

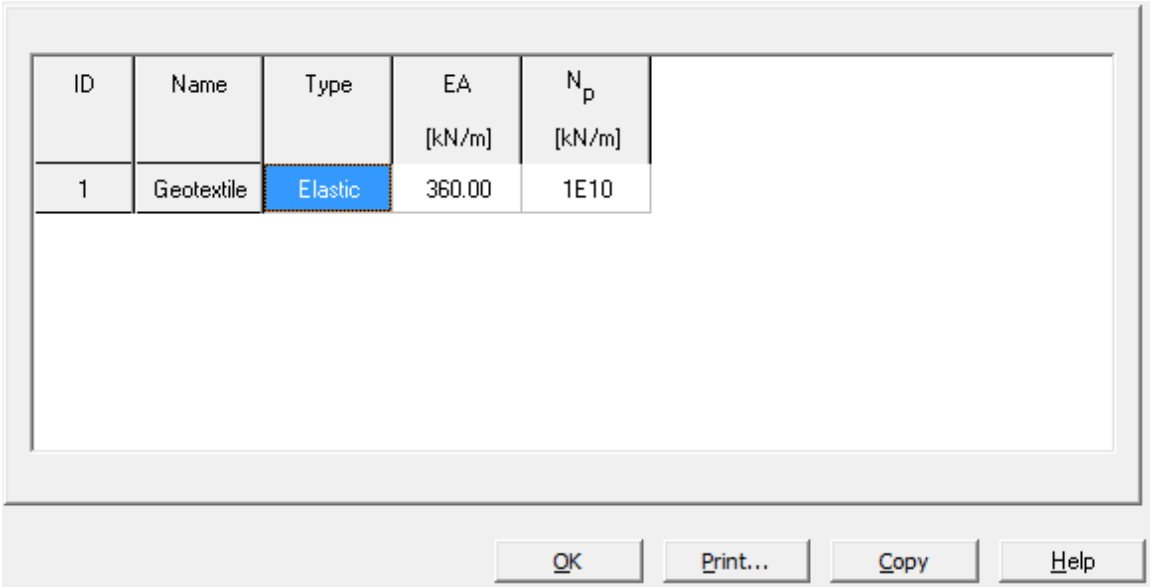

2. **Material data set for Geogrid**

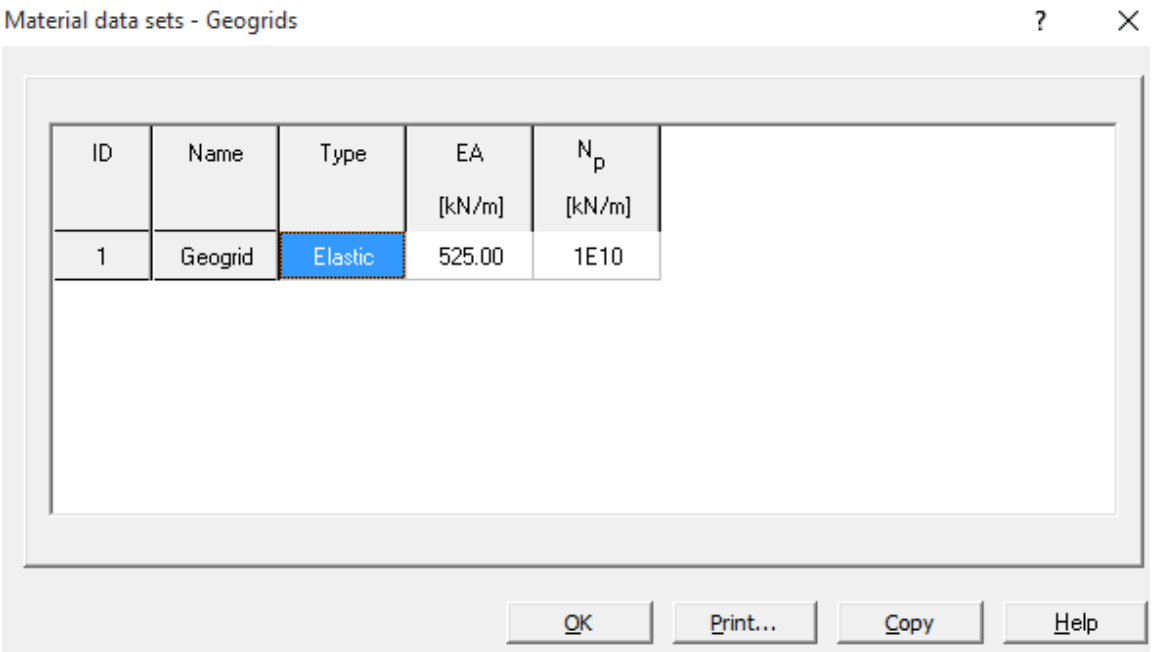

3. **Material data set for Geocomposite**

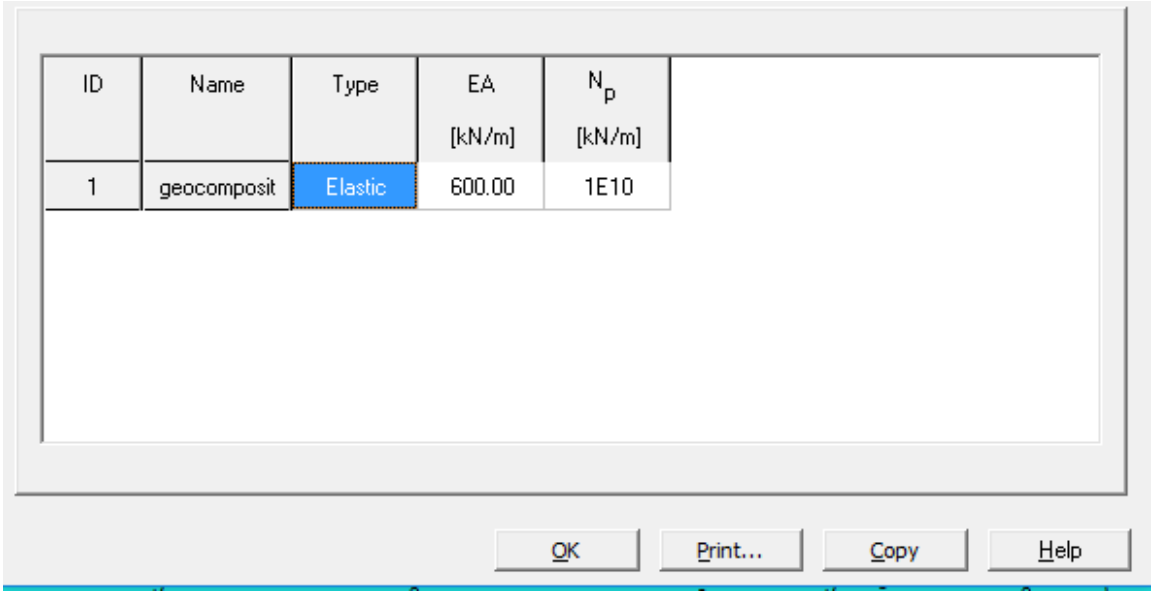
ID
Name
Type
EA [kN/m]
N_p [kN/m]
1
geocomposit
Elastic
600.00
1E10
OK
Print...
Copy
Help

APPENDIX B

Output spreadsheet data

Vertical displacement unreinforced track throughout the track depth under the sleeper

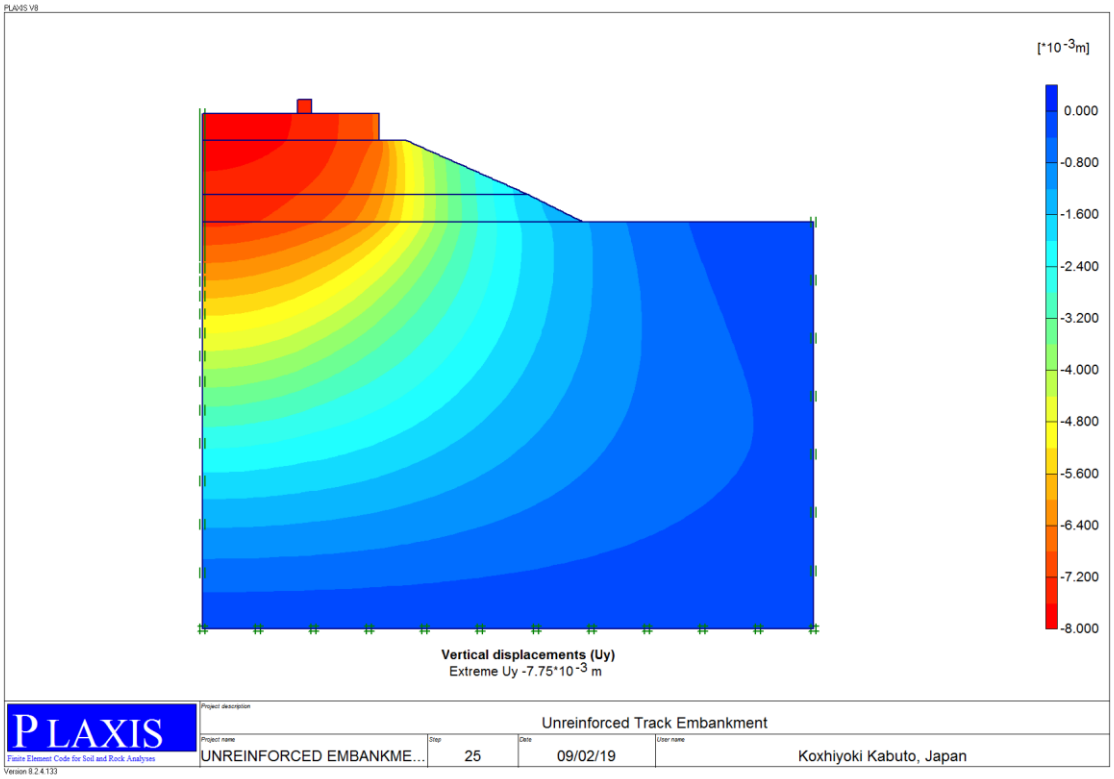

X [m]	Y [m]	U_y [m]
1.203488400000	3.634010900000	-0.006883822800
1.203488400000	3.600000000000	-0.006880943400
1.203488400000	3.600000000000	-0.006880943400
1.203488400000	3.572989200000	-0.006858520000
1.203488400000	3.572989200000	-0.006858520000
1.203488400000	3.557842200000	-0.006845973400
1.203488400000	3.557842200000	-0.006845973400

1.203488400000	3.528405600000	-0.006820517600
1.203488400000	3.528405600000	-0.006820517600
1.203488400000	3.523120900000	-0.006815766100
1.203488400000	3.523120900000	-0.006815766100
1.203488400000	3.495641000000	-0.006790669900
1.203488400000	3.495641000000	-0.006790669900
1.203488400000	3.465568800000	-0.006763015700
1.203488400000	3.465568800000	-0.006763015700
1.203488400000	3.454870500000	-0.006753260100
1.203488400000	3.454870500000	-0.006753260100
1.203488400000	3.447951200000	-0.006746990400
1.203488400000	3.447951200000	-0.006746990400
1.203488400000	3.408215700000	-0.006710706800
1.203488400000	3.408215700000	-0.006710706800
1.203488400000	3.402032300000	-0.006704920500
1.203488400000	3.402032300000	-0.006704920500
1.203488400000	3.359992300000	-0.006664531400
1.203488400000	3.359992300000	-0.006664531400
1.203488400000	3.354537600000	-0.006659140500
1.203488400000	3.354537600000	-0.006659140500
1.203488400000	3.347033700000	-0.006651662500

1.203488400000	3.347033700000	-0.006651662500
1.203488400000	3.316492200000	-0.006620444100
1.203488400000	3.316492200000	-0.006620444100
1.203488400000	3.299566000000	-0.006602556900
1.203488400000	3.299566000000	-0.006602556900
1.203488400000	3.271934200000	-0.006572365800
1.203488400000	3.271934200000	-0.006572365800
1.203488400000	3.244564500000	-0.006541151200
1.203488400000	3.244564500000	-0.006541151200
1.203488400000	3.224558900000	-0.006517452400
1.203488400000	3.224558900000	-0.006517452400
1.203488400000	3.200000000000	-0.006487282800
1.203488400000	3.200000000000	-0.006487282800
1.203488400000	3.170368500000	-0.006446656200
1.203488400000	3.170368500000	-0.006446656200
1.203488400000	3.159237100000	-0.006430874100
1.203488400000	3.159237100000	-0.006430874100
1.203488400000	3.120021500000	-0.006373246600
1.203488400000	3.120021500000	-0.006373246600
1.203488400000	3.115384200000	-0.006366211100
1.203488400000	3.115384200000	-0.006366211100

1.203488400000	3.114156800000	-0.006364340700
1.203488400000	3.114156800000	-0.006364340700
1.203488400000	3.108074700000	-0.006355021500
1.203488400000	3.108074700000	-0.006355021500
1.203488400000	3.079162800000	-0.006309531300
1.203488400000	3.079162800000	-0.006309531300
1.203488400000	3.066434500000	-0.006288860600
1.203488400000	3.066434500000	-0.006288860600
1.203488400000	3.045278000000	-0.006253598500
1.203488400000	3.045278000000	-0.006253598500
1.203488400000	3.032013100000	-0.006230900000
1.203488400000	3.032013100000	-0.006230900000
1.203488400000	3.000000000000	-0.006174190700
1.203488400000	3.000000000000	-0.006174190700
1.203488400000	2.954787100000	-0.005982293500

APPENDIX C

Vertical Displacement of Geotextile Reinforced Track throughout the Track Depth under the sleeper

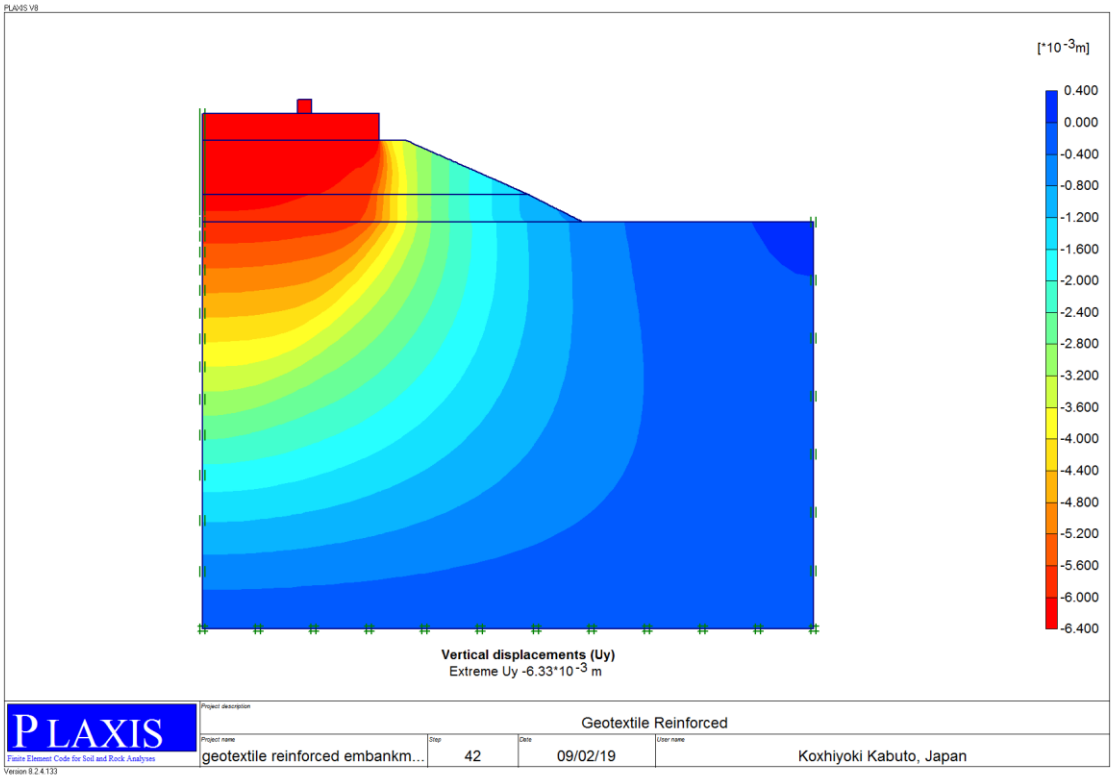

X	Y	U_y
[m]	[m]	[m]
1.203488400000	3.617059600000	-0.006120448200
1.203488400000	3.600000000000	-0.006118867900
1.203488400000	3.600000000000	-0.006118867900
1.203488400000	3.570019600000	-0.006102143200
1.203488400000	3.570019600000	-0.006102143200
1.203488400000	3.549454600000	-0.006089465900
1.203488400000	3.549454600000	-0.006089465900
1.203488400000	3.508037600000	-0.006061032200

1.203488400000	3.508037600000	-0.006061032200
1.203488400000	3.494255000000	-0.006050379100
1.203488400000	3.494255000000	-0.006050379100
1.203488400000	3.470255700000	-0.006032392900
1.203488400000	3.470255700000	-0.006032392900
1.203488400000	3.446566500000	-0.006012809700
1.203488400000	3.446566500000	-0.006012809700
1.203488400000	3.439003000000	-0.006005571600
1.203488400000	3.439003000000	-0.006005571600
1.203488400000	3.432448500000	-0.005999441200
1.203488400000	3.432448500000	-0.005999441200
1.203488400000	3.401521200000	-0.005973242400
1.203488400000	3.401521200000	-0.005973242400
1.203488400000	3.360856000000	-0.005942849700
1.203488400000	3.360856000000	-0.005942849700
1.203488400000	3.360492400000	-0.005942555900
1.203488400000	3.360492400000	-0.005942555900
1.203488400000	3.360170300000	-0.005942269700
1.203488400000	3.360170300000	-0.005942269700
1.203488400000	3.326566200000	-0.005871954500
1.203488400000	3.326566200000	-0.005871954500
1.203488400000	3.299449800000	-0.005845075800
1.203488400000	3.299449800000	-0.005845075800
1.203488400000	3.294747100000	-0.005841265000
1.203488400000	3.294747100000	-0.005841265000
1.203488400000	3.293278000000	-0.005840233500
1.203488400000	3.293278000000	-0.005840233500

1.203488400000	3.288147900000	-0.005836456200
1.203488400000	3.288147900000	-0.005836456200
1.203488400000	3.262876400000	-0.005798976200
1.203488400000	3.262876400000	-0.005798976200
1.203488400000	3.246781000000	-0.005777884000
1.203488400000	3.246781000000	-0.005777884000
1.203488400000	3.239813100000	-0.005771827000
1.203488400000	3.239813100000	-0.005771827000
1.203488400000	3.234871000000	-0.005767403800
1.203488400000	3.234871000000	-0.005767403800
1.203488400000	3.216082600000	-0.005746062700
1.203488400000	3.216082600000	-0.005746062700
1.203488400000	3.203566500000	-0.005731631000
1.203488400000	3.203566500000	-0.005731631000
1.203488400000	3.200000000000	-0.005727777700
1.203488400000	3.200000000000	-0.005704528700
1.203488400000	3.192983800000	-0.005700086300
1.203488400000	3.192983800000	-0.005700086300
1.203488400000	3.187199500000	-0.005695869500
1.203488400000	3.187199500000	-0.005695869500
1.203488400000	3.170133200000	-0.005680768600
1.203488400000	3.170133200000	-0.005680768600
1.203488400000	3.160116300000	-0.005671279000
1.203488400000	3.160116300000	-0.005671279000
1.203488400000	3.149601100000	-0.005661572800
1.203488400000	3.149601100000	-0.005661572800
1.203488400000	3.117089200000	-0.005634831500

1.203488400000	3.117089200000	-0.005634831500
1.203488400000	3.091329500000	-0.005609593200
1.203488400000	3.091329500000	-0.005609593200
1.203488400000	3.040367900000	-0.005533226500
1.203488400000	3.040367900000	-0.005533226500
1.203488400000	3.000000000000	-0.005455700500
1.203488400000	3.000000000000	-0.005455700500
1.203488400000	2.928118100000	-0.005136310000

APPENDIX D

Vertical displacement of geogrid reinforced track throughout the track depth under the sleeper

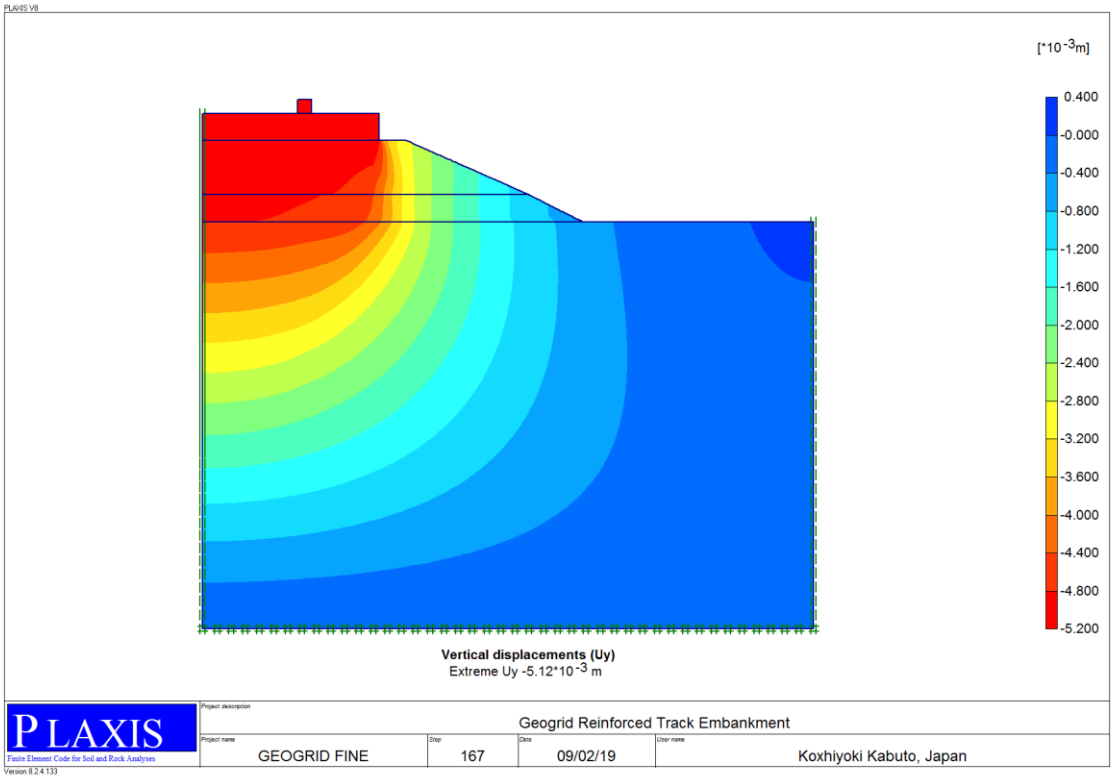

X	Y	U_y
[m]	[m]	[m]
1.203488400000	3.617059600000	-0.004943464900
1.203488400000	3.600000000000	-0.004942083500
1.203488400000	3.600000000000	-0.004942083500
1.203488400000	3.570019600000	-0.004928275200
1.203488400000	3.570019600000	-0.004928275200
1.203488400000	3.549454600000	-0.004917540400
1.203488400000	3.549454600000	-0.004917540400

1.203488400000	3.508037600000	-0.004893772600
1.203488400000	3.508037600000	-0.004893772600
1.203488400000	3.494255000000	-0.004885697000
1.203488400000	3.494255000000	-0.004885697000
1.203488400000	3.470255700000	-0.004870164400
1.203488400000	3.470255700000	-0.004870164400
1.203488400000	3.446566500000	-0.004848585000
1.203488400000	3.446566500000	-0.004848585000
1.203488400000	3.439003000000	-0.004841083300
1.203488400000	3.439003000000	-0.004841083300
1.203488400000	3.432448500000	-0.004834377500
1.203488400000	3.432448500000	-0.004834377500
1.203488400000	3.401521200000	-0.004803110900
1.203488400000	3.401521200000	-0.004803110900
1.203488400000	3.360856000000	-0.004768338100
1.203488400000	3.360856000000	-0.004768338100
1.203488400000	3.360492400000	-0.004767989900
1.203488400000	3.360492400000	-0.004767989900
1.203488400000	3.360170300000	-0.004767684800
1.203488400000	3.360170300000	-0.004767684800
1.203488400000	3.326566200000	-0.004733063400

1.203488400000	3.326566200000	-0.004733063400
1.203488400000	3.299449800000	-0.004704520900
1.203488400000	3.299449800000	-0.004704520900
1.203488400000	3.294747100000	-0.004699917300
1.203488400000	3.294747100000	-0.004699917300
1.203488400000	3.293278000000	-0.004698492600
1.203488400000	3.293278000000	-0.004698492600
1.203488400000	3.288147900000	-0.004693536200
1.203488400000	3.288147900000	-0.004693536200
1.203488400000	3.262876400000	-0.004669418000
1.203488400000	3.262876400000	-0.004669418000
1.203488400000	3.246781000000	-0.004652458400
1.203488400000	3.246781000000	-0.004652458400
1.203488400000	3.239813100000	-0.004645243800
1.203488400000	3.239813100000	-0.004645243800
1.203488400000	3.234871000000	-0.004640269800
1.203488400000	3.234871000000	-0.004640269800
1.203488400000	3.216082600000	-0.004621470600
1.203488400000	3.216082600000	-0.004621470600
1.203488400000	3.203566500000	-0.004608658800
1.203488400000	3.203566500000	-0.004608658800

1.203488400000	3.200000000000	-0.004604955000
1.203488400000	3.200000000000	-0.004565113800
1.203488400000	3.193632300000	-0.004561841300
1.203488400000	3.193632300000	-0.004561841300
1.203488400000	3.185803600000	-0.004557452200
1.203488400000	3.185803600000	-0.004557452200
1.203488400000	3.162631900000	-0.004542325100
1.203488400000	3.162631900000	-0.004542325100
1.203488400000	3.161020900000	-0.004541219500
1.203488400000	3.161020900000	-0.004541219500
1.203488400000	3.159772800000	-0.004540383400
1.203488400000	3.159772800000	-0.004540383400
1.203488400000	3.133576600000	-0.004523652500
1.203488400000	3.133576600000	-0.004523652500
1.203488400000	3.113946900000	-0.004512150400
1.203488400000	3.113946900000	-0.004512150400
1.203488400000	3.097902400000	-0.004500450100
1.203488400000	3.097902400000	-0.004500450100
1.203488400000	3.076916100000	-0.004478814400
1.203488400000	3.076916100000	-0.004478814400
1.203488400000	3.047278800000	-0.004444711100

1.203488400000	3.047278800000	-0.004444711100
1.203488400000	3.043855100000	-0.004440612700
1.203488400000	3.043855100000	-0.004440612700
1.203488400000	3.009681700000	-0.004398559000
1.203488400000	3.009681700000	-0.004398559000
1.203488400000	3.000000000000	-0.004386218700
1.203488400000	3.000000000000	-0.004386218700
1.203488400000	2.955972900000	-0.004244278900

APPENDIX E

Vertical displacement of geocomposit reinforced track throughout the track depth under the sleeper

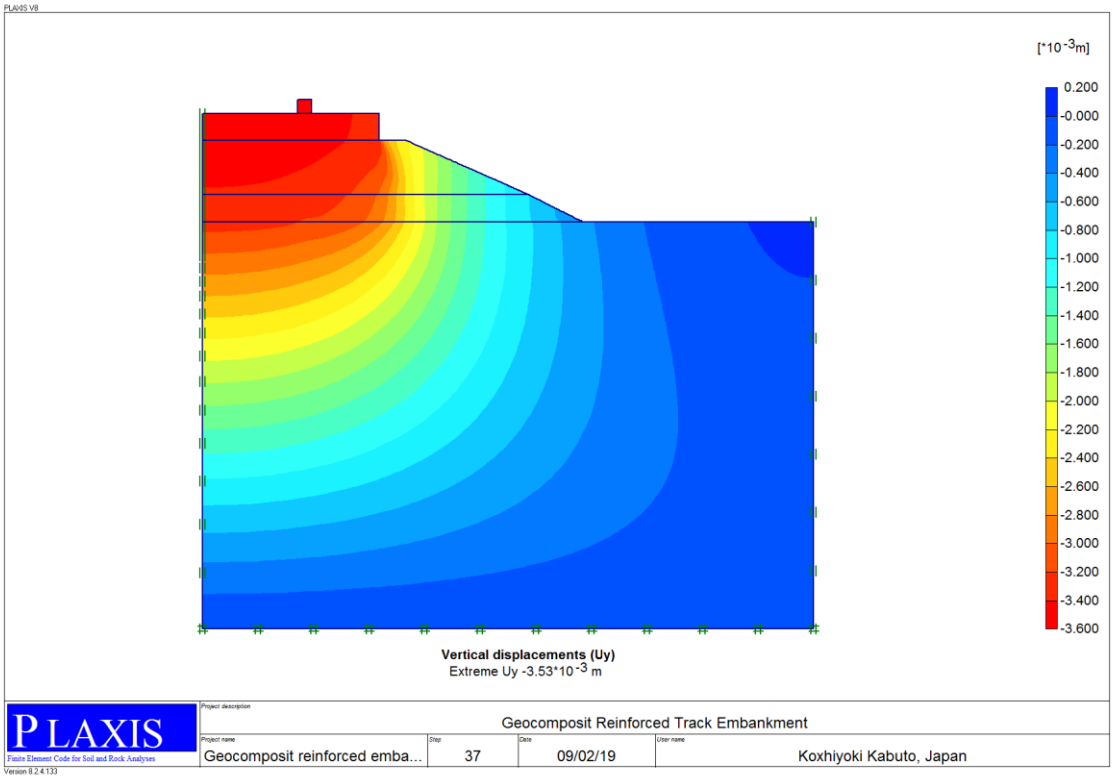

X	Y	U_y
[m]	[m]	[m]
1.203488400000	3.617059600000	-0.003352879000
1.203488400000	3.600000000000	-0.003351470200
1.203488400000	3.600000000000	-0.003351470200
1.203488400000	3.570019600000	-0.003339162600
1.203488400000	3.570019600000	-0.003339162600
1.203488400000	3.549454600000	-0.003329720300
1.203488400000	3.549454600000	-0.003329720300
1.203488400000	3.508037600000	-0.003309336800
1.203488400000	3.508037600000	-0.003309336800

1.203488400000	3.494255000000	-0.003302481000
1.203488400000	3.494255000000	-0.003302481000
1.203488400000	3.470255700000	-0.003289563500
1.203488400000	3.470255700000	-0.003289563500
1.203488400000	3.446566500000	-0.003273476100
1.203488400000	3.446566500000	-0.003273476100
1.203488400000	3.439003000000	-0.003267834800
1.203488400000	3.439003000000	-0.003267834800
1.203488400000	3.432448500000	-0.003262841900
1.203488400000	3.432448500000	-0.003262841900
1.203488400000	3.401521200000	-0.003239424700
1.203488400000	3.401521200000	-0.003239424700
1.203488400000	3.360856000000	-0.003212274400
1.203488400000	3.360856000000	-0.003212274400
1.203488400000	3.360492400000	-0.003212041100
1.203488400000	3.360492400000	-0.003212041100
1.203488400000	3.360170300000	-0.003211837000
1.203488400000	3.360170300000	-0.003211837000
1.203488400000	3.326566200000	-0.003190225300
1.203488400000	3.326566200000	-0.003190225300
1.203488400000	3.299449800000	-0.003173030800
1.203488400000	3.299449800000	-0.003173030800
1.203488400000	3.294747100000	-0.003170104700
1.203488400000	3.294747100000	-0.003170104700
1.203488400000	3.293278000000	-0.003169193100
1.203488400000	3.293278000000	-0.003169193100
1.203488400000	3.288147900000	-0.003166032700

1.203488400000	3.288147900000	-0.003166032700
1.203488400000	3.262876400000	-0.003150708400
1.203488400000	3.262876400000	-0.003150708400
1.203488400000	3.246781000000	-0.003141238400
1.203488400000	3.246781000000	-0.003141238400
1.203488400000	3.239813100000	-0.003137235500
1.203488400000	3.239813100000	-0.003137235500
1.203488400000	3.234871000000	-0.003134429900
1.203488400000	3.234871000000	-0.003134429900
1.203488400000	3.216082600000	-0.003123945500
1.203488400000	3.216082600000	-0.003123945500
1.203488400000	3.203566500000	-0.003117044000
1.203488400000	3.203566500000	-0.003117044000
1.203488400000	3.200000000000	-0.003115073900
1.203488400000	3.200000000000	-0.003100257200
1.203488400000	3.193632300000	-0.003097447800
1.203488400000	3.193632300000	-0.003097447800
1.203488400000	3.185803600000	-0.003093928900
1.203488400000	3.185803600000	-0.003093928900
1.203488400000	3.162631900000	-0.003083028200
1.203488400000	3.162631900000	-0.003083028200
1.203488400000	3.161020900000	-0.003082246700
1.203488400000	3.161020900000	-0.003082246700
1.203488400000	3.159772800000	-0.003081639300
1.203488400000	3.159772800000	-0.003081639300
1.203488400000	3.133576600000	-0.003068568600
1.203488400000	3.133576600000	-0.003068568600

1.203488400000	3.113946900000	-0.003058355300
1.203488400000	3.113946900000	-0.003058355300
1.203488400000	3.097902400000	-0.003049718900
1.203488400000	3.097902400000	-0.003049718900
1.203488400000	3.076916100000	-0.003037895800
1.203488400000	3.076916100000	-0.003037895800
1.203488400000	3.047278800000	-0.003019758100
1.203488400000	3.047278800000	-0.003019758100
1.203488400000	3.043855100000	-0.003017569200
1.203488400000	3.043855100000	-0.003017569200
1.203488400000	3.009681700000	-0.002994589400
1.203488400000	3.009681700000	-0.002994589400
1.203488400000	3.000000000000	-0.002987714900
1.203488400000	3.000000000000	-0.002987714900
1.203488400000	2.954787100000	-0.002906442400

Material properties used to validate the FEM software PLAXIS from [2]

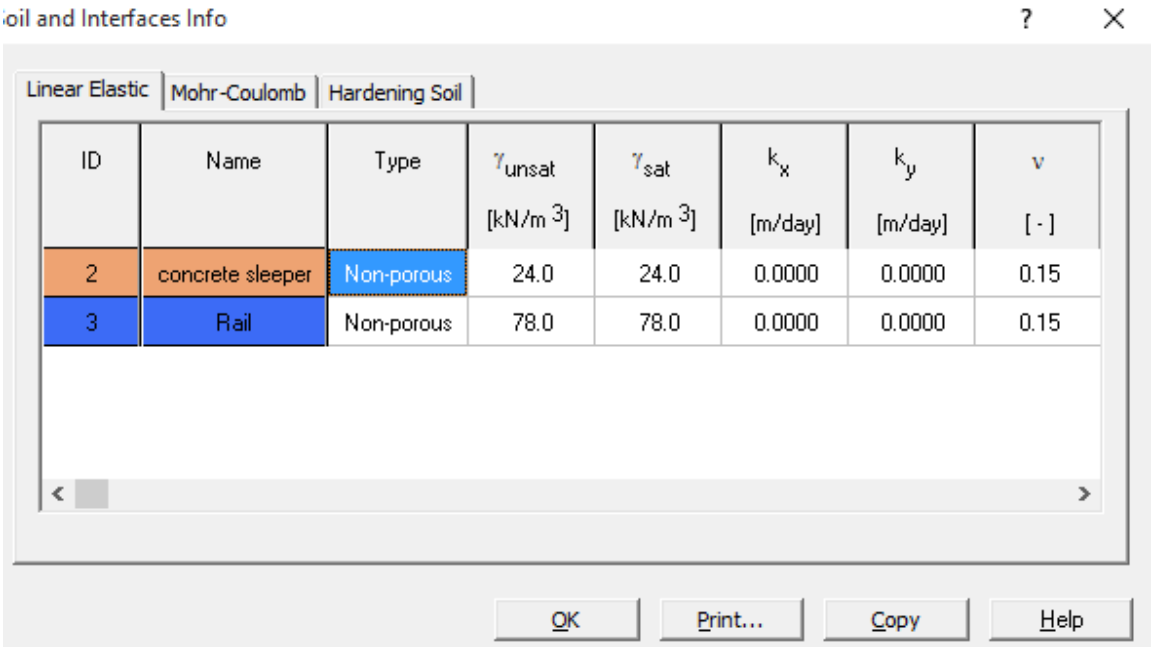

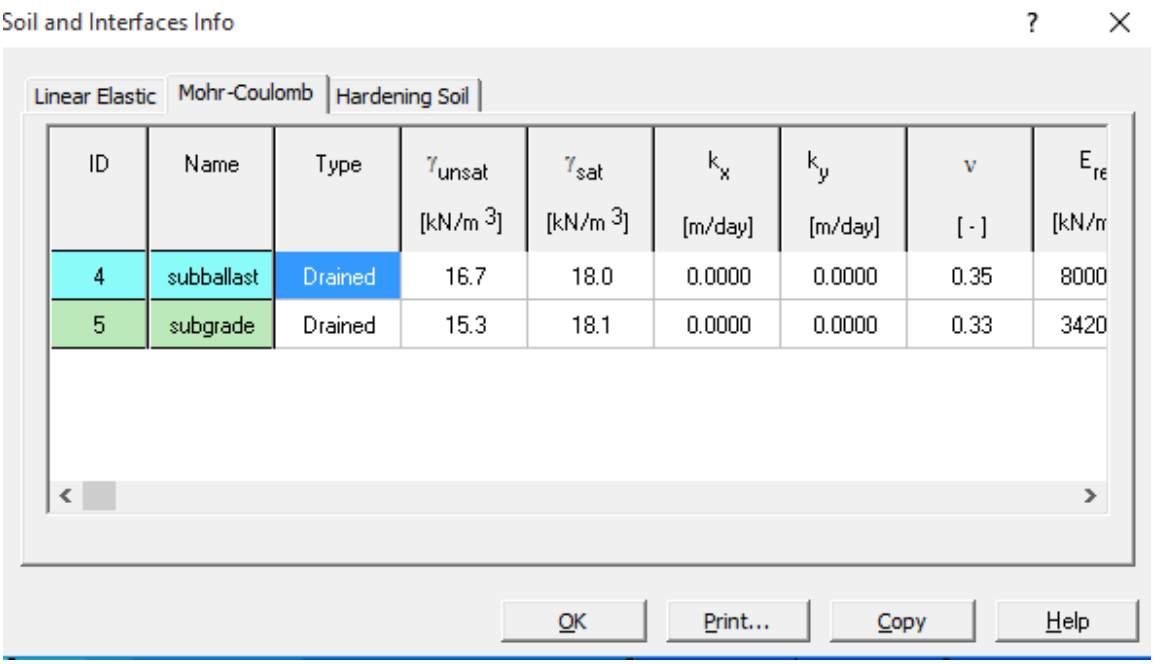

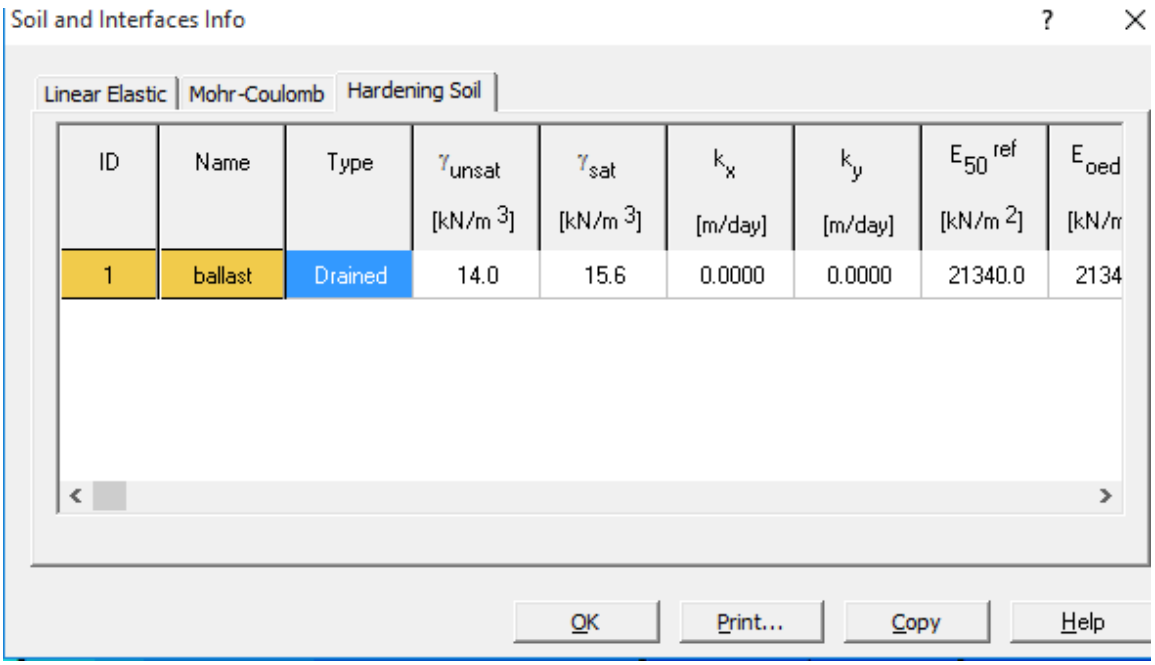

The analysis is a dynamic analysis and the loading condition that is extracted from

c

Point loads

Load no.	Load system	Node	X [10^{-3} m]	Y [m]	Fx [kN]	Fy [kN]
1	A	101	840.000	3.790	0.000	-171.675
2	B	101	840.000	3.790	0.000	0.000

OK Print Help